

For Reference

NOT TO BE TAKEN FROM THIS ROOM

THE UNIVERSITY OF ALBERTA

HYDRODYNAMIC PROPERTIES OF BOVINE CARDIAC

TROPONIN AND ITS SUBUNITS

by



DAVID MITCHELL BYERS

A THESIS

SUBMITTED TO THE FACULTY OF GRADUATE STUDIES AND RESEARCH
IN PARTIAL FULFILMENT OF THE REQUIREMENTS FOR THE DEGREE
OF DOCTOR OF PHILOSOPHY

DEPARTMENT OF BIOCHEMISTRY

EDMONTON, ALBERTA

SPRING, 1983



Digitized by the Internet Archive
in 2023 with funding from
University of Alberta Library

<https://archive.org/details/Byers1983>

ABSTRACT

The physical properties of bovine cardiac troponin, its individual subunits, and reconstituted complexes of the subunits were investigated in solution by a variety of hydrodynamic techniques. These included velocity and equilibrium ultracentrifugation, analytical gel chromatography and viscosity. The results suggest that troponin could extend over a considerable portion of the thin filament, in agreement with the majority of recent evidence from other sources.

Native, undissociated troponin, purified by ion-exchange chromatography on DEAE-Sephacel, consisted essentially of three major components: the Ca^{2+} -binding subunit (TN-C), the inhibitory subunit (TN-I) and the tropomyosin-binding subunit (TN-T). Sedimentation equilibrium studies indicated that native troponin self-associates in a reversible, concentration-dependent manner, although no tendency towards dissociation into subunits was observed at low protein concentrations. The limiting Stokes radius (52 \AA), obtained by gel filtration on Sephadryl S-300, suggests that monomeric troponin ($M_r \sim 80,000$) is an asymmetric molecule, with a frictional ratio of 1.85. Addition of 2 mM Ca^{2+} had very little influence on the hydrodynamic properties of troponin.

The gel filtration, sedimentation and viscosity behaviour of TN-C indicated that it is a monomeric protein ($M_r = 18,500$) of frictional ratio 1.52. TN-C undergoes a conformational change to a more compact shape (frictional ratio = 1.40) in the presence of 2 mM Ca^{2+} , although no effect on the molecular weight of the subunit occurs until higher levels of Ca^{2+} are reached. Most of the structural change induced by Ca^{2+} appears to be associated with cation binding to the $\text{Ca}^{2+}/\text{Mg}^{2+}$ sites of TN-C. The hydrodynamic data suggest that TN-C is a moderately asymmetric protein with an axial ratio of 4-6.

Density measurements were used to show that the partial specific volumes of whole troponin (0.71 ml/g) and TN-C (0.70 ml/g) are unaffected by Ca^{2+} and are significantly lower than expected from the amino acid compositions of these proteins. The major source of this discrepancy is probably the electrostriction of water around the highly-charged troponin subunits.

A new method for purifying TN-T and TN-I was developed, employing hydroxylapatite chromatography in 6 M urea. Monomeric TN-T ($M_r = 36,000$) could not be detected by sedimentation equilibrium, even at low protein concentrations, since this subunit undergoes a strong, reversible aggregation in non-denaturing buffers, probably to a tetramer. These TN-T aggregates appear to be very

asymmetric in solution, as they exhibited unusually large values of Stokes radius (~80 Å) and reduced viscosity (over 20 ml/g).

A tendency towards self-association was also observed for TN-I, although this subunit is essentially monomeric ($M_r = 23,000$) at protein concentrations below 1 mg/ml. The presence of reducing agent was shown to be necessary to avoid intermolecular disulfide bond formation. Gel filtration experiments indicated that TN-I, like TN-C, is not a completely globular protein (frictional ratio = 1.5). Similar physical properties were observed when both sulfhydryl groups of TN-I were modified by carboxamidomethylation.

Bimolecular interactions between cardiac troponin subunits were also investigated using hydrodynamic methods. Only TN-C and TN-I, mixed in a 1:1 molar ratio, are capable of forming a stable complex (TN-IC). The sedimentation coefficient (2.9 S) and Stokes radius from gel filtration (36 Å) suggest that the TN-IC complex is moderately asymmetric (frictional ratio = 1.5-1.6). No interaction between TN-C and TN-T was detected by these methods, while evidence for partial complex formation between TN-I and TN-T was obtained.

Gel filtration and sedimentation equilibrium experiments demonstrated that troponin can be fully

reconstituted by mixing all three subunits in an equimolar ratio (TN-ICT). The elution properties of TN-ICT and native troponin on Sephadryl S-300 were identical, suggesting that the native protein is 1:1:1 with respect to the subunits. In contrast, complexes reconstituted with excess TN-I or TN-C were unstable as monitored by this technique. The SDS gel staining ratios and amino acid composition of native troponin were also consistent with an equimolar subunit ratio.

ACKNOWLEDGEMENTS

I wish to express my sincere gratitude to Dr. Cyril Kay for his guidance and support during the course of this project. I would also like to thank Dr. Bill McCubbin, not only for sharing his expertise in protein chemistry, but also for making the lab a generally fun place to be. In addition, I am indebted to the other members of the lab, past and present, who have contributed to this congenial atmosphere: to Drs. Raj Mani, Max Hincke and Sonia Herasymowich for invaluable scientific input, to Toni Keri and Kim Oikawa for expert technical assistance, and to Vic Ledsham, who helped with the ultracentrifugal studies and was always willing to discuss sports. I am also grateful to the countless members of this Biochemistry department who assisted my research in a variety of ways, especially to Mike Nattriss for performing the amino acid analyses.

The excellent typing and graphics of A. Wiseman and Vic Ledsham, respectively, were greatly appreciated in the preparation of this thesis. I also thank my wife, Cathy, for proof-reading the final manuscript.

This work was made possible by a Medical Research Council of Canada Studentship and an Alberta Heritage Foundation for Medical Research Allowance.

TABLE OF CONTENTS

| CHAPTER | PAGE |
|---|------|
| I. INTRODUCTION..... | 1 |
| A. Muscle Contraction: An Overview..... | 1 |
| B. Thin Filament Regulation of Striated Muscle Contraction..... | 6 |
| C. Cardiac Troponin Subunits..... | 14 |
| 1. Troponin-C..... | 16 |
| 2. Troponin-I..... | 21 |
| 3. Troponin-T..... | 25 |
| D. The Study of Protein Structure by Hydrodynamic Methods..... | 26 |
| E. Aim of the Project..... | 33 |
| II EXPERIMENTAL PROCEDURES..... | 35 |
| A. Protein Preparation..... | 35 |
| 1. Purification of Troponin and its Subunits..... | 35 |
| 2. Preparation of Analytical Samples..... | 37 |
| B. Absorbance Spectrophotometry..... | 38 |
| C. SDS Polyacrylamide Gel Electrophoresis..... | 38 |
| D. Ultracentrifugal Analyses..... | 39 |
| 1. Sedimentation Velocity..... | 39 |
| 2. Sedimentation Equilibrium..... | 41 |
| 3. Extinction Coefficients..... | 46 |
| E. Analytical Gel Chromatography..... | 47 |

| | |
|--|-----------|
| F. Density Measurements..... | 49 |
| G. Viscometry..... | 51 |
| H. Hydrodynamic Analysis..... | 53 |
| I. Miscellaneous Methods..... | 54 |
| 1. Circular Dichroism..... | 54 |
| 2. Amino Acid Analysis..... | 55 |
| 3. Biological Activity Assays..... | 55 |
| III HYDRODYNAMIC PROPERTIES OF NATIVE TROPONIN..... | 57 |
| A. Results | 57 |
| 1. Preparation of Troponin..... | 57 |
| 2. Partial Specific Volume..... | 60 |
| 3. Molecular Weight..... | 60 |
| 4. Sedimentation Velocity..... | 62 |
| 5. Analytical Gel Chromatography..... | 65 |
| 6. Viscosity..... | 69 |
| B. Discussion..... | 69 |
| IV HYDRODYNAMIC PROPERTIES OF TROPONIN-C..... | 84 |
| A. Results | 84 |
| 1. Partial Specific Volume..... | 84 |
| 2. Molecular Weight..... | 84 |
| 3. Sedimentation Velocity..... | 86 |
| 4. Analytical Gel Chromatography..... | 88 |
| 5. Viscosity..... | 88 |
| B. Discussion..... | 91 |

| | | |
|--------------------|---|-----|
| V | HYDRODYNAMIC PROPERTIES OF TROPONIN-T..... | 101 |
| | A. Results | 101 |
| | 1. Preparation of TN-T..... | 101 |
| | 2. Molecular Weight..... | 103 |
| | 3. Sedimentation Velocity..... | 105 |
| | 4. Analytical Gel Chromatography..... | 105 |
| | 5. Viscosity..... | 105 |
| | B. Discussion..... | 109 |
| VI | HYDRODYNAMIC PROPERTIES OF TROPONIN-I..... | 117 |
| | A. Results | 117 |
| | 1. Preparation of TN-I..... | 117 |
| | 2. Molecular Weight..... | 119 |
| | 3. Sedimentation Velocity..... | 121 |
| | 4. Analytical Gel Chromatography..... | 124 |
| | 5. Viscosity..... | 124 |
| | B. Discussion..... | 126 |
| VII | TROPONIN SUBUNITS: BINARY COMPLEXES AND RECONSTITUTION OF WHOLE TROPONIN..... | 132 |
| | A. Results | 132 |
| | 1. TN-IC..... | 132 |
| | 2. TN-CT..... | 136 |
| | 3. TN-IT..... | 139 |
| | 4. Reconstituted Troponin..... | 140 |
| | B. Discussion..... | 143 |
| VIII | GENERAL DISCUSSION..... | 156 |
| Bibliography | | 162 |

LIST OF TABLES

| Table | | Page |
|-------|--|------|
| I | Dependence of shape factors on axial ratio for both prolate and oblate ellipsoids..... | 30 |
| II | Effects of pH, ionic strength and temperature on the sedimentation coefficient (leading peak) of troponin..... | 66 |
| III | Summary of the physical properties of TN-C..... | 93 |
| IV | Structural parameters of equivalent ellipsoids of revolution based on the hydrodynamic properties of TN-C..... | 98 |
| V | Comparison of the amino acid composition of native bovine cardiac troponin to that expected for TN-ICT and TN-I ₂ CT..... | 154 |

LIST OF FIGURES

| Figure | Page |
|---|------|
| 1. Schematic representation of striated muscle ultrastructure..... | 2 |
| 2. Current model for the fine structure of the striated muscle thin filament..... | 7 |
| 3. Steric model for the regulation of striated muscle contraction..... | 10 |
| 4. Evolution of the steric blocking hypothesis..... | 12 |
| 5. Amino acid sequence of bovine cardiac TN-C..... | 18 |
| 6. Amino acid sequence of rabbit cardiac TN-I..... | 23 |
| 7. Purification of troponin on DEAE-Sephacel..... | 58 |
| 8. Effect of protein concentration on the molecular weight of troponin..... | 61 |
| 9. Integration of schlieren peaks for troponin in 0.2 M KMED (- Ca ²⁺) at pH 7.2..... | 63 |
| 10. Effect of protein concentration on the sedimentation coefficient of troponin..... | 64 |
| 11. Calibration curve of standard proteins on Sephadryl S-300..... | 67 |
| 12. Effect of protein concentration on the apparent Stokes radius of troponin..... | 68 |
| 13. Viscosity of troponin in 0.2 M KMED (pH 7.2).... | 70 |
| 14. Protein association models for troponin in 0.2 M KMED (- Ca ²⁺) at pH 7.2..... | 76 |
| 15. Protein association models for troponin in 0.5 M NMED (pH 7.2)..... | 77 |
| 16. Effect of Ca ²⁺ on the molecular weight of TN-C..... | 85 |
| 17. Concentration dependence of the sedimentation coefficient of TN-C..... | 87 |

| | | |
|-----|---|-----|
| 18. | Stokes radius of TN-C as a function of protein concentration..... | 89 |
| 19. | Viscosity of TN-C in 0.2 M KMED (pH 7.2)..... | 90 |
| 20. | Purification of TN-T by hydroxylapatite chromatography..... | 102 |
| 21. | Molecular weight of TN-T as a function of protein concentration..... | 104 |
| 22. | Effect of protein concentration on the sedimentation coefficient of TN-T..... | 106 |
| 23. | Effect of protein concentration on the apparent Stokes radius of TN-T..... | 107 |
| 24. | Viscosity of TN-T in 0.5 M NMED (pH 7.2)..... | 108 |
| 25. | Protein association models for TN-T in 0.5 M NMED (pH 7.2)..... | 112 |
| 26. | Purification of TN-I by hydroxylapatite chromatography..... | 118 |
| 27. | Effect of protein concentration on the molecular weight of TN-I and CMC-TN-I..... | 120 |
| 28. | Sedimentation coefficient of TN-I as a function of protein concentration..... | 122 |
| 29. | Effect of protein concentration on the apparent Stokes radius of TN-I and CMC-TN-I..... | 124 |
| 30. | Viscosity of TN-I and CMC-TN-I in 0.5 M NMED (pH 7.2)..... | 125 |
| 31. | Analytical gel filtration of binary troponin complexes on Sephadryl S-300..... | 134 |
| 32. | Effect of protein concentration on the molecular weight of binary troponin complexes..... | 135 |
| 33. | Schlieren photographs of binary troponin complexes (pH 7.2)..... | 137 |
| 34. | Physical properties of TN-IC..... | 138 |

| | | |
|-----|--|-----|
| 35. | Analytical gel filtration of native and re-constituted troponin on Sephadryl S-300..... | 141 |
| 36. | Effect of protein concentration on the molecular weight of native troponin and reconstituted TN-ICT..... | 142 |

ABBREVIATIONS AND SYMBOLS

Terms appearing locally in a mathematical equation are defined at that point in the text. The units for mass, length, volume and time have been abbreviated according to standard procedures.

| | |
|--|---|
| ATP | adenosine 5'-triphosphate |
| BSA | bovine serum albumin |
| cAMP | cyclic adenosine 3',5'-monophosphate |
| CM- | carboxymethyl |
| CMC- | carboxamidomethylated |
| DEAE- | diethylaminoethyl |
| DTT | dithiothreitol |
| $E_{276 \text{ nm}}^{1\%, 1 \text{ cm}}$ | absorbance of a 1% protein solution in a 1 cm pathlength cell at a wavelength of 276 nm |
| EGTA | ethylene glycol bis(β -aminoethyl ether)-N,N,N',N'-tetraacetic acid |
| f/f_{\min} | experimental translational frictional ratio |
| f/f_o | translational frictional ratio component due to shape alone |
| k' | Huggins coefficient |
| K_a | association constant |
| $x \text{ M KMED (or NMED)}$ | analytical buffer consisting of x M KCl (or NaCl), 50 mM MOPS, 1 mM EGTA, and DTT |
| M_r | molecular weight |

| | |
|---|--|
| M_w | apparent weight-average molecular weight from sedimentation equilibrium experiments |
| MOPS | 3-(N-morpholino)propanesulfonic acid |
| n | degree of polymerization |
| NMR | nuclear magnetic resonance |
| R_s | experimental Stokes radius |
| $R_{s, \text{gel}} (R_{s, \text{sed}})$ | experimental Stokes radius determined by gel filtration (sedimentation velocity) |
| R_o | molecular radius of an equivalent sphere of identical molecular weight and partial specific volume |
| $s_{20,w}$ | sedimentation coefficient corrected to water at 20°C |
| $s^o_{20,w}$ | intrinsic sedimentation coefficient |
| S | Svedberg unit of sedimentation velocity (10^{-13} s) |
| S-1 | soluble subfragment (head region) of myosin |
| SDS | sodium dodecyl sulfate |
| TN-C | Ca^{2+} -binding subunit of troponin |
| TN-I | ATPase inhibitory subunit of troponin |
| TN-T | tropomyosin-binding subunit of troponin |
| TN-IC, TN-IT, TN-CT, TN-ICT, TN-I ₂ CT, TN-IC ₂ T | reconstituted complexes of the troponin subunits in the indicated molar ratios |
| Tris | tris(hydroxymethyl)aminomethane |
| \bar{v} | partial specific volume |
| w | protein hydration |

| | |
|--------------|--|
| β | structural parameter of Scheraga and Mandelkern (1953) |
| Δ_s | protein concentration corresponding to the trailing schlieren peak for associating systems ($n > 2$) |
| η_{red} | reduced viscosity |
| $[\eta]$ | density-corrected intrinsic viscosity |
| v_a | viscosity shape factor |
| σ | gel filtration partition coefficient |
| \sim | approximately |
| $>$ | greater than |
| $<$ | less than |

CHAPTER I

INTRODUCTION

A. MUSCLE CONTRACTION: AN OVERVIEW

Directed motion in vertebrates is accomplished by the concerted action of striated muscle. The structural organization of vertebrate striated (skeletal or cardiac) muscle is schematically illustrated in Figure 1. The muscle fibre is a long multinucleated cell which contains numerous specialized contractile organelles known as myofibrils. The myofibrils are longitudinally arranged, in register, and exhibit a repeating pattern of light and dark bands when viewed under the light microscope. As indicated in Figure 1, these periodic striations result from the overlap of two distinct types of protein fibres, known as the thick and thin filaments. Both filaments are bipolar and are bisected by transverse structural elements: the Z-line (thin filament) and the M-line (thick filament). The fundamental length unit of the myofibril, the sarcomere, is that portion between adjacent Z-lines.

The generally accepted mechanism of striated muscle contraction, descriptively referred to as the sliding filament theory, can be explained with reference to Figure

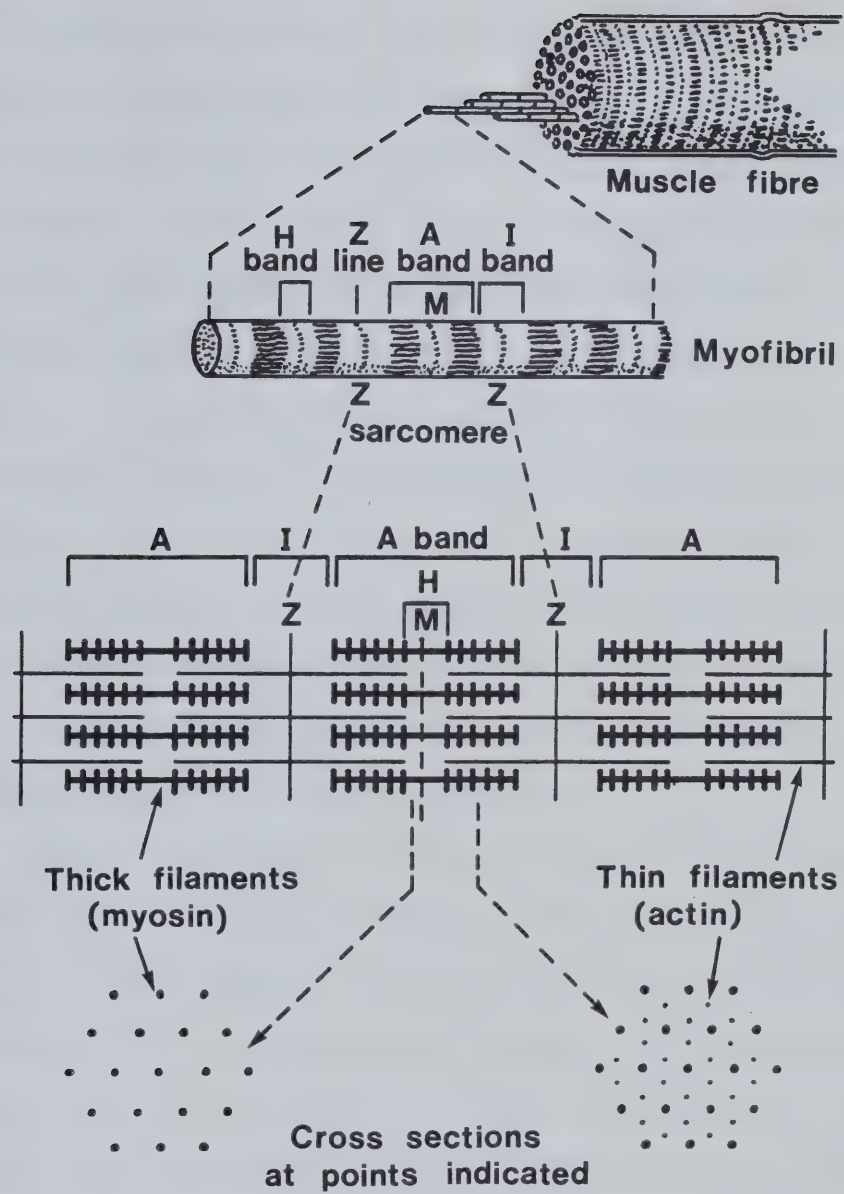


Figure 1. Schematic representation of striated muscle ultrastructure [from Lehninger (1970)].

1. During contraction, the thick and thin filaments are forced to slide past each other in a relative motion which moves opposing Z-lines closer together, thus shortening the sarcomere. Mechanically, this is accomplished by the cyclical, ATP-driven attachment and detachment of thick filament cross-bridges to the thin filament. These cross-bridges can be seen protruding from the core of the thick filament in electron micrographs of striated muscle. One important feature of the sliding filament model is that although contraction decreases the sarcomere length, typically from about 2.5 μ in the resting state to around 1.5 μ in the fully contracted state, the lengths of both filaments remain virtually constant.

Myosin, the major protein of the thick filament, is a hexamer ($M_r = 460,000$) composed of two heavy chains and two pairs of light chains. Myosin is an asymmetric molecule, consisting of two principal domains: a long rod-like tail at one end and two globular heads at the other. The highly helical tail portion of the molecule makes up the backbone of the thick filament, about 150 Å in diameter. The myosin head groups, which correspond to the cross-bridges seen under the electron microscope, contain sites for the binding of both ATP and actin, the major protein of the thin filament. These head groups can be prepared in a soluble form (subfragment S-1) by proteolytic digestion of myosin

with trypsin or papain. The ATPase activity of S-1, which is stimulated several hundred-fold by actin, is considered to be the in vitro correlate of muscle contraction. In addition to actin, the thin filament of vertebrate striated muscle also contains the regulatory proteins, troponin and tropomyosin.

Muscle contraction is regulated by the free Ca^{2+} concentration in the myofibrillar cytoplasm (sarcoplasm). Under resting conditions, the concentration of this ion in the sarcoplasm is around 10^{-8} M. A nerve signal arriving at the muscle fibre triggers the release of Ca^{2+} from storage vesicles (the sarcoplasmic reticulum) and the Ca^{2+} concentration increases to about 10^{-5} M, initiating contraction. There are basically three types of regulatory response to this rise in Ca^{2+} , depending upon the muscle source. In vertebrate striated muscle, Ca^{2+} binds to troponin on the thin filament, reversing the inhibition of the troponin-tropomyosin complex. This type of regulation is discussed in more detail in the following section. In molluscs, the interaction of actin and myosin is blocked in the resting state by a pair of regulatory light chains, one on each myosin cross-bridge. The binding of Ca^{2+} by these light chains allows activation of the actomyosin ATPase. Control at the level of the thick filament also occurs in vertebrate smooth muscle and in many non-muscle cells. In

these tissues, inhibition is relieved following the phosphorylation of myosin light chains analogous to those in molluscs. This phosphorylation is catalyzed by a specific kinase which is itself activated by the ubiquitous Ca^{2+} -binding protein, calmodulin, in response to an increase in Ca^{2+} concentration.

With the vast and expanding amount of research being carried out on the regulation of muscle, it is becoming clear that more than one regulatory system may be operative in a given muscle type. For example, thin filament-based regulation in smooth muscle has been reported (Ebashi et al., 1978; Marston et al., 1980). Conversely, there is some evidence for striated muscle regulation at the level of the myosin light chains (Lehman, 1978). In addition, contractile activity may also be modulated by secondary control mechanisms, such as the phosphorylation of troponin and tropomyosin.

Numerous excellent reviews dealing with various aspects of muscle contraction and regulation have appeared in recent years (Carlson and Wilkie, 1974; Mannherz and Goody, 1976; Harrington, 1979; Perry, 1979; Adelstein and Eisenberg, 1980; McCubbin and Kay, 1980).

B. THIN FILAMENT REGULATION OF STRIATED MUSCLE CONTRACTION

Ebashi (1963) first demonstrated that Ca^{2+} -regulation in skeletal muscle is conferred by a thin filament protein complex which he named "native tropomyosin". This regulatory component was later actually shown to be composed of two proteins, tropomyosin and a new protein called troponin (Ebashi and Kodama, 1965). Subsequently, troponin was also isolated from bovine cardiac muscle (Ebashi et al., 1967). Thanks to the contributions of a number of laboratories, it is now well established that both skeletal and cardiac troponin consist of three non-identical subunits. By the convention of Greaser and Gergely (1973), these are referred to as TN-C (the Ca^{2+} -binding subunit), TN-I (the inhibitory subunit) and TN-T (the tropomyosin-binding subunit).

Prior to a consideration of the regulatory mechanism in striated muscle, it is necessary to briefly examine the structure of the thin filament. A modern conception of this structure is depicted in Figure 2. The backbone of the thin filament, which has a diameter of about 60 Å, is made up of actin monomers ($M_r = 43,000$) polymerized to form two α -helical strands, wound around each other like a twisted pearl necklace. Into both grooves of this fibrous actin (F-actin) fit the long tropomyosin molecules, which lie end-to-end and overlap slightly. They form a repeating pattern of

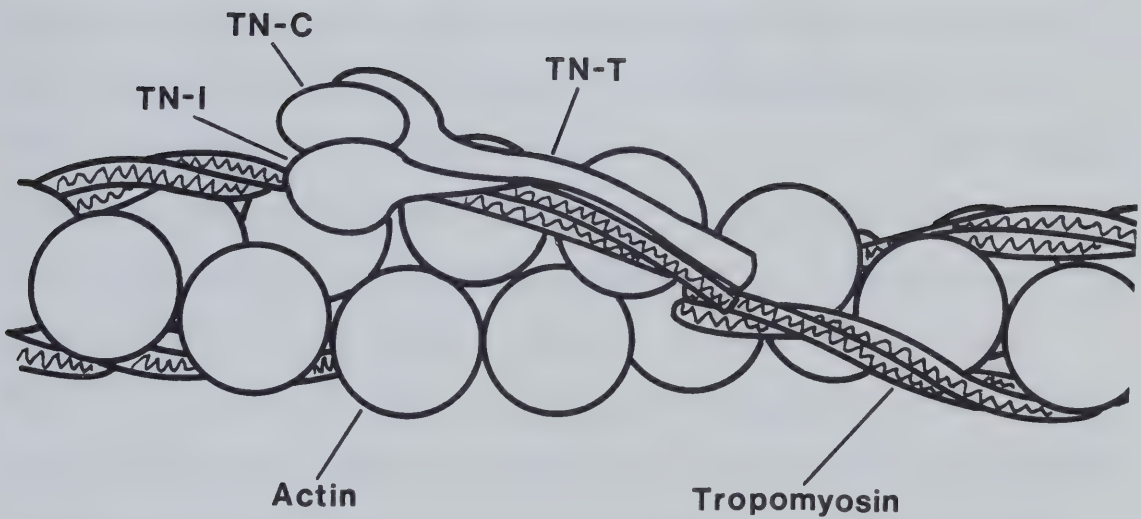


Figure 2. Current model for the fine structure of the striated muscle thin filament [from Mak and Smillie (1980), after Ebashi et al. (1969)].

380 Å along the filament axis, spanning seven actin monomers on each F-actin strand. Tropomyosin ($M_r = 66,000$) consists of two α -helical chains in a coiled-coil arrangement (Smillie, 1976). Associated with each molecule of tropomyosin is a single troponin complex ($M_r = 70,000-80,000$). Since the localization of troponin and its subunits on the thin filament is directly related to the structures of these proteins, a full discussion of this topic is deferred to the appropriate chapters in the Results section. For the present purpose, it is sufficient to note that the bulk of the troponin molecule is located about 100-130 Å from the tropomyosin overlap region (Stewart and McLachlan, 1976), although recent evidence (Ohtsuki, 1979; Mak and Smillie, 1981) suggests that a portion of the TN-T subunit extends to the C-terminal end of the tropomyosin molecule, as illustrated in Figure 2.

The stoichiometry of the major structural proteins in skeletal muscle is believed to be 7:1:1:1:1:1 (actin:myosin:tropomyosin:TN-C:TN-I:TN-T) (Ebashi et al., 1969; Potter, 1974), although there is still some uncertainty regarding the relative amounts of each troponin subunit (Sperling et al., 1979). The ratio of actin to TN-C in rabbit cardiac muscle is also 7:1 (Head and Perry, 1974), suggesting a similar stoichiometry to that of skeletal muscle.

Over the past decade, the most popular theory of thin filament regulation has been the steric blocking hypothesis (Huxley, 1972; Parry and Squire, 1973), proposed on the basis of X-ray diffraction studies on relaxed and contracting muscle. These experiments revealed that tropomyosin is shifted to a position deeper in the F-actin groove under activating conditions. The binding location of the myosin cross-bridge on actin had been established earlier from electron micrograph reconstructions of subfragment S-1-decorated actin filaments (Moore et al., 1970). In conjunction with biochemical evidence (Hitchcock et al., 1973; Margossian and Cohen, 1973; Potter and Gergely, 1974), this data was used to suggest a model (Figure 3) in which actin-myosin interaction is physically blocked in the resting state by tropomyosin, perhaps anchored in this "off" position by the binding of TN-I to actin. Contraction is signalled by the binding of Ca^{2+} to TN-C, followed by a conformational change in troponin which releases TN-I from its actin site. Tropomyosin would then be free to occupy the "on" position and thus allow cross-bridge attachment to the thin filament. This model has received some experimental support over the years, including additional electron microscopic evidence of tropomyosin movement in actin paracrystals (Wakabayashi et al., 1975). Moreover, the results of a biochemical study (Bremel et al.,

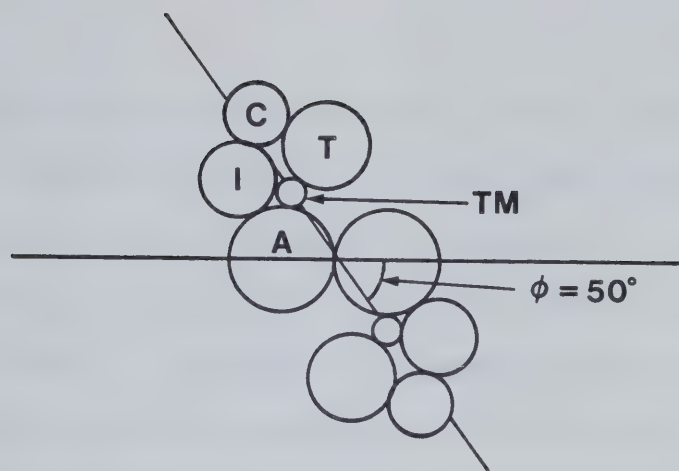
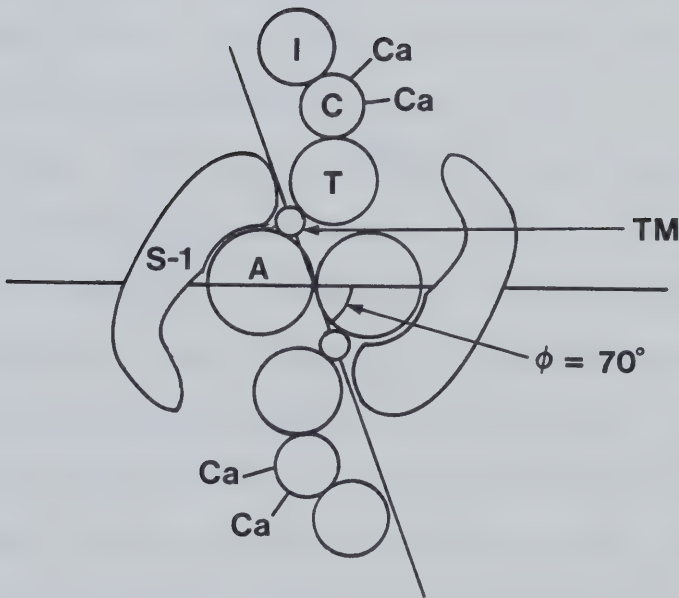
A. -Ca⁺⁺**B. +Ca⁺⁺**

Figure 3. Steric model for the regulation of striated muscle contraction. The view looking down the thin filament axis towards the Z-line is schematically depicted. The proteins represented are: A (actin), TM (tropomyosin), C (TN-C), I (TN-I), T (TN-T), S-1 (myosin subfragment S-1). (A) relaxed muscle, $[Ca^{2+}] \sim 10^{-8} M$. (B) contracting muscle, $[Ca^{2+}] \sim 10^{-5} M$ [from Potter and Gergely (1974)].

1972) are partially in accord with the steric hypothesis. These workers observed that, at low ATP concentration, saturating amounts of S-1 can push tropomyosin from its inhibitory position, thus rendering the ATPase activity insensitive to Ca^{2+} . Although the geometry of the steric model has been altered by approximately 180° as a consequence of more recent evidence regarding the positions of tropomyosin (Seymour and O'Brien, 1980) and S-1 binding (Taylor and Amos, 1981), the basic structural requirements of the model remain satisfied (Figure 4).

Nevertheless, the current status of the steric hypothesis, as envisioned in Figures 3 and 4, has been jeopardized by a number of independent investigations. To begin with, there is some evidence that tropomyosin does not bind actin at two discrete sites (Johnson et al., 1981), as suggested by the structural data presented above. Moreover, the steric model is at a loss to explain why the binding of S-1 actually increases the affinity of F-actin for tropomyosin (Eaton, 1976) or how tropomyosin plus actin can stimulate higher ATPase rates than actin alone (Bremel et al., 1972). A steady-state kinetic investigation has also demonstrated that tropomyosin is a non-competitive inhibitor of actomyosin ATPase, indicating that myosin and tropomyosin do not compete directly for the same binding site on actin (Sobieszek, 1982). Perhaps the most damaging evidence

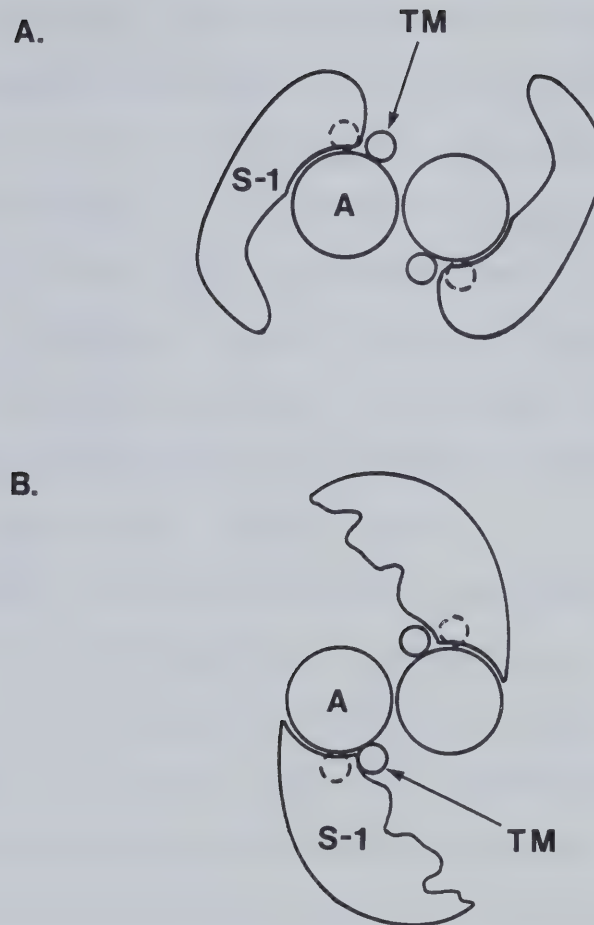


Figure 4. Evolution of the steric blocking hypothesis. (A) Original model based on the structural data of Moore et al. (1970), Huxley (1972), Parry and Squire (1973) and others. (B) Revised model based on more recent data of Seymour and O'Brien (1980) and Taylor and Amos (1981). This schematic diagram shows tropomyosin (TM) in the activating (—) and relaxing (---) positions. The other proteins are represented as in Figure 3 and the viewer is looking down the thin filament towards the Z-line [from Squire (1981)].

against the steric hypothesis is the observation that, despite dramatic changes in the ATPase activity, the actual binding of the S-1 subfragment to regulated thin filaments is not influenced by the addition or removal of Ca^{2+} (Chalovich et al., 1981; Chalovich and Eisenberg, 1982). It should be cautioned, however, that the soluble proteolytic fragments of myosin employed in many of these studies may not be valid representations of intact myosin in the thick filament (Wagner and Giniger, 1981).

Although no alternate model comparable in scope and popularity to the steric hypothesis has yet been proposed, research in this area is currently proceeding in a number of directions. To explain the Ca^{2+} -insensitivity of S-1 binding to actin, Chalovich and Eisenberg (1982) have suggested that troponin-tropomyosin control is exerted at a subsequent step in the ATPase cycle, perhaps the release of inorganic phosphate from the actomyosin complex, following ATP hydrolysis. This relatively slow step is believed to be accompanied by a change in the angle of attachment of S-1 to actin, from 90° to 45° (Lynn and Taylor, 1971). This rotation of the myosin cross-bridge could be blocked by the regulatory proteins in the absence of Ca^{2+} .

A more active role of actin, perhaps in the form of a conformational change (Yanagida et al., 1974; Eaton, 1976) has also been considered as a possible mechanism for the

troponin-mediated Ca^{2+} -response. Some investigators now believe that thin filament control should not be approached as an "all-or-none" phenomenon at all, but rather as a complicated allosteric system, with Ca^{2+} and the myosin heads acting as effectors. A recent demonstration that Ca^{2+} reduces the cooperativity between adjacent tropomyosin-troponin units along the thin filament is quite interesting in this regard (Greene and Eisenberg, 1980).

C. CARDIAC TROPONIN SUBUNITS

Individual troponin subunits have been the subject of intensive study ever since the realization that these proteins retain their basic functional properties in solution and can be reconstituted to form a biologically-active complex. Although most of this work has been carried out with the subunits from rabbit skeletal muscle, cardiac troponin is believed to operate in an analogous fashion. In an early investigation, Ebashi et al. (1967) observed that both skeletal and cardiac troponin can confer Ca^{2+} -sensitivity to actomyosin from either muscle type. The subsequent isolation of purified cardiac troponin subunits (Brekke and Greaser, 1976; Burtnick, 1977) has led to the discovery that these proteins are qualitatively similar to their skeletal counterparts in size, amino acid composition and biological properties. Indeed, Hincke et al. (1977)

have demonstrated that hybrid troponin complexes, formed from various skeletal and cardiac subunit combinations, are generally capable of regulating actomyosin in vitro.

Nonetheless, there are important differences between skeletal and cardiac muscle (Katz, 1970; Ebashi et al., 1974a). For example, skeletal muscle must be available for rapid and complete contraction or relaxation, whereas cardiac muscle contracts in a continuous, rhythmical manner, displaying a relatively high resting tension. There is substantial evidence that these altered regulatory requirements are, in fact, reflected at the level of the troponin subunits. With the sequences of TN-C (van Eerd and Takahashi, 1975) and TN-I (Wilkinson and Grand, 1978) from a number of sources now known, it has been established that variations in primary structure are tissue, rather than species, dependent. That is, sequences are generally more homologous between skeletal (or cardiac) subunits of different species than between skeletal and cardiac subunits of the same species. Also, antiserum raised against a given cardiac or skeletal troponin subunit often does not cross react with the same protein from the other muscle source (Hirabayashi and Perry, 1974; Cummins and Perry, 1978).

In the following sections, a brief outline of the chemical, physical and biological properties of bovine cardiac troponin subunits is presented, with special

reference to any similarities or differences with the corresponding proteins from rabbit skeletal muscle. Details of troponin subunit interactions will be discussed in Chapter VII.

1. Troponin-C

The Ca^{2+} -binding subunit of troponin, TN-C, is part of a family of homologous Ca^{2+} -binding proteins which are thought to have evolved from a common ancestral protein by gene duplication (Collins, 1974). Others in this family include calmodulin, parvalbumin, and the regulatory light chains of myosin. From the X-ray crystal structure of parvalbumin, Kretsinger and Nockolds (1973) observed that each Ca^{2+} -binding site consists of a "helix-loop-helix" arrangement in the polypeptide chain which is folded around the bound cation. Four such regions, exhibiting remarkable homology, were found in the sequence of rabbit skeletal TN-C (Collins et al., 1973), and later studies showed that this protein indeed binds four Ca^{2+} ions (Potter and Gergely, 1975). These Ca^{2+} -binding sites are usually labelled I to IV, starting from the N-terminus. Van Eerd and Takahashi (1975) noticed extensive amino acid replacements in the site I region of the bovine cardiac TN-C sequence and suggested that this protein would only be able to bind three Ca^{2+} ions. Again, this prediction has been confirmed experimentally (Burtnick and Kay, 1977; Leavis and Kraft, 1978).

TN-C at pH 7 is a highly negatively-charged protein with numerous aspartic and glutamic acid residues, many of which are involved in Ca^{2+} binding (Reid and Hodges, 1980). The amino acid sequence of bovine cardiac TN-C is shown in Figure 5 (van Eerd and Takahashi, 1975). The molecular weight of this protein (18,459) is similar to that of rabbit skeletal TN-C ($M_r = 17,840$; Collins, 1974). Cardiac TN-C contains one more tyrosine (3) and cysteine (2) than skeletal TN-C, but lacks histidine. Tryptophan is not found in either protein, but both molecules contain a relatively large number of phenylalanine residues. So far, no X-ray structural determination has been reported for any TN-C subunit, although crystals suitable for this purpose have been obtained for chicken skeletal TN-C (Strasburg et al., 1980).

The Ca^{2+} -binding properties of TN-C have been thoroughly characterized. Rabbit skeletal TN-C contains two Ca^{2+} -specific sites ($K_a \sim 2 \times 10^5 \text{ M}^{-1}$) and two Ca^{2+} -sites of higher affinity ($K_a \sim 2 \times 10^7 \text{ M}^{-1}$) which can also bind Mg^{2+} competitively ($K_a \sim 5 \times 10^3 \text{ M}^{-1}$) (Potter and Gergely, 1975). Chemical modification studies (Sin et al., 1978) and experiments with defined fragments of skeletal TN-C (Leavis et al., 1978) have revealed that sites I and II are the Ca^{2+} -specific sites while the remaining two (III and IV) are

Ac-Met-Asp-Asp-Ile-Tyr-Lys-Ala-Ala-Val-Glu-Gln-Leu-Thr-Glu-Glu-
Gln-Lys-Asn-Glu-Phe-Lys-Ala-Ala-Phe-Asp-Ile-Phe-Val-Leu-Gly- (15)
Ala-Glu-Asp-Gly-Cys-Ile-Ser-Thr-Lys-Glu-Leu-Gly-Lys-Val-Met-
Arg-Met-Leu-Gly-Gln-Asn-Pro-Thr-Pro-Glu-Glu-Leu-Gln-Glu-Met- (45)
Ile-Asp-Glu-Val [Asp-Glu-Asp-Gly-Ser-Gly-Thr-Val-Asp-Phe-Asp-
Glu] Phe-Leu-Met-Met-Val-Arg-Cys-Met-Lys-Asp-Asp-Ser-Lys- (60)
Gly-Lys-Ser-Glu-Glu-Leu-Ser-Asp-Leu-Arg-Met-Phe [Asp-
Lys-Asn-Ala-Asp-Gly-Tyr-Ile-Asp-Leu-Glu-Glu] Leu-Lys-Ile-Met- (75)
Leu-Gln-Ala-Thr-Gly-Glu-Thr-Ile-Thr-Glu-Asp-Asp-Ile-Glu-Glu- (90)
Leu-Met-Lys-Asp-Gly [Asp-Lys-Asn-Asp-Gly-Arg-Ile-Asp-Tyr-
Asp-Glu] Phe-Leu-Glu-Phe-Met-Lys-Gly-Val-Glu-OH (105)
Leu-Gln-Ala-Thr-Gly-Glu-Thr-Ile-Thr-Glu-Asp-Asp-Ile-Glu-Glu- (120)
Leu-Met-Lys-Asp-Gly [Asp-Lys-Asn-Asp-Gly-Arg-Ile-Asp-Tyr-
Asp-Glu] Phe-Leu-Glu-Phe-Met-Lys-Gly-Val-Glu-OH (135)
Leu-Met-Lys-Asp-Gly [Asp-Lys-Asn-Asp-Gly-Arg-Ile-Asp-Tyr-
Asp-Glu] Phe-Leu-Glu-Phe-Met-Lys-Gly-Val-Glu-OH (150)

Figure 5. Amino acid sequence of bovine cardiac TN-C (van Eerd and Takahashi, 1975). The proposed Ca^{2+} -binding sites are enclosed with square brackets.

the $\text{Ca}^{2+}/\text{Mg}^{2+}$ sites. Bovine cardiac TN-C also has two $\text{Ca}^{2+}/\text{Mg}^{2+}$ sites, with binding affinities similar to those of the skeletal protein (Hincke et al., 1978; Holroyde et al., 1980). However, only a single Ca^{2+} -specific site is present on cardiac TN-C, with an affinity of $2 \times 10^5 \text{ M}^{-1}$ (Holroyde et al., 1980). Comparison with skeletal TN-C suggests that this lone Ca^{2+} -specific site is site II. In whole troponin, or in the TN-C - TN-I complex, the Ca^{2+} -affinity of each class of binding site is increased by one order of magnitude (Potter and Gergely, 1975; Holroyde et al., 1980). The presence of actin may also influence the Ca^{2+} -binding properties of TN-C (Potter and Zot, 1982).

Upon binding of Ca^{2+} to TN-C, numerous spectroscopic and hydrodynamic changes occur (reviewed by McCubbin and Kay, 1980). Perhaps the most dramatic effect observed is the increase in the amount of ordered secondary structure in the "plus Ca^{2+} " state. Circular dichroism studies have indicated that Ca^{2+} -binding increases the α -helical content by 60% in rabbit skeletal TN-C (Murray and Kay, 1972) and by 30% in the bovine cardiac protein (Burtnick et al., 1975a). Most of this change results from the occupation of the $\text{Ca}^{2+}/\text{Mg}^{2+}$ sites (Hincke et al., 1978; Johnson and Potter, 1978). On the other hand, only relatively minor conformational alterations are associated with Ca^{2+} binding to the Ca^{2+} -specific sites. For the cardiac subunit, these

changes include NMR-detected variations in phenylalanine environment (Hincke et al., 1981a) and a 2-fold increase in the fluorescence of an extrinsic probe (Johnson et al., 1980). Comparable results have been reported for skeletal TN-C.

Nevertheless, it appears that the Ca^{2+} -specific site(s) in TN-C is responsible for the regulation of muscle contraction. Actomyosin ATPase is activated in the same range of free Ca^{2+} concentration that is required to saturate the two Ca^{2+} -specific sites on skeletal troponin (Potter and Gergely, 1975) or the single site on cardiac troponin (Holroyde et al., 1980). Kinetic studies with skeletal TN-C also support a biologically-important role for these sites (Johnson et al., 1979). Stopped-flow fluorescence measurements with dansylaziridine-labelled TN-C indicated that Ca^{2+} removal from the Ca^{2+} -specific sites occurs with a half-life ($t_{1/2}$) of 2-3 ms, while $t_{1/2}$ for the removal of Ca^{2+} from the $\text{Ca}^{2+}/\text{Mg}^{2+}$ sites is ~700 ms. Similar results were observed for cardiac TN-C (Johnson et al., 1978a). Since these $t_{1/2}$ values would be even higher in native troponin, because of the increased affinity for Ca^{2+} in the complex, Ca^{2+} -exchange in the $\text{Ca}^{2+}/\text{Mg}^{2+}$ sites is clearly too slow to participate in a rapid switching mechanism where contraction-relaxation events must be complete within about 50 ms of excitation (Carlson and

Wilkie, 1974; McCubbin and Kay, 1980). In any case, the intracellular concentrations of Ca^{2+} ($\sim 10^{-8}$ M) and Mg^{2+} (a few millimolar) are sufficiently high that the $\text{Ca}^{2+}/\text{Mg}^{2+}$ sites would be occupied even under relaxing conditions (Potter et al., 1981). Recent studies have suggested a structural role for these sites (Zot and Potter, 1982).

2. Troponin-I

Skeletal TN-I is capable of inhibiting the actomyosin ATPase by itself, although this inhibition is greatly enhanced by tropomyosin (Wilkinson et al., 1972). TN-C alleviates this inhibition by forming a complex with TN-I (Schaub et al., 1972). Full Ca^{2+} -sensitivity requires the further addition of TN-T, thus completing the thin filament regulatory unit (Eisenberg and Kielley, 1974). The principal inhibitory region of TN-I has been located on a cyanogen bromide fragment of the protein (residues 96-117) (Syska et al., 1976). This fragment alone is very effective in binding to actin and inhibiting the actomyosin ATPase. The amino acid residues essential for inhibition have been studied by using synthetic peptide analogues of this region (Talbot and Hodges, 1981a). The mechanism of cardiac TN-I inhibition appears to be similar to that of the skeletal subunit. TN-I from bovine cardiac muscle can inhibit rabbit skeletal actomyosin, and vice versa, although each type of TN-I is most effective in its own system (Hincke et al., 1977). There may be some species specificity at this level,

however, since rabbit skeletal TN-I is a better inhibitor than rabbit cardiac TN-I in both skeletal and cardiac actomyosin assay systems from rabbit (Talbot and Hodges, 1981b).

The primary structures of rabbit cardiac and three types of skeletal TN-I have been determined (Wilkinson and Grand, 1978). The rabbit cardiac TN-I sequence is shown in Figure 6. Although there is a fair degree of homology between the skeletal and cardiac TN-I molecules, the cardiac protein is significantly larger ($M_r = 23,550$) than the skeletal subunits ($M_r \sim 21,000$), containing an extra 26 amino acid residues at its N-terminus. Rabbit cardiac TN-I has a substantially lower methionine content than its skeletal counterpart, as well as one less cysteine residue (2). Both skeletal and cardiac TN-I molecules possess a net positive charge at pH 7 which interferes with the molecular weight determination of these proteins by SDS-polyacrylamide gel electrophoresis (Burtnick, 1977).

Although the sequence of bovine cardiac TN-I is not yet known, this protein appears to be very similar to rabbit cardiac TN-I. The apparent molecular weight of bovine cardiac TN-I is 23,000, determined by sedimentation equilibrium in 6 M urea (Burtnick et al., 1975b). The amino acid compositions of the two proteins are almost identical, although the bovine subunit has a slightly higher tyrosine and proline content (Burtnick et al., 1975b; Brekke and Greaser, 1976).

X-Ala-Asp-Glu-Ser-Arg-Asp-Ala-Ala-Glu-Glu-Ala-Lys-Pro-Ala-Pro- (115)
 Ala-Val-Arg-Arg-Ser-Asp-Arg-Ala-Tyr-Ala-Thr-Glu-Pro-His-Ala- (30)
 Lys-Ser-Lys-Lys-Ile-Ser-Ala-Ser-Arg-Lys-Leu-Gln-Leu-Lys- (45)
 Thr-Leu-Met-Leu-Gln-Ile-Ala-Lys-Gln-Glu-Leu-Glu-Arg-Glu-Ala- (60)
 Glu-Glu-Arg-Arg-Gly-Glu-Lys-Gly-Arg-Ala-Leu-Ser-Thr-Arg-Cys- (75)
 Gln-Pro-Leu-Glu-Ala-Gly-Leu-Gly-Phe-Ala-Glu-Leu-Gln-Asp- (90)
 Leu-Cys-Arg-Gln-Leu-His-Ala-Arg-Val-Asp-Lys-Val-Asp-Glu-Glu- (105)
 Arg-Tyr-Asp-Val-Glu-Ala-Lys-Val-Thr-Lys-Asn-Ile-Thr-Glu-Ile- (120)
 Ala-Asp-Leu-Thr-Gln-Lys-Ile-Phe-Asp-Leu-Arg-Gly-Lys-Phe-Lys- (135)
 Arg-Pro-Thr-Leu-Arg-Leu-Arg-Val-Arg-Ile-Ser-Ala-Asp-Ala-Met- (150)
 Met-Gln-Ala-Leu-Glu-Gly-Thr-Arg-Ala-Lys-Glu-Thr-Leu-Asp-Leu- (165)
 Arg-Ala-His-Leu-Lys-Gln-Val-Lys-Lys-Glu-Asp-Thr-Glu-Lys-Glu- (180)
 Asn-Arg-Glu-Val-Gly-Asp-Trp-Arg-Lys-Asn-Ile-Asp-Leu-Leu-Ser- (195)
 Gly-Met-Glu-Gly-Arg-Lys-Lys-Phe-Glu-Gly-OH

Figure 6. Amino acid sequence of rabbit cardiac TN-I (Grand et al., 1976). X denotes an unknown blocking group.

The phosphorylation of TN-I has been the subject of a great deal of interest (reviewed by Perry, 1979). Rabbit cardiac TN-I can be phosphorylated by either phosphorylase kinase (at serine 72) or by cAMP-dependent protein kinase (at serines 20 and 146). The phosphorylation of residues 72 and 146 is blocked in the native troponin complex, as is the phosphorylation of the corresponding residues (threonine 11 and serine 117) in rabbit skeletal TN-I. Thus, no biological role has yet been indicated for these sites.

In contrast, the phosphorylation of serine 20 in cardiac TN-I does appear to be physiologically relevant. This residue, which is in a region of the polypeptide chain that has no analogue in the skeletal subunit, can be phosphorylated in native troponin by cAMP-dependent protein kinase in vitro (Stull and Buss, 1977). Moreover, studies with perfused hearts have demonstrated that β -adrenergic stimulation increases the phosphate content of TN-I by 1 mol/mol (England, 1975; Solaro et al., 1976), specifically modifying serine 20 (Moir et al., 1980). Solaro et al. (1976) have suggested that this is a negative feedback mechanism, smoothing out the regulatory response to the increased force brought about by the primary action of β -adrenergic agents. They have further speculated that, since the phosphate group would introduce negative charges into a positively-charged region of the protein, the basis of this

response might be a decreased TN-I - TN-C interaction, ultimately leading to reduced Ca^{2+} -sensitivity. Recent Ca^{2+} -binding experiments with bovine cardiac troponin have confirmed that phosphorylation in fact does decrease the Ca^{2+} -affinity at the Ca^{2+} -specific site (Robertson et al., 1982).

3. Troponin-T

TN-T is responsible for anchoring the troponin complex to tropomyosin on the thin filament. The interaction between TN-T and tropomyosin is manifested by changes in a variety of physical properties of these proteins, such as an increased head-to-tail aggregation of tropomyosin in the complex (Ebashi and Kodama, 1965). For cardiac TN-T, this interaction can be demonstrated by cosedimentation analysis (Burtnick et al., 1976) and circular dichroism (Burtnick and Kay, 1976). Both skeletal (Yamaguchi et al., 1974) and cardiac (Brekke and Greaser, 1976) TN-T also produce changes in the paracrystal patterns formed by tropomyosin, although specific differences have been observed in each system (Yamaguchi and Greaser, 1979).

Rabbit skeletal TN-T has been sequenced and has a molecular weight of 30,503 (Pearlstone et al., 1976). The amino acid composition of this protein is striking in that about 50% of the residues would be expected to be charged at pH 7. Although no TN-T sequence from a cardiac muscle

source has yet been reported, the bovine cardiac subunit appears to be larger ($M_r = 36,000$) than its skeletal counterpart and exhibits significant differences in amino acid composition as well (Brekke and Greaser, 1976; Burtnick et al., 1976). For example, the cardiac subunit has a higher acidic amino acid content and, unlike skeletal TN-T, contains a cysteine residue.

D. THE STUDY OF PROTEIN STRUCTURE BY HYDRODYNAMIC METHODS

The relationship between protein structure and function is one of the most intriguing problems in molecular biology. At the present time, only X-ray crystallography is capable of determining the complete three dimensional structure of proteins, although this monopoly is being challenged by some powerful NMR techniques (Wuthrich et al., 1982). Nevertheless, countless other approaches, such as hydrodynamics, can be used to give lesser degrees of structural information. Hydrodynamic techniques study how proteins move in solution and thereby affect the bulk properties of the solvent. The associated parameters are a function of the size and shape of the dissolved macromolecule. Most experimental methods are designed to examine either the translational (sedimentation, gel filtration, electrophoresis) or the rotational (viscosity) motions of proteins. Several good reviews, outlining the

theoretical and practical aspects of hydrodynamic measurements, have been published (Schachman, 1959; Tanford, 1961; Yang, 1961; Kuntz and Kauzmann, 1974; Cantor and Schimmel, 1980).

The study of protein structure by translational hydrodynamic methods is based on the Stokes equation:

$$f = 6 \pi \eta r \quad [1]$$

This equation relates the translational frictional coefficient (f) of a sphere to its radius (r), where η is the viscosity of the medium. Derivation of the Stokes law in this form requires the assumption that the solvent molecules are negligibly small relative to the particle and that no slippage occurs at the solvent-particle interface. Although there is no a priori reason to believe that these conditions should be true for proteins, Squire and Himmel (1979) have demonstrated the validity of Equation 1 in water for molecules greater than 7 Å in radius.

The quantity usually determined in experiments of this type is the frictional ratio (f/f_{\min}), or the ratio of the observed frictional coefficient to that of an idealized spherical particle of identical molecular weight:

$$f/f_{\min} = R_s/R_o = R_s/[3 M_r \bar{v}/4 \pi N]^{1/3} \quad [2]$$

In this relationship, R_s is the experimental Stokes radius of the protein while R_o is the Stokes radius of the equivalent unhydrated sphere of molecular weight M_r and partial specific volume \bar{v} (N is Avogadro's number). In practice, f/f_{\min} will be greater than unity, since real proteins are not spherical and are substantially hydrated, thus increasing their effective hydrodynamic size. Most water-soluble globular proteins have f/f_{\min} values between 1.15 and 1.30, while much higher values can be exhibited by very asymmetric proteins, such as myosin ($f/f_{\min} = 3.5$) (Tanford, 1961). If the degree of hydration is known, or can be estimated, the contribution to the frictional ratio due to asymmetry alone (f/f_o) can be evaluated (Oncley, 1941) by:

$$f/f_o = (f/f_{\min})/[1 + (w/\bar{v}\rho)]^{1/3} \quad [3]$$

where w is the hydration expressed as grams of water bound per gram of protein, \bar{v} is the partial specific volume and ρ is the solvent density.

The level of detail obtainable from hydrodynamic methods is inherently low. Experimental values of f/f_o must be compared to theoretical values calculated for various geometric models. The choice of a plausible model that best

fits the data is then made. Although a number of more complex models have been developed for this purpose (Bloomfield et al., 1967; Teller et al., 1979), ellipsoidal models are still the most commonly used. Equations relating f/f_o to the axial ratio of both prolate (cigar-shaped) and oblate (disc-shaped) ellipsoids of revolution have been derived (Perrin, 1936). Representative f/f_o values are listed in Table I, as a function of axial ratio.

A similar approach is employed in determining structural parameters from viscosity data. The corresponding frictional equation for rotational motion is:

$$f_{\text{rot}} = 6 \eta v \quad [4]$$

where f_{rot} is the rotational frictional coefficient, η is the viscosity of the medium and v is the particle volume. The assumptions for this relationship are the same as for Equation 1. The experimentally-measured intrinsic viscosity ($[\eta]$) can likewise be separated into contributions from hydration (w) and asymmetry (v_a) according to:

$$[\eta] = v \bar{\eta} = v_a [1 + (w/\bar{\eta}\rho)] \bar{\eta} \quad [5]$$

where v is the experimental viscosity increment. Equations relating v_a to the axial ratios of prolate and oblate

TABLE I: DEPENDENCE OF SHAPE FACTORS ON AXIAL RATIO FOR
BOTH PROLATE AND OBLATE ELLIPSOIDS^a

| Axial ratio | Prolate | | | Oblate | | |
|-------------|----------------------|----------------------|--|---------|---------|---------------------------------|
| | f/f_O ^b | ν_a ^c | β ^d ($\times 10^{-6}$) | f/f_O | ν_a | β ($\times 10^{-6}$) |
| 1 | 1.000 | 2.50 | 2.12 | 1.000 | 2.50 | 2.12 |
| 2 | 1.044 | 2.91 | 2.13 | 1.042 | 2.85 | 2.12 |
| 3 | 1.112 | 3.68 | 2.16 | 1.105 | 3.43 | 2.13 |
| 4 | 1.182 | 4.66 | 2.20 | 1.165 | 4.06 | 2.13 |
| 5 | 1.255 | 5.81 | 2.23 | 1.224 | 4.71 | 2.13 |
| 6 | 1.314 | 7.10 | 2.28 | 1.277 | 5.36 | 2.14 |
| 8 | 1.433 | 10.10 | 2.35 | 1.374 | 6.70 | 2.14 |
| 10 | 1.543 | 13.63 | 2.41 | 1.458 | 8.04 | 2.14 |
| 12 | 1.645 | 17.76 | 2.47 | 1.534 | 9.39 | 2.14 |
| 15 | 1.784 | 24.8 | 2.54 | 1.636 | 11.42 | 2.14 |
| 20 | 1.996 | 38.6 | 2.64 | 1.782 | 14.8 | 2.15 |
| 25 | 2.183 | 55.2 | 2.72 | 1.908 | 18.2 | 2.15 |
| 30 | 2.356 | 74.5 | 2.78 | 2.020 | 21.6 | 2.15 |
| 40 | 2.668 | 120.8 | 2.89 | 2.212 | 28.3 | 2.15 |
| 50 | 2.946 | 176.5 | 2.97 | 2.375 | 35.0 | 2.15 |

^aAdapted from Schachman (1959). The axial ratios of prolate and oblate ellipsoids of revolution are a/b and b/a , respectively, where a is the semiaxis of revolution and b is the equatorial semiaxis.

^b f/f_O is the frictional ratio due to asymmetry, calculated from the equations of Perrin (1936).

^c ν_a is the shape component of the viscosity increment and corresponds to the intrinsic viscosity when concentration is expressed as volume fraction (Simha, 1940).

^d β is the combined parameter of Scheraga and Mandelkern (1953), defined in Equation 6.

ellipsoids have been derived (Simha, 1940) (see Table I). It should be noted that viscosity is inherently more sensitive to changes in shape than f/f_{\min} because it is a function of the molecular volume rather than of the radius. Intrinsic viscosity values typically range from 3-5 ml/g for globular proteins to over 200 ml/g for proteins like myosin (Tanford, 1961).

Obviously, both shape and hydration parameters cannot be uniquely determined from a single type of experiment. However, viscosity data can be combined with f/f_{\min} measurements to solve for both w and the shape factor (Oncley, 1941). Alternatively, the value of w is often estimated from the amino acid composition or an average protein value is used. Typical hydration values, determined by such methods as NMR, calorimetry, and isopiestic measurements, are usually about 0.3-0.4 g water/g protein (Kuntz and Kauzmann, 1974). As expected, some variability in w determined by these techniques is observed, since different methods are no doubt sensitive to varying degrees of hydration. In any case, detailed structural inferences based on assumed values of w are subject to considerable uncertainty.

Some investigators have criticized the whole approach of separating shape and hydration factors, noting that the effective hydrodynamic volume of a protein need not

necessarily equal the sum of its partial specific volume and the amount of water bound. Indeed, non-ideal solvent-solute interactions might be expected to invalidate this common assumption. For this reason, Scheraga and Mandelkern (1953) proposed that experimental quantities be used to eliminate the explicit hydration and \bar{v} terms. They combined sedimentation and viscosity data to describe a new parameter (β) which is a function of the axial ratio only:

$$\beta = [N/(16,200 \pi^2)]^{1/3} v^{1/3} / (f/f_{\min}) \quad [6]$$

where N is Avogadro's number, v is the experimental viscosity increment and f/f_{\min} is the observed frictional ratio. The value of β , which is typically about 2.15×10^6 for the average globular protein, varies only slightly with axial ratio for prolate ellipsoids and practically not at all for oblate ellipsoids (see Table I).

It is interesting to evaluate predictions based on hydrodynamic methods using proteins whose structures have been determined by other techniques. With electron microscopy as a standard, Erickson (1982) concluded that strict interpretation of hydrodynamic results can lead to serious overestimation of axial ratios when average hydration values (~0.3 g/g) are used. Squire and Himmel (1979) compared hydrodynamic and X-ray structural data for

21 proteins and calculated an average hydration of 0.53 ± 0.26 g/g. It can be argued that these higher values of "hydration" are actually just correlation coefficients relating the two structural methods. As such, they would include not only the effects of bound water, but also those of surface irregularities and any deficiencies in the model used. It is clear from studies like these that a semi-empirical approach, in which the protein in question is compared to known proteins with similar physical properties, is the safest way in which to interpret hydrodynamic data.

E. AIM OF THE PROJECT

Structural knowledge of troponin and its subunits is vital to a complete understanding of thin filament regulation. Although this knowledge could probably best be obtained from a complete X-ray crystallographic investigation, the prospects for such an analysis are not good due to the practical difficulties involved in working with these proteins. TN-I and TN-T, in particular, are relatively difficult to purify and are only reluctantly solubilized in non-denaturing media. For this reason, a project was undertaken to examine the structures of these regulatory proteins in solution using hydrodynamic techniques. The choice of bovine cardiac, as opposed to skeletal, troponin is a reflection of our recent interest in

this muscle system. Much of the current information about the physico-chemical properties of the bovine cardiac proteins has been obtained in our laboratory (Burtnick, 1977; Hincke, 1981). The present project is, in a sense, a continuation of this pioneering work.

Research for this thesis fell naturally into three separate categories. Initially, the hydrodynamic properties of native, undissociated troponin were examined (Chapter III). This was followed by a similar investigation of the individual troponin subunits (Chapters IV-VI). Finally, this approach was extended to the characterization of binary and ternary complexes of the subunits (Chapter VII). Most of the material presented in this thesis has either been published or accepted for publication (Byers et al., 1979; Byers and Kay, 1982 a,b,c).

CHAPTER II

EXPERIMENTAL PROCEDURES

A. PROTEIN PREPARATION

1. Purification of Troponin and its Subunits

The starting material for all preparative work was crude cardiac troponin (37-55% ammonium sulfate fraction) isolated either by the LiCl extraction procedure of Tsukui and Ebashi (1973) or by the muscle powder method (Murray and Kay, 1971). Modifications introduced by Burtnick (1977) were included in these procedures and both methods yielded final products of equal purity.

Native cardiac troponin was purified using a single ion-exchange chromatography step. Crude troponin dialyzed vs 20 mM Tris-Cl, 0.5 mM DTT (pH 7.8) was centrifuged to remove any precipitate and applied to a DEAE-Sephacel column equilibrated with the same buffer. The column was eluted with a linear 0-0.4 M KCl gradient in 20 mM Tris-Cl, 0.5 mM DTT (pH 7.8). Fractions containing troponin were pooled, dialyzed extensively vs 20 mM NH₄HCO₃, 0.1 mM DTT and lyophilized. All preparative operations were carried out at 4°C.

Individual subunits were isolated from crude troponin by DEAE-Sephadex A25 chromatography in 6 M urea as previously described (Burtnick et al., 1975a). TN-C was further purified by ion-exchange chromatography on DEAE-Sephadex (Hincke, 1981) while CM-Sephadex chromatography in 6 M urea was used to separately purify TN-I (Burtnick et al., 1975b) and TN-T (Burtnick et al., 1976). These chromatography steps were occasionally repeated to improve purity.

Alternatively, TN-T and TN-I were purified by hydroxylapatite chromatography. Lyophilized protein was dissolved in and dialyzed vs 6 M urea, 0.1 M NaCl, 1 mM Na-phosphate, 0.5 mM DTT (pH 7). This material was applied to a Biogel HTP column equilibrated with the starting buffer. The column was eluted with a linear 1-200 mM (for TN-T) or 1-120 mM (for TN-I) Na-phosphate gradient at 20°C. The appropriate fractions were pooled, desalted on a Biogel P2 column (100 × 5 cm) in 2% formic acid and lyophilized. The Biogel HTP column was regenerated in situ by washing with several column volumes of 6 M urea, 1 M NaCl, 0.4 M Na-phosphate followed by the starting buffer.

Carboxamidomethylated TN-I (CMC-TN-I) was prepared from cardiac TN-I and iodoacetamide by the method of Hincke et al. (1979). Amino acid analysis revealed essentially complete modification of both cysteine residues.

2. Preparation of Analytical Samples

All analytical experiments were performed in a buffer system consisting of 50 mM MOPS, 1 mM EGTA, 1 or 2 mM DTT and either KCl (KMED buffer) or NaCl (NMED buffer). The salt concentration is specified before the buffer abbreviation, i.e. 0.2 M NMED buffer contains 0.2 M NaCl. Unless otherwise indicated, all experiments were conducted at pH 7.2 and buffers representing the "plus Ca²⁺" state also contained 2 mM CaCl₂ (about 1 mM free Ca²⁺). All analytical solvents were millipored (0.8 µ filter) prior to use.

The more soluble proteins (native troponin and TN-C) were dissolved directly in the analytical solvent and dialyzed at least 24 h at 4°C. On the other hand, TN-I and TN-T were initially dissolved in 6 M urea, 0.5 M NMED and dialyzed vs the analytical buffer at 4°C. Due to the susceptibility of TN-I and TN-T to proteolytic degradation, only buffers containing NaCl were used for these proteins so that samples could be analyzed by SDS polyacrylamide gel electrophoresis following selected experiments.

All analytical samples were clarified by centrifugation on a Beckman Model L centrifuge (20 min, 50,000 g).

B. ABSORBANCE SPECTROPHOTOMETRY

Protein concentrations were determined using a Cary 118C recording spectrophotometer with quartz cuvettes (0.2-1.0 cm pathlength). Spectra were recorded between 250 nm and 320 nm for this purpose but no attempt was made to correct for light scattering unless this effect was unduly large. Absorbance measurements were done as soon as possible after dialysis in order to minimize the absorbance errors resulting from any increased oxidation of DTT in the protein sample relative to the dialyzate. Routine absorbance measurements were performed using a Gilford 240 spectrophotometer.

C. SDS POLYACRYLAMIDE GEL ELECTROPHORESIS

Standard methodology was employed for SDS gel analysis of protein composition (Shapiro et al., 1967; Weber and Osborn, 1969). Protein samples were dissolved in 2% SDS containing 10 mM DTT and heated for 5 min in a boiling water bath. Bromophenol Blue (a dye marker) and urea (to increase the density) were also added to the samples. Electrophoresis was performed on 10 or 15% polyacrylamide gels for 3-5 h at 6 mamp/tube. The gels were stained with Coomassie Brilliant Blue for 30 min and destained in several changes of 7.5% methanol, 7% acetic acid (by volume). The

gels were scanned at 600 nm on a Gilford 250 Spectrophotometer equipped with a Gilford Linear Transport Scanner. The recordings were photocopied onto heavier paper and the peaks were cut out and weighed to determine relative quantities of the troponin subunits.

D. ULTRACENTRIFUGAL ANALYSES

Ultracentrifugal studies were performed at 20°C in a Beckman Spinco Model E analytical ultracentrifuge equipped with an RTIC temperature-control unit and electronic speed control. Rayleigh interference and schlieren optics were employed for most investigations although the photoelectric scanner was also used for preliminary work. Optical alignment and focussing was carried out according to manufacturer's instructions and sapphire windows were used in all experiments.

1. Sedimentation Velocity

Sedimentation coefficients were measured at 60,000 rpm from schlieren photographs taken at constant time intervals. Aluminum synthetic-boundary or charcoal-filled Epon centerpieces (12 or 30 mm) were used for these experiments. In studies designed to examine the effect of Ca^{2+} on native troponin or TN-C, data were collected for both plus and minus Ca^{2+} states in a single run using two

cells and a 1° positive-wedge window. These samples were prepared by adding small aliquots of water or 0.2 M CaCl₂ to the protein solution immediately prior to the run.

Sedimentation coefficients (*s*) were calculated by measuring the distance (*r*) between the center of rotation and the maximum ordinate of the schlieren gradient as a function of time (*t*) according to:

$$s = \left(\frac{1}{\omega^2}\right) \left(\frac{d \ln r}{dt}\right) \quad [7]$$

where ω is the angular velocity in radians per second. The value of *s*, expressed in Svedberg units (1 S = 10⁻¹³ s), was calculated from the slope of a ln *r* vs *t* plot and was then corrected to the standard conditions of water at 20°C (Svedberg and Pedersen, 1940) by:

$$s_{20,w} = s \left(\frac{\eta_T}{\eta_{20,w}} \right) \left(\frac{\eta}{\eta_w} \right)_T \left(\frac{1 - \bar{v} \rho_{20,w}}{1 - \bar{v} \rho_T} \right) \quad [8]$$

where $(\eta_T/\eta_{20})_w$ is the ratio of the viscosity of water at the experimental temperature (*T*) to that at 20°C, $(\eta/\eta_w)_T$ is the viscosity correction factor of the solvent relative to water at the temperature, *T*, $\rho_{20,w}$ is the density of water at 20°C, ρ_T is the density of the solvent at T°C, and \bar{v} is the partial specific volume of the protein. Viscosity and density values used in sedimentation calculations were

either measured experimentally or taken from the Handbook of Chemistry and Physics.

The Stokes radius ($R_{s, \text{sed}}$) of an unknown protein was calculated from the extrapolated value of $s_{20,w}$ at infinite dilution ($s_{20,w}^0$) by the relationship:

$$R_{s, \text{sed}} = M_r(1 - \bar{v}\rho)/(6N\pi n_0 s_{20,w}^0) \quad [9]$$

where M_r is the molecular weight, \bar{v} is the partial specific volume, ρ is the solvent density, N is Avogadro's number, and n_0 is the solvent viscosity in poise.

Schlieren peaks were integrated by tracing magnified (10 \times) photographic images from the microcomparator onto paper; the peaks were then cut out and weighed.

2. Sedimentation Equilibrium

Weight-average molecular weights were measured using either meniscus depletion (Yphantis, 1964) or conventional low-speed (Richards et al., 1968) sedimentation equilibrium techniques. Double-sector charcoal-filled Epon centerpieces (12 mm) and Rayleigh interference optics were employed in these experiments. Equilibrium photos were taken at periodic intervals after 20 h until no further change was apparent. Following certain experiments, the integrity of the protein sample was checked by SDS polyacrylamide gel

electrophoresis and the effective DTT concentration was determined by the procedure of Ellman (1959).

Meniscus depletion experiments were carried out according to the basic methodology reviewed by Teller (1973) on samples with protein concentrations less than 1 mg/ml. Optimal rotor speeds were selected from graphical data (Teller, 1973) and no attempt was made to decrease the time required to reach equilibrium by overspeeding. Periodically, baseline linearity of the interference fringe pattern was checked following an experiment by performing a separate run (1,400 rpm, 30 min) after shaking the rotor in order to destroy thermal and concentration gradients in the cell (Teller, 1973).

Protein samples for conventional equilibrium experiments were dialyzed at least 48 h at 4°C to ensure complete equilibration (Casassa and Eisenberg, 1964). Initial protein concentrations (c_0) of these samples were determined in duplicate using synthetic boundary runs (Richards et al., 1968). In this procedure, the dialyzate (0.40 ml) was layered onto the protein solution (0.12 ml) by centrifugation at 8,000 rpm and several photos of the boundary were taken. The number of fringes crossed horizontally between the solvent and solution plateau regions, which is directly proportional to the protein concentration, was determined for each photo and back-

extrapolated to the beginning of the run. For molecular weight calculations, c_0 was expressed in length units by multiplying the fringe count by the average vertical distance between fringes. Equilibrium experiments were then performed with 0.1 ml of the protein solution, using rotor speeds chosen from graphical data (Chervenka, 1969).

Equilibrium photographs were measured manually at a magnification of 50 \times . Several vertical readings of fringe displacement (y) were taken at equally-spaced horizontal points (x), where x and y were set to zero at the meniscus. In meniscus depletion experiments, x -intervals of no more than 100 μ were used while intervals of 200 μ were employed in conventional equilibrium runs. These intervals typically allowed the collection of 20 to 40 x - y data points across the cell. The horizontal x -readings were converted to values of radial distance (r) using the position of the counterbalance reference hole ($r = 7.28$ cm) and the camera magnification factor.

The apparent weight-average molecular weight (M_w) was calculated from the protein concentration (c) as a function of r according to:

$$M_w(r) = \left[\frac{2RT}{(1 - \frac{v_p}{\omega})^2} \right] \left(\frac{d \ln c(r)}{dr^2} \right) \quad [10]$$

where R is the universal gas constant, T is the experimental temperature (K), \bar{v} is the partial specific volume of the protein, ρ is the solvent density and ω is the angular velocity. In meniscus depletion experiments, the concentration at a given region in the cell is usually assumed to be proportional to the vertical fringe displacement (y) relative to the meniscus, at which point the concentration is considered to be zero due to the high rotor speed. In practice, the true meniscus concentration (c_m) was determined by an iterative procedure (Teller, 1973), using the initial x-y data points. The refined value of c_m , usually in the order of 5-15 μ , was then added to the original y values to give the actual concentration. For the calculation of M_w , all data with y less than 100 μ (~ 0.1 mg/ml) were discarded. The meniscus concentration for conventional equilibrium experiments was calculated using the initial protein concentration (c_o) by the equation:

$$c_m = c_o - \left[\frac{\frac{r_b^2(c_b - c_m)}{r_m^2} - \int_{c_m}^{c_b} r^2 dc}{(r_b^2 - r_m^2)} \right] \quad [11]$$

where the subscripts m and b refer to values at the cell meniscus and the cell bottom, respectively. The concentration at any point r was then obtained by adding the value of c_m to the value of y at that point.

All molecular weight calculations were carried out by computer using programs written in the APL language (Wolodko, 1974). The $\ln c$ vs r^2 data were fitted to a 2nd-degree polynomial equation using least-squares techniques and the point-average M_w values were calculated (Equation 10) from the slope of this equation.

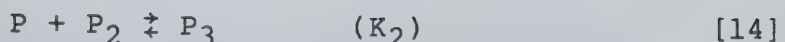
Sedimentation equilibrium data were used to estimate protein association parameters for monomer-polymer and isodesmic indefinite types of association as outlined by Van Holde (1975). The general monomer-polymer reaction is described by:

$$nP \not\propto P_n \quad [12]$$

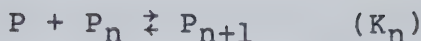
where n is the degree of association of the protein (P). The association constant (K_a) for this reaction was calculated from the experimental weight-average molecular weight (M_w) as a function of concentration (c), according to:

$$Q/[1-(Q/(n-1))]^n = K_a (n-1) c^{n-1} \quad [13]$$

where $Q = (M_w/M_1) - 1$ and M_1 is the monomer molecular weight. An indefinite association of the form:



⋮ ⋮



is considered to be isodesmic if $K_1 = K_2 = \dots = K_n$, etc.

The experimental data were treated for this type of reaction according to:

$$(M_w/M_1)^2 - 1 = 4 K_a c \quad [15]$$

If the association is ideal, a plot of the left hand side of Equation 13 or 15 vs the appropriate concentration term on the right hand side will be linear for the correct model of association and the value of K_a can thus be determined from the slope.

3. Extinction Coefficients

New and altered preparative methods for cardiac troponin subunits have been developed since the original work of Burtnick (1977). Therefore, the extinction coefficients of these proteins, and of native troponin, were reevaluated in order to provide a reliable basis for concentration determination. New values were established

using the refractometric method of Babul and Stellwagen (1969), in which the absorbance of a protein sample is correlated with its weight concentration, the latter determined from synthetic boundary experiments in the ultracentrifuge. An average refractive increment of 4.1 fringes/mg/ml was used in these calculations. The accuracy of the method was checked with standard proteins (ribonuclease and BSA) and the experimental extinction coefficients were found to be within 2% of the literature values. Theoretical extinction coefficients were also calculated from the tyrosine and tryptophan content, using molar extinction values for these amino acids in both water and ethanol*. These solvents were chosen to represent the environments in the protein exterior and interior, respectively, thus giving an expected range of extinction coefficients.

E. ANALYTICAL GEL CHROMATOGRAPHY

Gel filtration experiments were performed at room temperature ($21 \pm 2^\circ\text{C}$) in silicone-treated columns packed with either Biogel A 1.5 m (100/200 mesh, BioRad) or Sephadryl S-300 Superfine (Pharmacia). Column packing was

* CRC Handbook of Biochemistry and Molecular Biology, Proteins, vol. 1)

carried out according to manufacturer's instructions after the gel had been equilibrated with starting buffer and degassed under vacuum. Flow rate was maintained during all column operations with a peristaltic pump (Perista). Elution volumes were determined gravimetrically, followed by collection of 0.4 ml fractions in the region of interest. For samples with initial protein concentration greater than 1 mg/ml, fractions were monitored by absorbance at 276 nm, while the dye binding assay of Bradford (1976) was used for more dilute samples.

Gel filtration columns were calibrated with respect to Stokes radius (R_s) using protein standards chosen from the following list: β -galactosidase, 69 Å (de Riel and Paulus, 1978); catalase, 52 Å (Siegel and Monty, 1966); lactate dehydrogenase, 41 Å (de Riel and Paulus, 1978); BSA, 35 Å (Siegel and Monty, 1966); ovalbumin, 28.4 Å (Henn and Ackers, 1969; Martenson, 1978; Pharmacia calibration kit); α -chymotrypsinogen, 21.9 Å (Dedman et al., 1977; Pharmacia calibration kit); myoglobin, 19.8 Å (Henn and Ackers, 1969; Dedman et al., 1977); cytochrome c, 17.2 Å (Siegel and Monty, 1966; Henn and Ackers, 1969). In cases of discrepancy between published R_s values for a given protein standard, the numerical average was used. All gel standards (between 4 and 9 were employed for each column) and protein samples were run individually and elution volumes were

reproducible to within at least 0.2 ml. The void volume (V_O) and total included volume (V_T) were measured with Blue dextran 2000 (Pharmacia) and potassium chromate, respectively. Elution volumes (V_e) were estimated by interpolation of the peak position (Andrews, 1965) and were used to calculate the partition coefficient (σ) by the relationship:

$$\sigma = (V_e - V_O)/(V_T - V_O) \quad [16]$$

The Stokes radius of an unknown protein sample ($R_{S,gel}$) was then calculated from a standard curve of $\log R_S$ vs σ (Siegel and Monty, 1966).

In reconstitution experiments, column fractions were analyzed for troponin subunit composition using SDS polyacrylamide gel electrophoresis. Pooled fractions were treated with an equal volume of 20% trichloroacetic acid and centrifuged. The precipitated protein was dissolved in 100-200 μ l of 2% SDS, 50 mM unbuffered Tris, 10 mM DTT and prepared for electrophoresis as described earlier.

F. DENSITY MEASUREMENTS

Partial specific volumes of native troponin and TN-C were determined from precision density measurements

performed at 20°C using a digital density meter of the mechanical oscillator type (Kratky et al., 1973). This instrument consisted of a processing unit and an external measuring cell (Anton Paar DMA 60 and DMA 601, respectively). Prior to density measurements, the cell was cleaned with a solution of 3N HCl/50% ethanol, rinsed with water and methanol, and finally air-dried. Protein samples for these experiments were extensively dialyzed for at least 48 h.

The period of oscillation (T) of the vibrating cell was measured for at least 20 min following the injection of solvent or sample (1.0 ml). Individual readings of T , each one displayed after 20,000 oscillations (about 70 s), were averaged. The density difference ($\rho_2 - \rho_1$) between two arbitrary solutions is related to the difference in the measured time periods by the equation:

$$\rho_2 - \rho_1 = A(T_2^2 - T_1^2) \quad [17]$$

where A is a constant. The value of A was established experimentally using dry air ($\rho = 0.001205$ g/ml) and water ($\rho = 0.998196$ g/ml) and was then used to calculate the densities of solvent and protein solutions from Equation 17 using the corresponding values of T . Instrument performance was checked with solutions of sucrose and BSA; the observed

densities were within 0.01% of expected values in each case.

Density data were used to calculate the partial specific volume (\bar{v}) of the solute according to:

$$\bar{v} = \frac{1}{\rho_0} \left(1 - \frac{\rho - \rho_0}{c} \right) \quad [18]$$

where ρ_0 and ρ are the densities of the solvent and protein solutions, respectively, and c is the protein concentration in g/ml.

Partial specific volumes were also estimated from the amino acid compositions of troponin and its subunits as described by Cohn and Edsall (1943). For sedimentation equilibrium experiments conducted in 6 M urea, the value of \bar{v} used was decreased by 0.01 ml/g to correct for the reduction of excluded volume effects in this solvent (Kay, 1960).

G. VISCOMETRY

Viscosity measurements were conducted at 20°C using a Cannon-Manning semimicroviscometer with a water flow time of about 530 s. Temperature in these experiments was controlled to within 0.01°C with a viscosity water bath (Scientific Development Co.). Dust contamination was avoided by washing the viscometer and all sample handling

apparatus, such as pipettes, cuvettes and sample tubes, with chromic acid followed by rinsing with water and methanol.

In a typical experiment, measurements were performed on 3 or 4 samples (0.5 ml) obtained by sequential dilution of the most concentrated sample. Several flow time readings, normally reproducible to within 0.2 s, were taken for each sample after allowing about 10 min for thermal equilibration. The reduced kinematic viscosity (η_{red}) was calculated by:

$$\eta_{red} = (t - t_0) / (t_0 c) \quad [19]$$

where t_0 and t are the flow times of the solvent and protein solution, respectively, and c is the protein concentration in g/ml. In cases where the dependence of reduced viscosity on protein concentration allowed a reasonably accurate extrapolation of η_{red} to zero concentration, the data were treated according to:

$$\eta_{red} = [\eta]_u + k' [\eta]_u^2 c \quad [20]$$

where $[\eta]_u$ is the uncorrected intrinsic viscosity and k' is the dimensionless Huggins coefficient. The values of $[\eta]_u$ were corrected for the difference in density between solvent and protein solution (Tanford, 1955) to give the true

intrinsic viscosity [η]. This adjustment generally amounts to an increase in [η] of about 0.3 ml/g.

H. HYDRODYNAMIC ANALYSIS

Many of the hydrodynamic relationships used have already been presented in the Introduction (Equations 1-6). Translational frictional ratios (f/f_{\min}) were calculated from the experimental Stokes radii obtained by sedimentation velocity ($R_{s,\text{sed}}$) or gel filtration ($R_{s,\text{gel}}$) using Equation 2. The frictional ratio contribution due to asymmetry (f/f_0) was determined from Equation 3. The degree of hydration (w) was estimated from the amino acid composition (Kuntz and Kauzmann, 1974), using amino acid hydration values determined from NMR measurements on frozen solutions. No correction was made to account for the expected relative exposure of each type of amino acid on the protein surface (Chothia, 1975). The estimated hydration values were also used to calculate the shape factor (v_a) from the intrinsic viscosity (Equation 5).

Axial ratios for both prolate and oblate ellipsoids were interpolated from f/f_0 and v_a values using Table I. This tabulated data is based on equations for the frictional resistance experienced by ellipsoids of revolution undergoing translational (Perrin, 1936), or rotational (Simha, 1940) motion in solution. Additional comparison was

made by using the Scheraga-Mandelkern β -function (Scheraga and Mandelkern, 1953) defined in Equation 6 (see Table I).

In favourable cases, unhydrated protein dimensions were predicted from axial ratio values using prolate and oblate models. The maximum dimension (length or width) for an ellipsoid was evaluated from:

length (prolate)

$$\underline{\text{or}} \quad = 2 R_o (r_1^2 r_2)^{1/3} \quad [21]$$

width (oblate)

where r_1 is the ratio of the longest axis to the intermediate axis and r_2 is the ratio of the intermediate axis to the shortest axis. For a prolate ellipsoid, r_1 is the axial ratio and r_2 is unity, while for an oblate ellipsoid, r_2 is the axial ratio and r_1 is unity.

I. MISCELLANEOUS METHODS

The following methods were used to compare the quality of protein preparations to published standards. The reader is referred to more detailed accounts of the procedures employed.

1. Circular Dichroism

Circular dichroism measurements were carried out using a Cary 60 recording spectropolarimeter with a Cary 6001 circular dichroism attachment, as described by Oikawa et al. (1968). The far ultraviolet region (200–250 nm) was used exclusively in these studies. The mean residue ellipticity ($[\theta]_{\lambda}$), at a given wavelength (λ) was calculated from the equation:

$$[\theta]_{\lambda} = \frac{\theta_{\text{obs}}^{\text{MRW}}}{100 l c} \quad [22]$$

where θ_{obs} is the observed ellipticity at the wavelength (λ), MRW is the mean residue weight (assumed to be 115 in these studies), l is the cell pathlength in dm and c is the protein concentration in g/ml.

2. Amino Acid Analysis

Amino acid analyses were performed as described by Moore and Stein (1963) using a Durrum D500 or D502 (Dionex) automated amino acid analyzer. Samples were hydrolyzed for at least 24 h in constant-boiling 6N HCl with 1% phenol included to limit tyrosine degradation.

3. Biological Activity Assays

The biological activity of native troponin was checked using a synthetic cardiac actomyosin assay system as

outlined by Burtnick et al. (1975b). This assay system contained 750 μ g synthetic actomyosin and 50 μ g tropomyosin in 2.5 mM ATP, 2.5 mM MgCl₂, 25 mM Tris-Cl, and 1 mM EGTA (pH 8). The hydrolysis of ATP was followed by monitoring the release of inorganic phosphate (Fiske and SubbaRow, 1925).

CHAPTER III

HYDRODYNAMIC PROPERTIES OF NATIVE TROPONIN

A. RESULTS

1. Preparation of Troponin

The 37-55% ammonium sulfate fraction obtained from a LiCl extraction of bovine cardiac muscle (Tsukui and Ebashi, 1973) consists primarily of the three troponin subunits, as demonstrated by SDS polyacrylamide gel electrophoresis (Burtnick, 1977). However, there are also a large number of minor proteins present which might be expected to interfere with a biophysical investigation. Thus, it was considered necessary to further purify native cardiac troponin, preferably without disrupting interactions within the complex. This was achieved by ion-exchange chromatography on DEAE-Sephadex (Figure 7): troponin eluted in a sharp peak at a KCl concentration of about 0.3 M at pH 7.8. SDS gels of this material revealed essentially three major components (Figure 7, inset), corresponding in migration to the subunits of cardiac troponin (Burtnick, 1977). A faint protein band of apparent molecular weight 23,000 was also invariably present; densitometric scans of SDS gels indicated that this component represents less than 3% of the

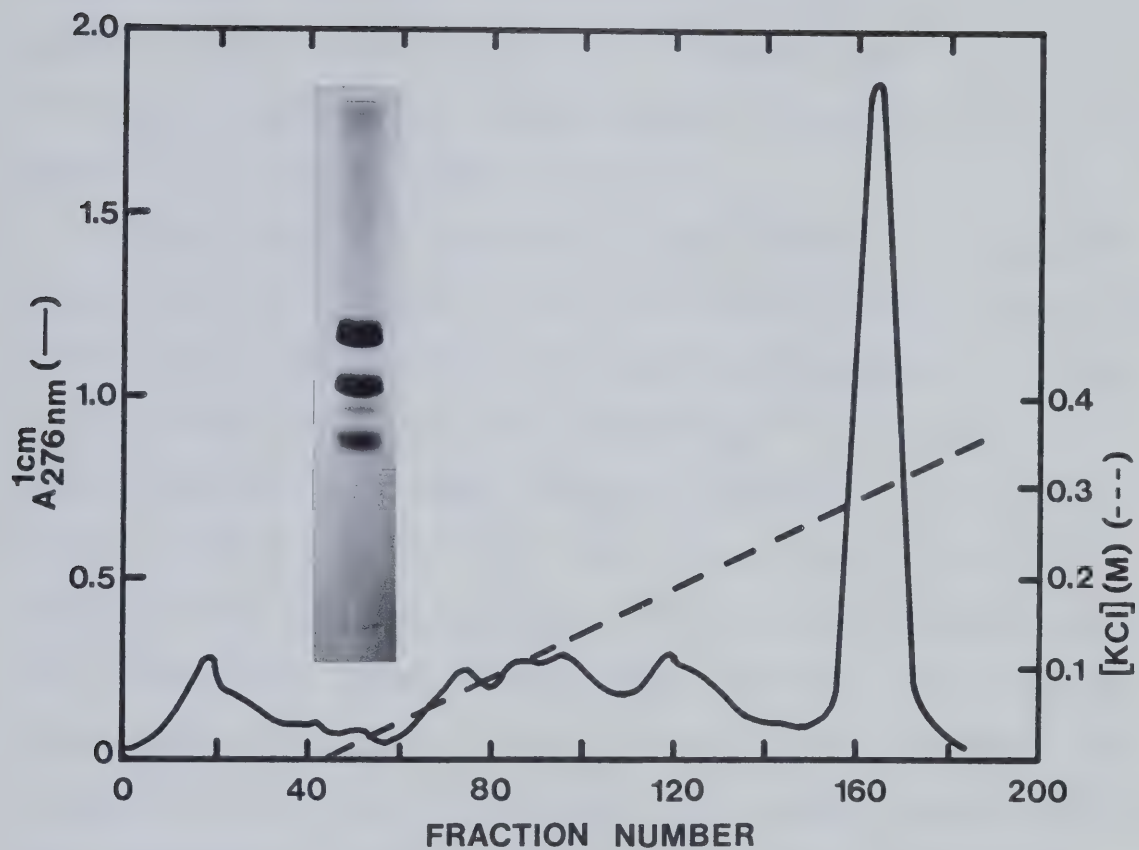


Figure 7. Purification of troponin on DEAE-Sephadex. Crude troponin (1.1 g) in 20 mM Tris-Cl, 0.5 mM DTT at pH 7.8 was applied to the column (30×3 cm) and eluted with a linear 0-0.4 M KCl gradient (1 litre total). The flow rate was 50 ml/h and 6 ml fractions were collected. The yield of lyophilized troponin was 270 mg. Inset: SDS polyacrylamide gel of the major fraction.

total protein. Attempts to remove this impurity by either gel filtration or hydroxylapatite chromatography in non-denaturing solvents were unsuccessful, suggesting that this component is tightly bound to troponin.

Cardiac troponin purified in this manner was stable for several days in solution at 20°C and for at least 3 years in lyophilized form at -20°C. The average ellipticity (222 nm) of this material was -14,000 deg cm² dmol⁻¹, similar to values reported from other circular dichroism studies with native (Lin and Cassim, 1978) and reconstituted (Burtnick and Kay, 1976) cardiac troponin. The amino acid composition (see Chapter VII, Table V) was also consistent with expected values (Burtnick, 1977; Lin and Cassim, 1978). Addition of troponin (200 µg) to a biological assay system consisting of 750 µg synthetic cardiac actomyosin and 50 µg tropomyosin resulted in 50% inhibition of ATP hydrolysis in the absence of Ca²⁺. The inhibition which is similar to that reported earlier with reconstituted cardiac troponin (Hincke et al., 1977), was almost fully (96%) reversed by adding 2 mM Ca²⁺. The extinction coefficient for a 1% solution of troponin in a 1 cm pathlength cell at 277 nm ($E_{277 \text{ nm}}^{1\%, 1 \text{ cm}}$) was 4.4 ± 0.1 (average of 13 samples), determined by refractometry in the ultracentrifuge. This value is in good agreement with the range of values calculated from the aromatic amino acid content, 3.8 (in water) to 4.4 (in

ethanol), assuming 10 tyrosine and 3 tryptophan residues per molecule (Burtnick, 1977).

2. Partial Specific Volume

The partial specific volume (\bar{v}) of native troponin was determined from precision density measurements of rigorously-dialyzed protein solutions. No dependence of \bar{v} on protein concentration was observed. The value of \bar{v} for troponin in 0.2 M KMED (pH 7.2), in the absence of Ca^{2+} , was $0.710 \pm 0.002 \text{ ml/g}$ (average of 9 samples). There was no significant change in \bar{v} ($0.708 \pm 0.001 \text{ ml/g}$, 3 samples) when 2 mM Ca^{2+} was present in the solution.

3. Molecular Weight

Conventional and meniscus depletion sedimentation equilibrium techniques were used to examine the molecular weight behaviour of native troponin (Figure 8). The apparent weight-average molecular weight (M_w) of troponin in 0.2 M KMED (pH 7.2) increased as a function of protein concentration, varying from about 100,000 to 300,000 over the concentration range examined. The limiting value of M_w (80,000), obtained by extrapolation to zero protein concentration, is indistinguishable from the combined molecular weights of the cardiac troponin subunits (78,000). The M_w data were sensitive to rotor speed and initial loading concentration as the results from different

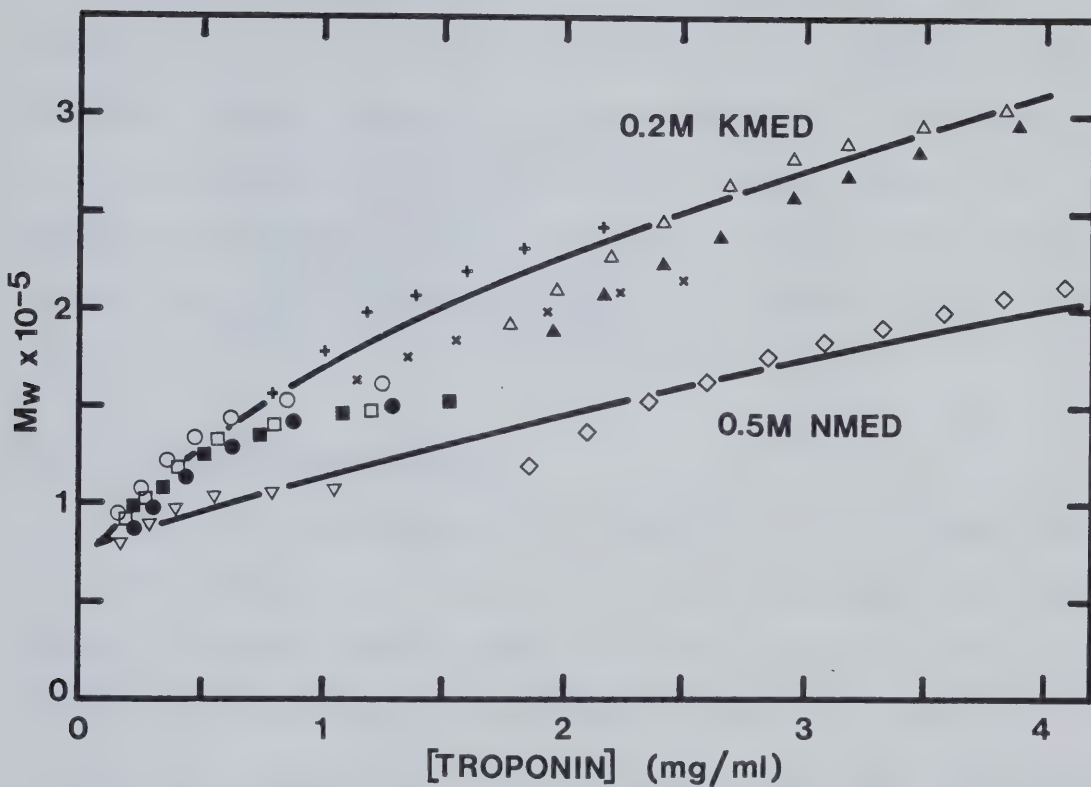


Figure 8. Effect of protein concentration on the molecular weight of troponin. Conventional and meniscus depletion sedimentation equilibrium experiments were performed on samples of troponin in 0.2 M KMED or 0.5 M NMED at pH 7.2. Most runs were recorded with interference optics although two scanner experiments in 0.2 M KMED ($-Ca^{2+}$) are also included (+, x). The solid lines were visually drawn through the data. Initial protein concentrations and equilibrium rotor speeds were: (○, ●) 0.58 mg/ml, 16,000 rpm; (□, ■) 1.1 mg/ml, 14,000 rpm; (Δ) 2.53 mg/ml, 3,600 rpm; (\blacktriangle) 2.78 mg/ml, 3,600 rpm; (+) 1.35 mg/ml, 4,800 rpm; (x) 2.0 mg/ml, 4,800 rpm; (∇) 0.98 mg/ml, 17,000 rpm; (\diamond) 2.8 mg/ml, 4,800 rpm. Open symbols: $-Ca^{2+}$; closed symbols: $+2 mM Ca^{2+}$.

experiments did not always overlap completely. Thus, the significance of the slight decrease in M_w observed when 2 mM Ca^{2+} was added (Figure 8) is questionable. Increasing the ionic strength of the solvent (0.5 M NMED) reduced the degree of aggregation of troponin but did not appear to alter the limiting value of M_w at low concentration (Figure 8).

4. Sedimentation Velocity

Schlieren photographs of troponin in 0.2 M KMED (pH 7.2) did not exhibit a single, symmetrical peak but rather a bimodal boundary consisting of a major leading peak and a smaller trailing peak or shoulder (Figure 9, inset). Integration of the schlieren boundary revealed that the size of the leading peak increases with total protein concentration while that of the slower component remains relatively constant (Figure 9).

The effect of varying protein concentration on the sedimentation coefficients ($s_{20,w}$) of the two peaks is shown in Figure 10. The value of $s_{20,w}$ for the major peak decreased dramatically at troponin concentrations below 2 mg/ml, whereas $s_{20,w}$ for the trailing peak was more or less independent of concentration. The small size of this shoulder made accurate estimation of $s_{20,w}$ difficult, but least squares treatment of the data gave an intrinsic value ($s_{20,w}^0$) of 3.5-4.0 S. Addition of 2 mM Ca^{2+} to troponin in

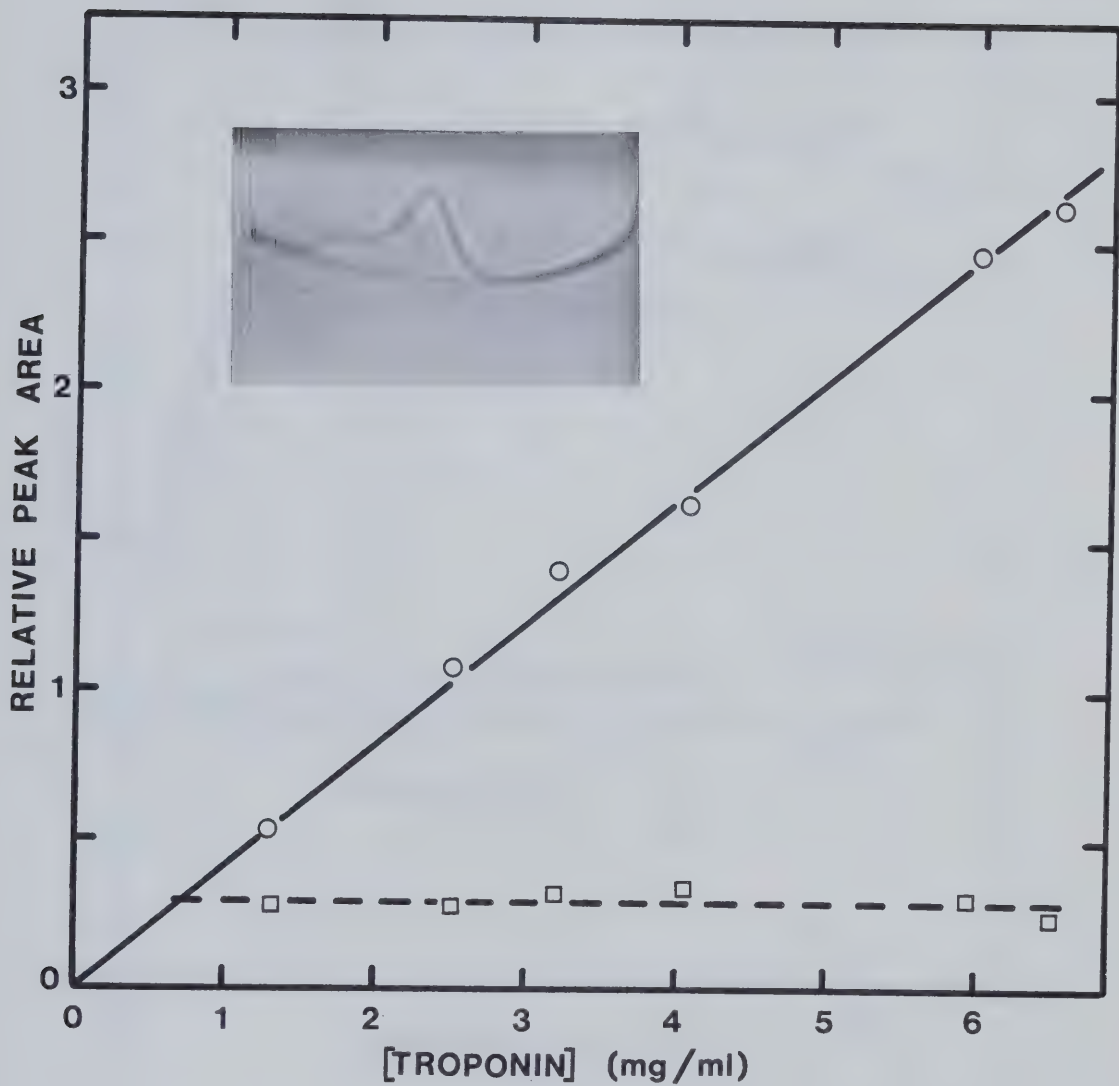


Figure 9. Integration of schlieren peaks for troponin in 0.2 M KMED ($- \text{Ca}^{2+}$) at pH 7.2. Traced peaks from photos taken at 50 min were weighed to determine relative areas. (—), total area; (---), area of trailing peak. Inset: schlieren photograph of troponin (4.1 mg/ml, $- \text{Ca}^{2+}$) taken at 50 min.

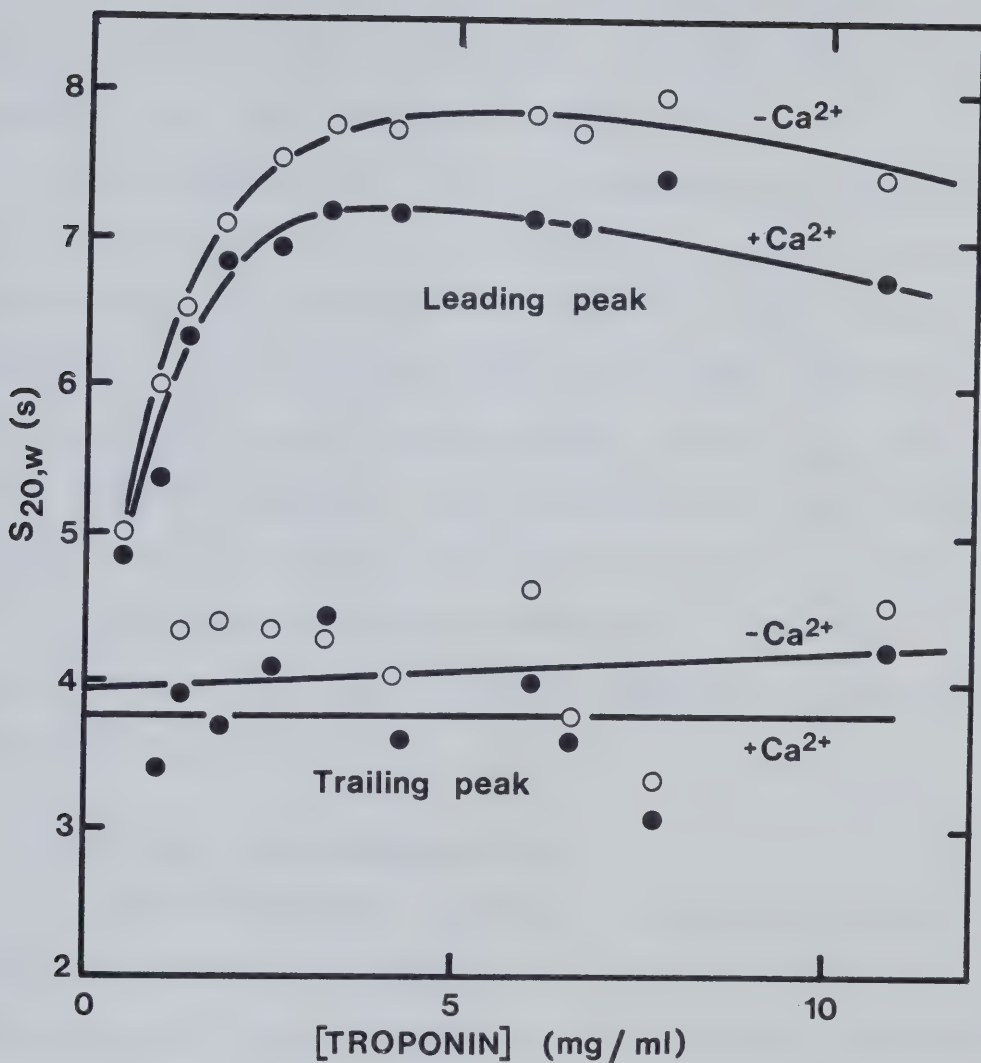


Figure 10. Effect of protein concentration on the sedimentation coefficient of troponin. Troponin samples (0.5 ml) in 0.2 M KMED (pH 7.2) were sedimented at 60,000 rpm and schlieren photos were taken at 16 min intervals. Double sector cells of width 12 mm were used except at the two lowest protein concentrations (30 mm cells). Ca^{2+} concentrations were: (○) no Ca^{2+} , (●) 2 mM Ca^{2+} .

0.2 M KMED resulted in a small but definite decrease in $s_{20,w}$ for the major component but no significant effect was noted for the trailing peak (Figure 10).

The sedimentation velocity behaviour of troponin was also sensitive to the ionic strength, pH and temperature of the solvent, as indicated in Table II. The relative magnitude of the trailing peak became more prominent with increasing pH and KCl concentration, while $s_{20,w}$ for the major peak was reduced. The sedimentation coefficient of troponin was also decreased when the temperature was lowered to 4°C, although a detailed comparison is perhaps unjustified because of the large temperature corrections required to calculate $s_{20,w}$ from runs at 4°C.

5. Analytical Gel Chromatography

Due to the apparent tendency of cardiac troponin to aggregate, gel filtration was used to study the physical properties at very low protein concentrations. Figure 11 illustrates a representative Sephadryl S-300 calibration curve constructed with globular proteins of known Stokes radii. Troponin in 0.2 M KMED (pH 7.2) eluted in a single, symmetrical peak and the apparent Stokes radius ($R_{s,gel}$) increased with the concentration of the applied sample (Figure 12). This observation suggests that troponin undergoes a concentration-dependent aggregation. The limiting value of $R_{s,gel}$ was about 52 Å, estimated from runs

TABLE II: EFFECTS OF pH, IONIC STRENGTH AND TEMPERATURE ON THE SEDIMENTATION COEFFICIENT (LEADING PEAK) OF TROPONIN^a

| Buffer (- Ca ²⁺) | $s_{20,w}$ (S) |
|----------------------------------|----------------|
| 0.2 M KMED (pH 7.2) | 7.06 |
| 0.2 M KMED (pH 6.7) | 7.65 |
| 0.2 M KMED (pH 7.7) | 6.77 |
| 0 M KMED (pH 7.2) ^b | 7.58 |
| 0.5 M KMED (pH 7.2) | 5.30 |
| 1.0 M KMED (pH 7.2) | 5.30 |
| 0.2 M KMED (pH 7.2) ^c | 6.53 |

^aThese experiments were done as described in the text and in the legend to Figure 10. Protein concentrations were 4.3-4.5 mg/ml.

^bThe concentration refers to KCl, all other buffer components being constant.

^cThis experiment was performed at 4°C.

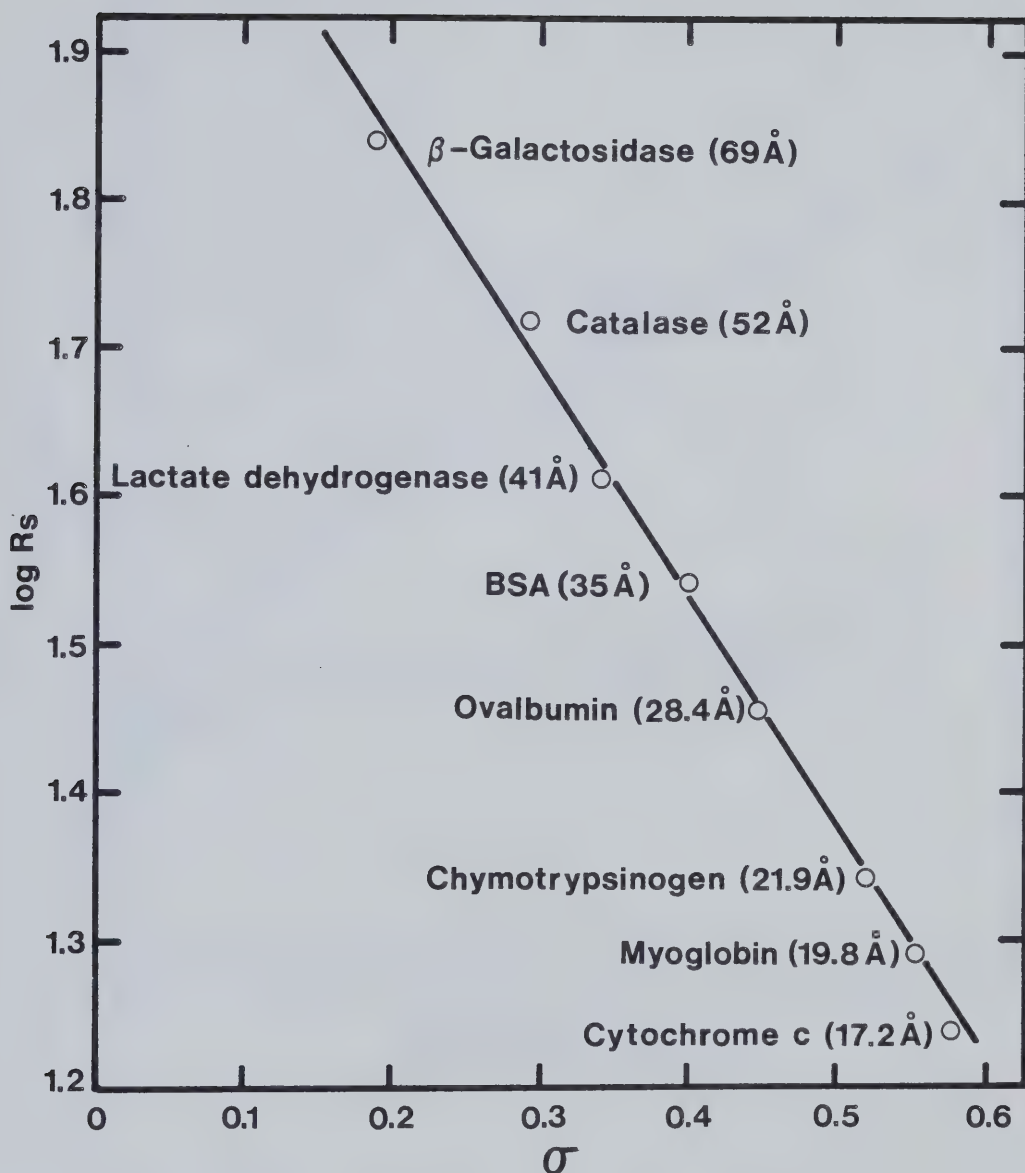


Figure 11. Calibration curve of standard proteins on Sephadryl S-300. Samples (300 μl) in 0.2 M KMED (pH 7.2) were applied to a 74 \times 1.1 cm column. Flow rate was 15 ml/h and 0.4 ml fractions were collected. Partition coefficients (σ) were calculated from the peak elution volumes.

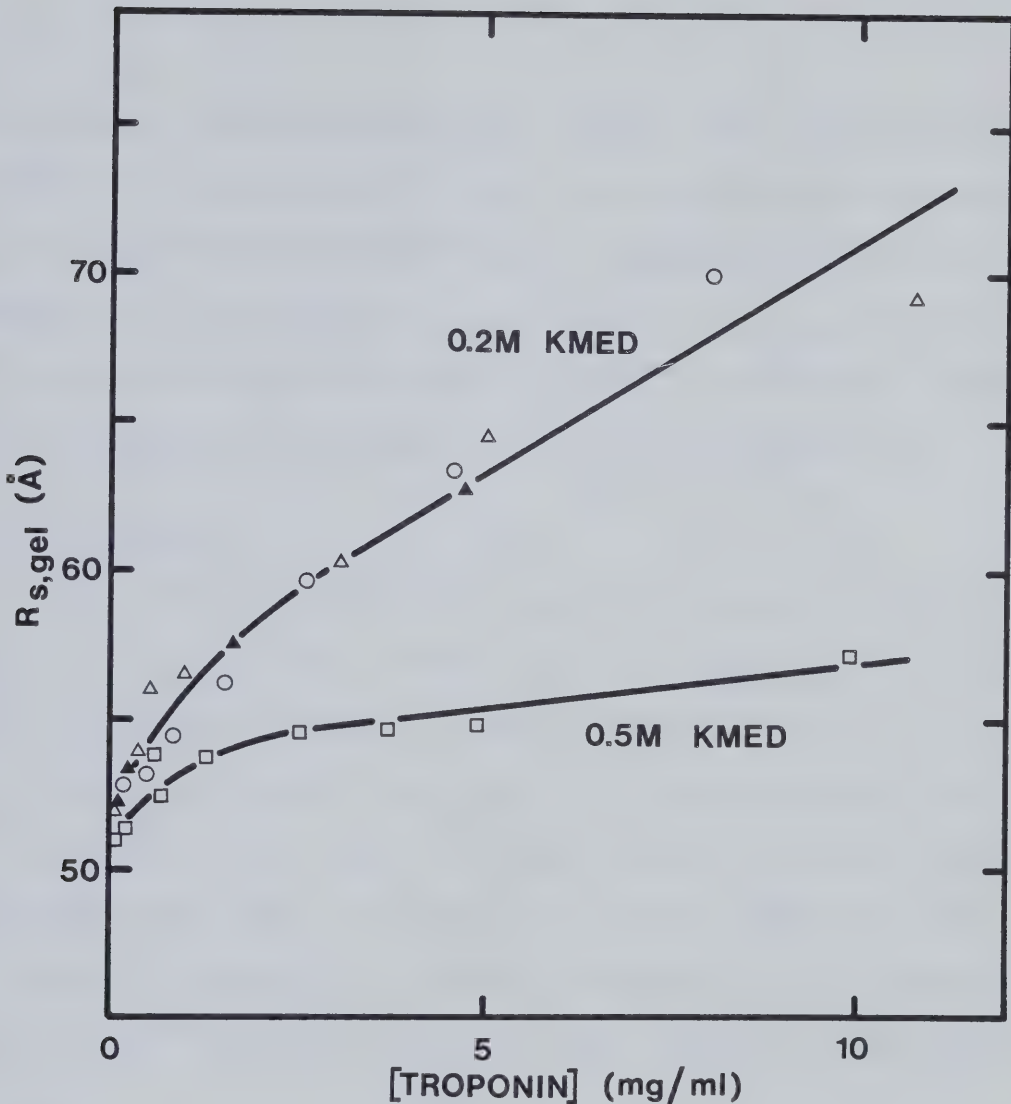


Figure 12. Effect of protein concentration on the apparent Stokes radius of troponin. Two types of gel filtration columns were used: (a) Sephadryl S-300 (74×1.1 cm) in 0.2 M (○) or 0.5 M (□) KMED (pH 7.2). Flow rate: 15 ml/h. (b) Biogel A 1.5 m (55×0.9 cm) in 0.2 M KMED at pH 7.2 (Δ, \blacktriangle). Flow rate: 6 ml/h. Samples ($300 \mu\text{l}$) at the concentrations indicated were applied and 0.4 ml fractions were collected. Ca^{2+} concentrations were: (○, □, Δ) no Ca^{2+} , (\blacktriangle) 2 mM Ca^{2+} .

with very dilute samples (<5 µg/ml). The presence of 2 mM Ca²⁺ had no appreciable effect on the elution properties of either the protein standards or troponin samples in 0.2 M KMED. In 0.5 M KMED, the dependence of $R_{s,gel}$ on sample concentration was decreased, although no apparent change in the limiting $R_{s,gel}$ value was observed (Figure 12).

6. Viscosity

The reduced viscosity (η_{red}) of troponin in 0.2 M KMED (pH 7.2) exhibited a marked biphasic dependence on protein concentration (Figure 13), behaviour not typical of normal monomeric proteins. η_{red} could not be accurately measured at concentrations below 0.5 mg/ml because of the increased experimental error in dilute solutions. However, the intrinsic viscosity of troponin appeared to be around 10 ml/g. Ca²⁺ produced no significant change in the values of η_{red} .

B. DISCUSSION

Whereas both skeletal and cardiac troponin subunits have been fairly well-characterized, relatively little attention has been directed towards the parent molecule: the native troponin complex. This neglect has undoubtedly resulted from the difficulty in achieving clean preparations, free of endogenous proteases, without

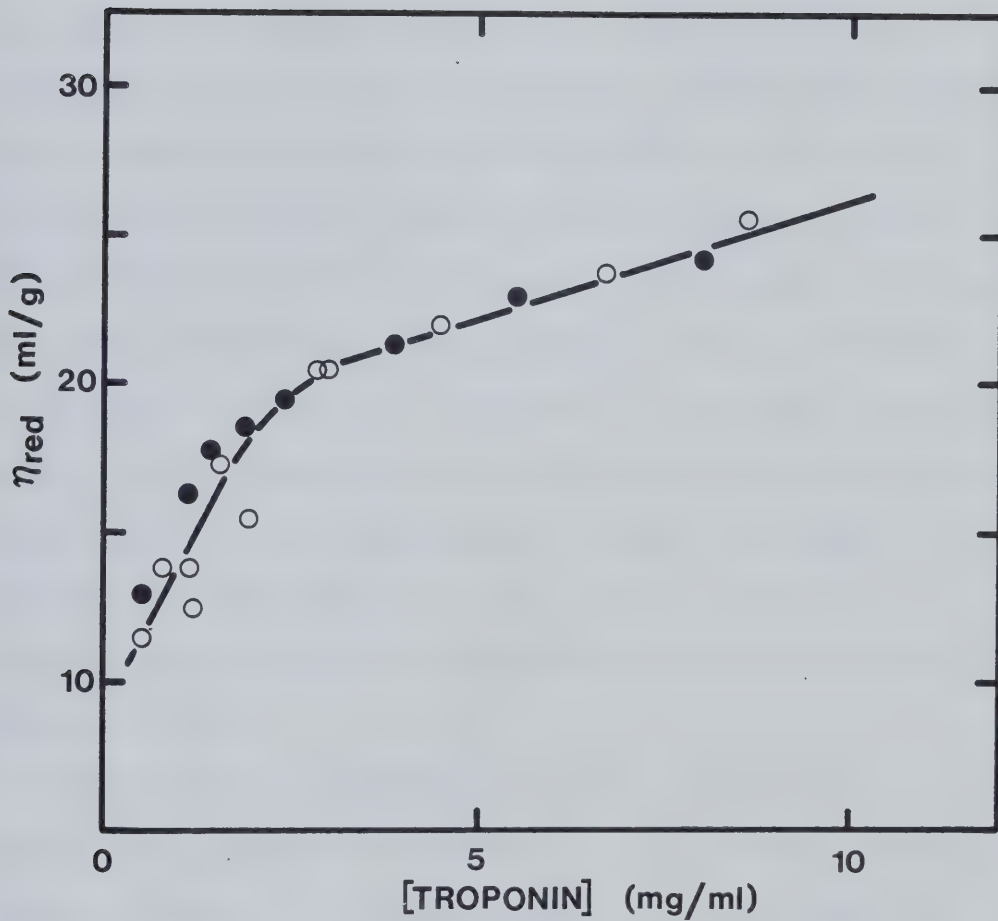


Figure 13. Viscosity of troponin in 0.2 M KMED (pH 7.2). Reduced viscosity (η_{red}) was measured for samples (0.5 ml) in the absence (○) or presence (●) of 2 mM Ca^{2+} .

resorting to denaturing conditions. The situation is particularly grim with respect to cardiac muscle because of the high proteolytic activity and large number of contaminants present in this tissue (Tsukui and Ebashi, 1973). Cardiac troponin purified using the present methodology (Figure 7) is at least as pure as other reported preparations (Brekke and Greaser, 1976; Stull and Buss, 1977; Lin and Cassim, 1978; Potter, 1982). The only significant impurity not removed, a tenacious protein of apparent molecular weight 23,000, has also been observed by other workers. It has been attributed to a degradation product of TN-T (Ebashi et al., 1974b) or to an intramolecular disulfide-linked form of TN-I (Brekke and Greaser, 1976).

The detailed hydrodynamic investigation of any protein requires an accurate knowledge of its partial specific volume. Errors in the estimation of \bar{v} are magnified substantially in the calculation of molecular weights and hydrodynamic parameters. In many cases \bar{v} is calculated from the amino acid composition (Cohn and Edsall, 1943), with the assumption that the amino acid specific volumes are additive. Although this approach generally gives good results, and is certainly easier than experimental measurement, it ignores the dependence of \bar{v} on the three dimensional structure of the protein. For example, the

electrostriction of water around charged groups on the protein surface will tend to decrease the partial specific volume (Cohn and Edsall, 1943) while any "excluded volumes", or solvent-inaccessible pockets in the folded polypeptide chain, will result in an increase in \bar{v} (Linderstrom-Lang, 1950). The dangers inherent in the above procedure are especially evident in the case of native cardiac troponin: the calculated value of \bar{v} (0.727 ml/g) is significantly higher than the observed value (0.710 ml/g), determined by densitometry. Thus, it would seem that electrostriction influences the partial specific volume of troponin, a result not unexpected in view of the large number of charged amino acid residues in the protein. Using methodology identical to ours, Lovell and Winzor (1977) demonstrated that bovine skeletal troponin also exhibits a relatively low value of \bar{v} , ranging from 0.715 ml/g (0.1 M KCl) to 0.680 ml/g (1.0 M KCl) at pH 7.

The aggregating tendency of troponin was evident in every type of experiment performed. The high molecular weight of the protein in 0.2 M KMED (Figure 8) is probably due to a concentration-dependent reversible association rather than an irreversible aggregation since the observed values of M_w generally increased with initial loading concentration in different sedimentation equilibrium experiments. Moreover, troponin eluted from gel filtration

columns in a single peak, with a Stokes radius markedly dependent on sample concentration. On the other hand, the presence of two or more distinct non-interacting proteins, such as troponin monomer and its aggregate(s), would be expected to result in multiple gel filtration peaks with $R_{s,gel}$ values corresponding to the individual molecules.

In light of this conclusion, the bimodal schlieren profiles observed in sedimentation velocity experiments might appear to be somewhat confusing. However, complex sedimentation boundaries have been noted for many reversible protein associations, even when the rates of interconversion are much faster than the rates of separation of the different species (Cann, 1970). In particular, Gilbert (1955) has theoretically predicted sedimentation behaviour remarkably similar to that depicted in Figures 9 and 10, for rapid-equilibrium protein associations of the type $nP \rightleftharpoons P_n$, where $n > 2$. According to these predictions, which neglect the spreading effects of diffusion, a single schlieren peak is observed at very low protein concentrations. As the total sample concentration is increased, the size of this peak also increases proportionately until a critical concentration (Δ_s) is reached, above which this peak remains constant in area and in $s_{20,w}$. A second, faster-moving peak appears which continues to increase in size and velocity with total protein concentration. The equilibrium constant

(K_a) for a given degree of polymerization (n) is related to the size of the small trailing peak (Δ_s) according to:

$$K_a = \Delta_s^{1-n} [2(n^2-1)]^{n-1} (n-2)/[n(2n-1)]^n \quad [23]$$

It should be noted that neither of the peaks rigorously correspond to any distinct macromolecular entity, although in practice the movement of the slower peak is usually taken to approximate $s_{20,w}$ for the monomer (Cann, 1970).

Skeletal troponin apparently also undergoes self-association, based on velocity and equilibrium sedimentation observations (Wakabayashi and Ebashi, 1968; Lovell and Winzor, 1977). There is, however, one important difference between the skeletal and cardiac proteins. Lovell and Winzor (1977) have reported substantial dissociation of bovine skeletal troponin into subunits at protein concentrations below 1 mg/ml. In contrast, no evidence of cardiac troponin dissociation was observed (Figure 8): M_w was larger than the expected monomer value (78,000), even at the lowest concentrations examined (~0.1 mg/ml). This was also true at a higher ionic strength (0.5 M), as demonstrated by the limiting behaviour of M_w (Figure 8) and $R_{s,gel}$ (Figure 12) in dilute protein solutions. It is still possible that troponin dissociates into subunits at concentrations too low to be detected by these techniques.

Sedimentation equilibrium experiments can often be used to gain insight into the modes and parameters of protein association reactions (Van Holde, 1975). M_w vs concentration data for troponin in 0.2 M KMED (- Ca²⁺) were analyzed according to the monomer-polymer (Equation 12) and isodesmic indefinite (Equation 14) types of association. The results for representative trial models are shown in Figure 14. The best fit, over the entire data range, is obtained for the isodesmic model and the association constant (K_a) calculated from Equation 15 is 0.93 ml/mg. However, a monomer-pentamer association cannot be ruled out because of the excellent agreement in the association constants estimated for this model from both equilibrium and velocity sedimentation results. The value of K_a (0.68 ml⁴/mg⁴) derived from the linear portion of the curve shown in Figure 14B is virtually identical to the value (0.65 ml⁴/mg⁴) calculated from schlieren photos (see Equation 23, above) where $\Delta_s = 0.6$ mg/ml (Figure 9). Analogous treatment of the M_w data for troponin in 0.5 M NMED (Figure 15) also yields a good fit for the isodesmic model ($K_a = 0.31$ ml/mg). The speculative nature of these predictions must be emphasized due to the large degree of scatter in the molecular weight data (Figure 8) and the exclusion of non-ideality in the treatment. Nevertheless, the key point to note is that the self-association of troponin is reduced at

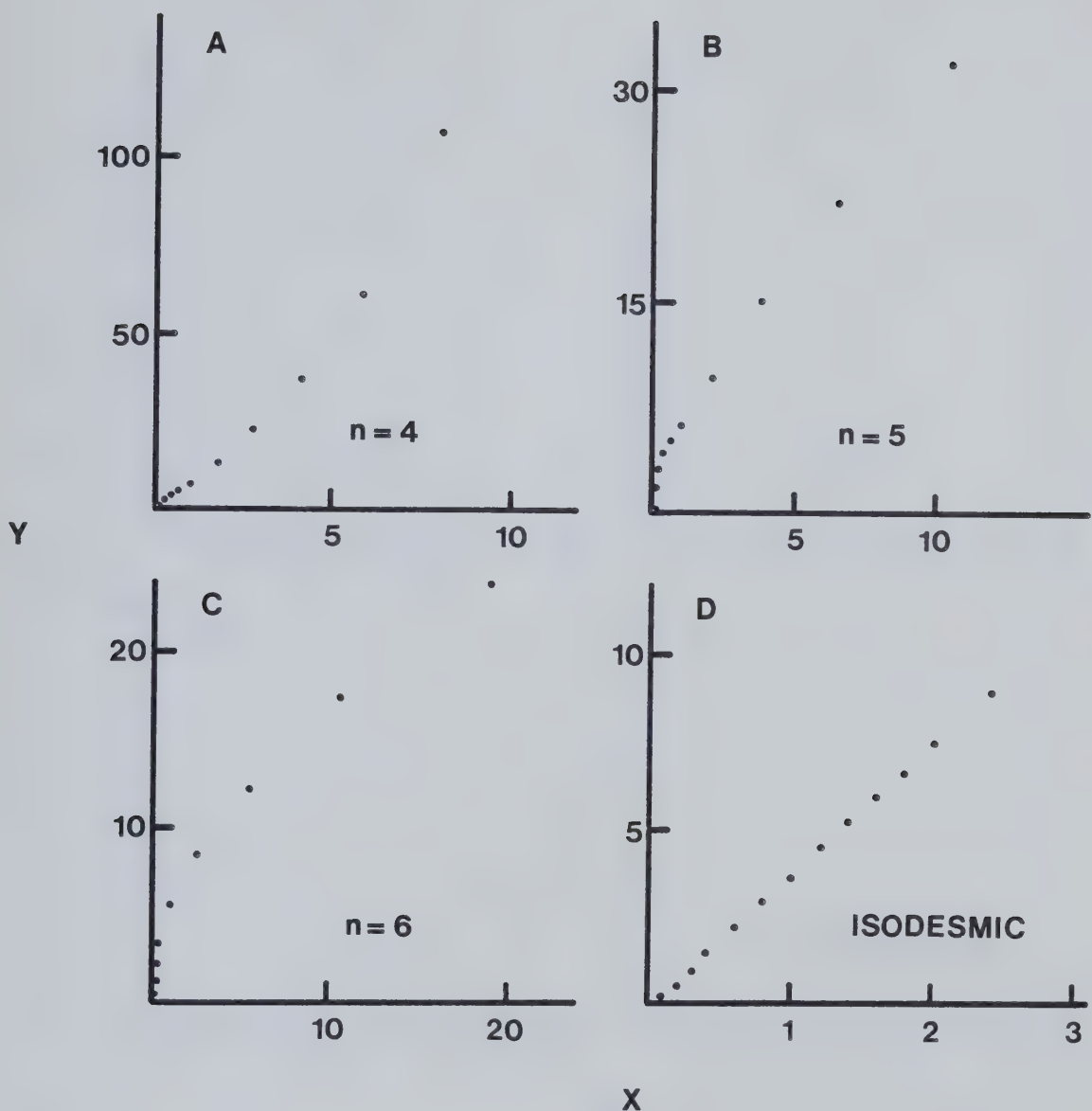


Figure 14. Protein association models for troponin in 0.2 M KMED ($- \text{Ca}^{2+}$) at pH 7.2. M_w vs concentration data from Figure 8 (solid line) were treated according to Equations 13 and 15, where the coordinates X and Y are defined. Panels A-C: monomer-n-mer association (Equation 12). Panel D: isodesmic indefinite association (Equation 14). The monomer molecular weight (M_1) was taken as 78,000.

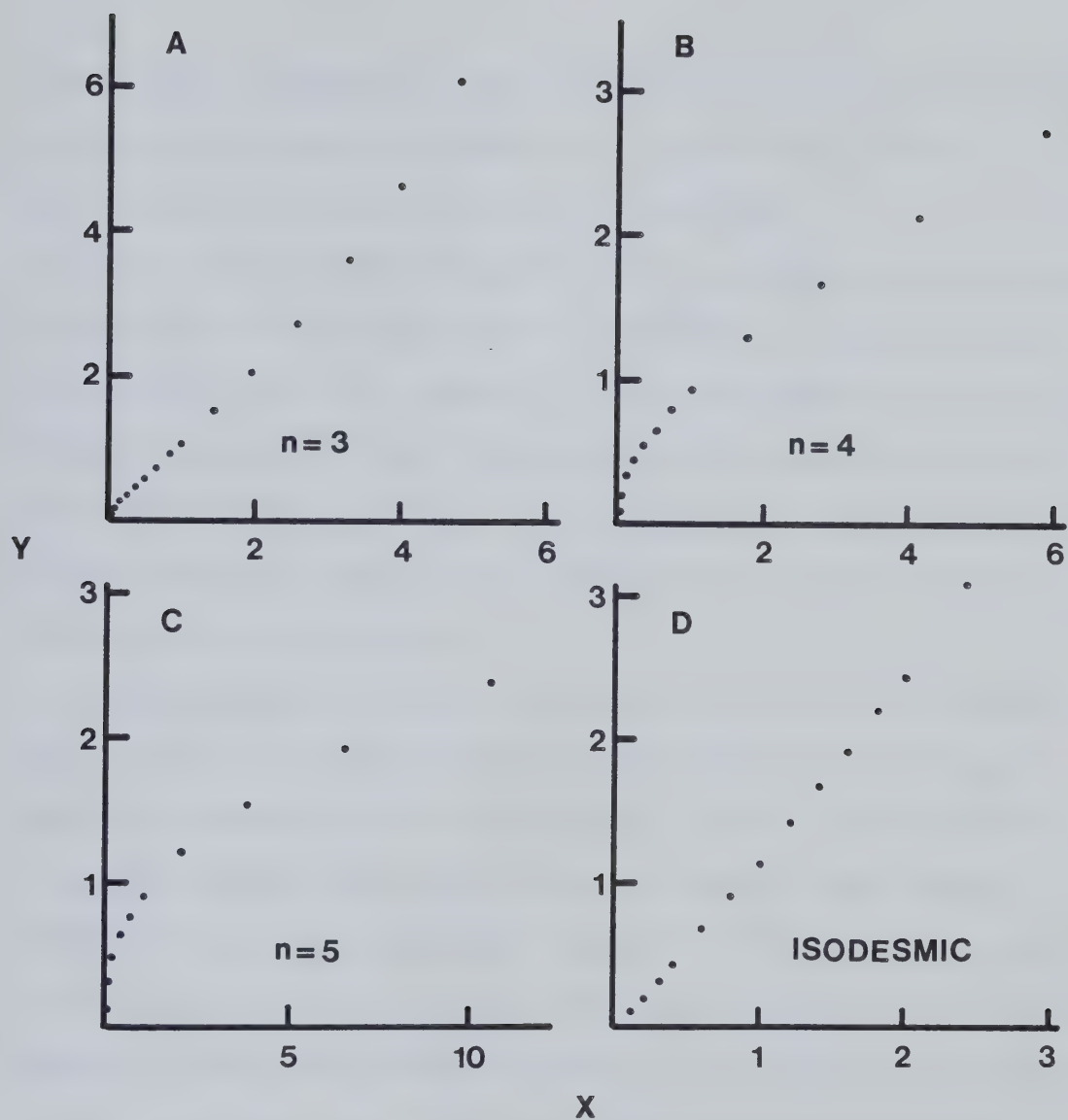


Figure 15. Protein association models for troponin in 0.5 M NMED (pH 7.2). M_w vs concentration data from Figure 8 (solid line) were treated according to Equations 13 and 15, where the coordinates X and Y are defined. Panels A-C: monomer-n-mer association (Equation 12). Panel D: isodesmic indefinite association (Equation 14). The monomer molecular weight (M_1) was assumed to be 78,000.

higher ionic strength. This is supported by the sedimentation velocity results (Table II), which also indicate a similar effect upon raising the pH of the solvent. These observations suggest a role of electrostatic attractions in the aggregation of cardiac troponin. Such attractions would be expected to become less prominent at higher pH values, since troponin already possesses a net negative charge at pH 7.2. Comparable ionic strength and pH effects have also been seen with bovine skeletal troponin (Lovell and Winzor, 1977).

Hydrodynamic analysis of cardiac troponin is complicated by the self-association of the protein, since most physical parameters can be measured only at concentrations in which a number of macromolecular species may coexist. Analytical gel chromatography appears to be the sole technique capable of determining the Stokes radius at troponin concentrations sufficiently dilute to suppress this aggregation. Assuming the limiting value of $R_{s,gel}$ (52 Å) corresponds to monomeric troponin ($M_r = 78,000$, $R_o = 28 \text{ \AA}$), the translational frictional ratio (f/f_{min}) is 1.85 (Equation 2). Since the range of f/f_{min} for most globular proteins is 1.15-1.30, this value indicates that troponin is an unusually asymmetric molecule. This conclusion is illustrated by noting that the limiting $R_{s,gel}$ of troponin is identical to that of the gel standard catalase ($R_s = 52 \text{ \AA}$,

Figure 11), a much larger protein ($M_r = 250,000$).

Substituting $R_{S,gel}$ (52 Å) for $R_{S,sed}$ in Equation 9, the theoretical sedimentation coefficient of troponin can be estimated. The resulting value of $s_{20,w}$ (3.8 S) is close to that observed for the slower peak in the sedimentation velocity experiments (Figure 10). Additional support for the asymmetry of troponin is provided by the viscosity data (Figure 13); the relatively high reduced viscosity of troponin (>10 ml/g) is substantially larger than the values (3-5 ml/g) normally exhibited by globular proteins. Hydrodynamic behaviour consistent with an asymmetric molecule has also been observed for skeletal troponin (Sperling et al., 1979).

Structural information about proteins can generally be obtained from the frictional ratio if the contribution from hydration is known. The degree of hydration (w), calculated from the amino acid composition, is 0.49 g/g troponin. This value is consistent with average protein hydration values determined by correlating hydrodynamic and X-ray structural data (Squire and Himmel, 1979). Using this estimate of w , the frictional ratio due to asymmetry alone (f/f_0 , calculated from Equation 3) is 1.56. This corresponds to a prolate ellipsoid of axial ratio 10 (total length ~ 270 Å) or to an oblate ellipsoid of axial ratio 13 (total width ~ 130 Å) (see Table I and Equation 21). Although accurate

determination of the intrinsic viscosity of troponin was hampered by aggregation, the estimated value of this parameter ($\sim 10 \text{ ml/g}$, Figure 13) is too low to be consistent with a strictly rod-like shape for the protein. If troponin were a long, thin molecule (i.e. a prolate ellipsoid of axial ratio 10), it would exhibit a much larger value of $[\eta]$, in the range of 16-18 ml/g for $w = 0.5 \text{ g/g}$ (Equation 5). In any case, detailed structural predictions based on ellipsoidal models are probably not justified. After all, troponin is composed of three non-identical subunits and an ellipsoidal model is unlikely to be a valid representation. Any irregularities in the shape of the troponin complex would be expected to increase the frictional ratio above that due to asymmetry and hydration alone.

The present indication that cardiac troponin is an elongated, rather than a globular, molecule finds support in a number of independent investigations with the skeletal protein. Early electron microscopic evidence, which examined the binding of troponin to tropomyosin crystals (Higashi and Ooi, 1968) or Mg^{2+} -paracrystals (Nonomura et al., 1968), suggested that troponin is a globular protein, situated approximately one-third of the distance, or about 130 Å, from the C-terminus of tropomyosin (Stewart and McLachlan, 1976). This conclusion was supported by the

location of certain irregularities in the tropomyosin sequence (McLachlan and Stewart, 1976). However, immunoelectron microscopy studies by Oktsuki (1975,1979) have demonstrated that troponin binds over a much larger region of the thin filament. His experiments showed that while antibodies directed towards TN-I or TN-C do indeed bind at the location suggested earlier, TN-T antibodies form a broad band which covers the entire C-terminal third of the tropomyosin molecule. These observations have since been confirmed and extended by examining the interactions between various fragments of TN-T and tropomyosin (Pearlstone and Smillie, 1977, 1981; Mak and Smillie, 1981; Pato et al., 1981). This combined effort has resulted in a picture of troponin on the thin filament similar to that depicted in Figure 2. According to this conception, the bulk of the troponin molecule, including TN-C, TN-I and part of TN-T, is located about one-third of the distance from the C-terminus of tropomyosin, while another portion of TN-T extends to tropomyosin overlap region, over 100 Å away.

Very recently, a preliminary report has appeared in which rotary-shadowed skeletal troponin and TN-T have been directly visualized by electron microscopy (Flicker et al., 1979). Troponin apparently consists of both a globular and a rod-like domain, with a total length of 265 ± 40 Å. Images of TN-T suggest that this subunit comprises the tail

portion of the whole protein. Although the shape of troponin observed by electron microscopy is very similar to that predicted by the localization studies discussed in the paragraph above, the length of troponin estimated by this technique indicates that it could actually span up to two-thirds of the tropomyosin molecule. A more detailed investigation is probably required to ensure that troponin is neither unfolded nor aggregated under the conditions of these experiments. In any case, the hydrodynamic properties of cardiac troponin are consistent with an elongated, but not completely rod-like, molecule.

In view of the essential role of troponin in striated muscle regulation, the small effect of Ca^{2+} on the hydrodynamic properties of the protein is perhaps surprising. The gel filtration and viscosity behaviour were independent of Ca^{2+} , while a barely-significant decrease in M_w was observed. Only the sedimentation coefficient of the major schlieren peak was substantially altered when Ca^{2+} was added (Figure 10). As mentioned previously, however, this peak is not directly related to a specific macromolecular species. Taken together, these observations could be consistent with a slight Ca^{2+} -induced dissociation of troponin coupled with a minor increase in f/f_{\min} . The relative insensitivity to Ca^{2+} cannot be due to irreversible protein damage resulting from the method of preparation

since our troponin was completely active in a synthetic actomyosin assay system.

Other investigators have reported variable effects of Ca^{2+} on the structural properties of bovine cardiac troponin. No influence of Ca^{2+} on the secondary structure of the protein was detected in a circular dichroism study (Lin and Cassim, 1978), an observation also made in this investigation. On the other hand, an increase in thermal stability (Jacobson et al., 1981) and a decrease in sulphhydryl reactivity (Barskaya and Gusev, 1981) have suggested that cardiac troponin becomes a tighter, more compact molecule in the presence of Ca^{2+} . The results of the present study indicate, however, that these changes probably do not reflect a drastic conformational alteration at the level of the isolated troponin complex.

CHAPTER IV

HYDRODYNAMIC PROPERTIES OF TROPONIN-C

A. RESULTS

1. Partial Specific Volume

The partial specific volume of TN-C in 0.2 M KMED ($- \text{Ca}^{2+}$) at pH 7.2 was $0.701 \pm 0.003 \text{ ml/g}$ (average of 5 samples). This value was unchanged ($0.701 \pm 0.002 \text{ ml/g}$, 3 samples) in the presence of 2 mM Ca^{2+} . No dependence of \bar{v} on protein concentration was observed.

2. Molecular Weight

The molecular weight of TN-C in 0.2 M KMED (pH 7.2) was measured by conventional low-speed sedimentation equilibrium (Figure 16). In the absence of Ca^{2+} , the apparent molecular weight of TN-C decreased slightly as a function of protein concentration across the cell and the value of M_w extrapolated to zero protein concentration was 18,000. This value is similar to that calculated from the amino acid sequence of cardiac TN-C ($M_r = 18,459$, van Eerd and Takahashi, 1975), indicating that the subunit is monomeric under these conditions. This conclusion is not seriously altered by considering the non-ideality effects resulting from the large net charge (-28) of TN-C at pH 7. In 0.2 M

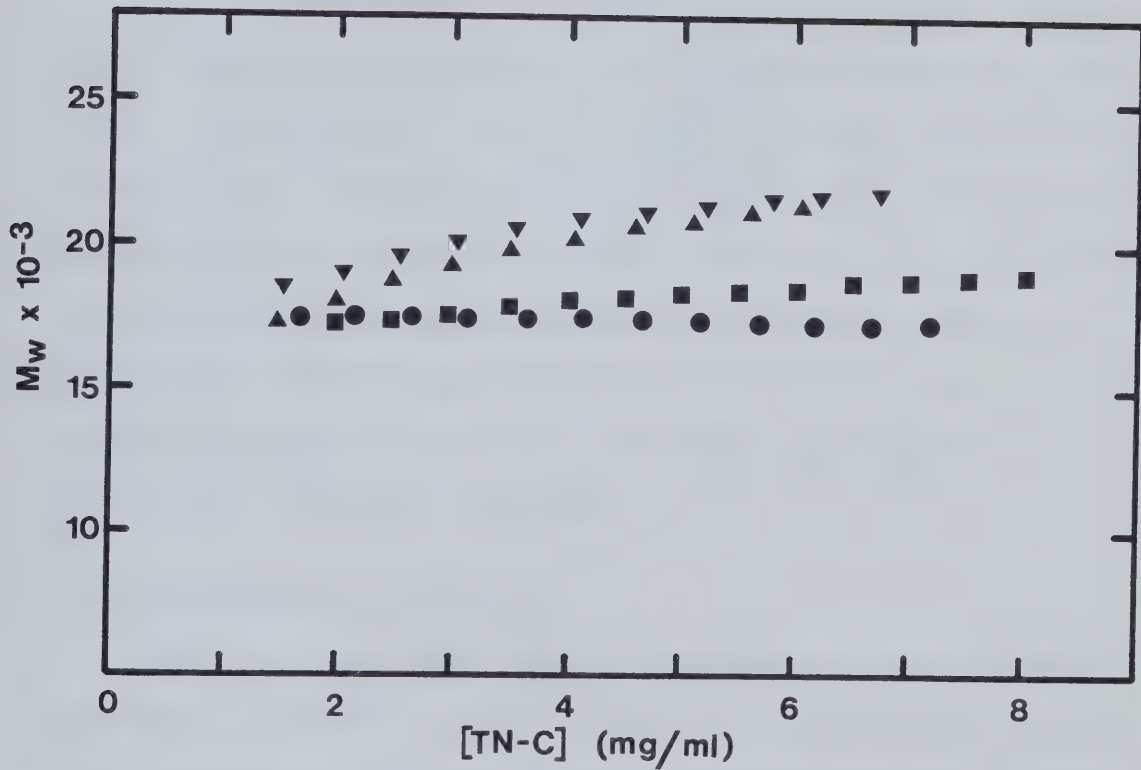


Figure 16. Effect of Ca^{2+} on the molecular weight of TN-C. Conventional sedimentation equilibrium experiments were conducted in 0.2 M KMED (pH 7.2) at an initial TN-C loading concentration of 4 mg/ml and a rotor speed of 18,000 rpm. Ca^{2+} concentrations were: (●) no Ca^{2+} , (■) 2 mM Ca^{2+} , (▲) 10 mM Ca^{2+} , and (▼) 25 mM Ca^{2+} .

KMED, this contribution would only amount to an observed decrease in M_w of about 2,000 at a TN-C concentration of 5 mg/ml (Margossian and Stafford, 1982).

In the presence of 2 mM Ca^{2+} , no significant increase in M_w was observed at concentrations below 4 mg/ml, although a small increase was noted at higher protein concentrations (Figure 16). Raising the Ca^{2+} concentration to 10 mM or 25 mM resulted in a more pronounced increase in M_w , although even at high TN-C concentrations the apparent molecular weight did not approach the dimer value of 37,000. The molecular weight behaviour of TN-C was unchanged when DTT was omitted from the solution.

3. Sedimentation Velocity

TN-C in 0.2 M KMED (pH 7.2) sedimented as a single, symmetrical schlieren peak, with $s_{20,w}^0$ decreasing slightly as a function of protein concentration (Figure 17). The extrapolated sedimentation coefficient ($s_{20,w}^0$) of TN-C in the absence of Ca^{2+} was 1.87 S. Addition of 2 mM Ca^{2+} produced a significant increase in $s_{20,w}^0$ to 2.04 S, suggesting that TN-C undergoes a conformational change to a more compact shape. The corresponding Stokes radii ($R_{s,\text{sed}}$) calculated from these $s_{20,w}^0$ values (Equation 9) are 26.2 Å (- Ca^{2+}) and 24.0 Å (+ Ca^{2+}).

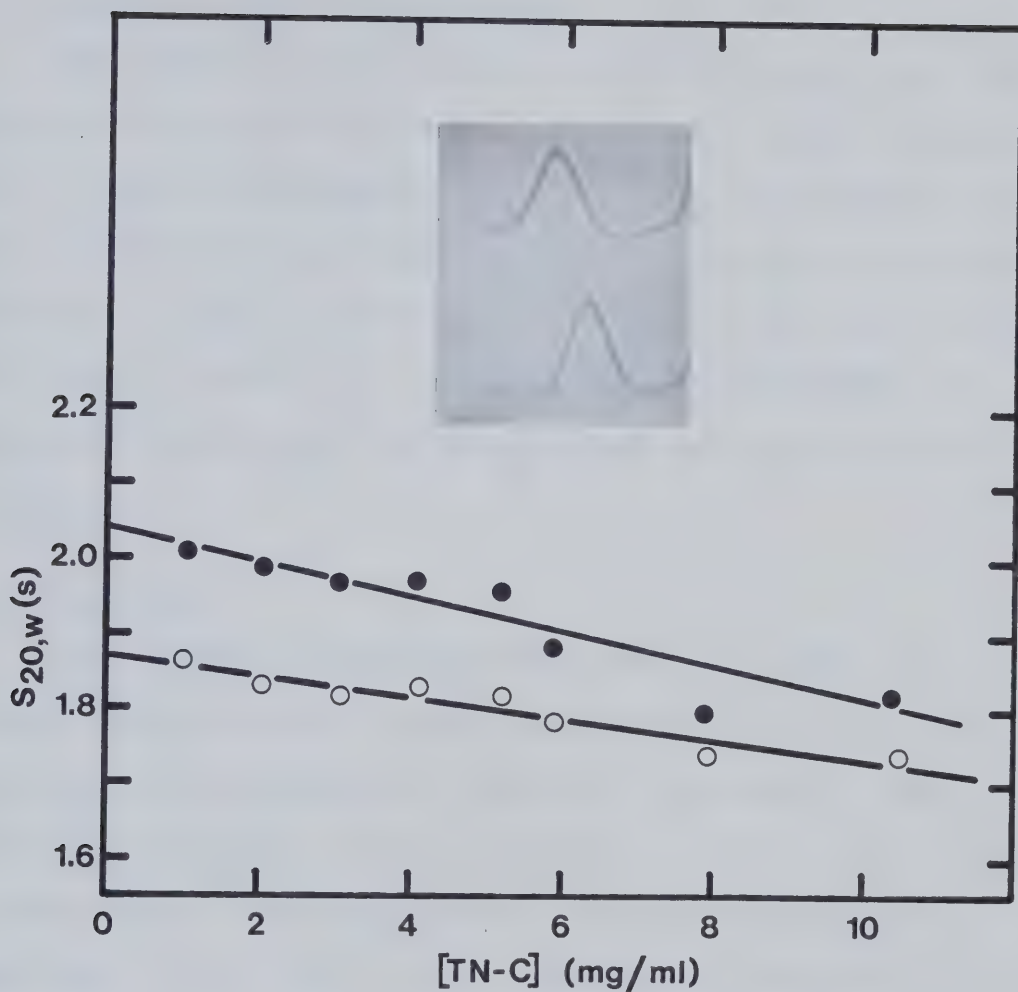


Figure 17. Concentration dependence of the sedimentation coefficient of TN-C. TN-C samples (0.4 ml) in 0.2 M KMED (pH 7.2) were sedimented at 60,000 rpm in aluminum synthetic boundary cells (12 mm). Schlieren photos were taken at 16 min intervals. Inset: schlieren photo of TN-C (5.1 mg/ml), minus (lower) or plus (upper) Ca^{2+} , taken at 50 min. Ca^{2+} concentrations were: (○) no Ca^{2+} , (●) 2 mM Ca^{2+} .

4. Analytical Gel Chromatography

The apparent Stokes radius of TN-C ($R_{s,gel}$) was also determined by gel filtration on Sephadryl S-300 (Figure 18). TN-C in 0.2 M KMED (pH 7.2) eluted in a single peak and no concentration dependence of the elution volume was observed. Adding 2 mM Ca^{2+} resulted in a decrease in $R_{s,gel}$ from 26.3 Å to 24.3 Å. Both values are consistent with the corresponding $R_{s,sed}$ values obtained from sedimentation velocity.

5. Viscosity

The reduced viscosity of TN-C in 0.2 M KMED (pH 7.2) varied linearly with protein concentration (Figure 19), thus allowing the estimation of intrinsic viscosity. The density-corrected intrinsic viscosity ($[\eta]$) of TN-C in the absence of Ca^{2+} was 6.4 ml/g. The value of $[\eta]$ was decreased to 5.4 ml/g in the presence of 2 mM Ca^{2+} , further indication of a conformational change. Using 10^{-4} M instead of 10^{-3} M Ca^{2+} did not significantly affect the intrinsic viscosity of TN-C (+ Ca^{2+}). The Huggins coefficient (k'), determined from the dependence of η_{red} on protein concentration (Equation 20), was 2.3 (- Ca^{2+}) and 2.1 (+ Ca^{2+}). These values suggest that TN-C behaves as a spherical or mildly asymmetric molecule in solution (Bradbury, 1970).

The effect of Mg^{2+} on the viscosity of TN-C was also

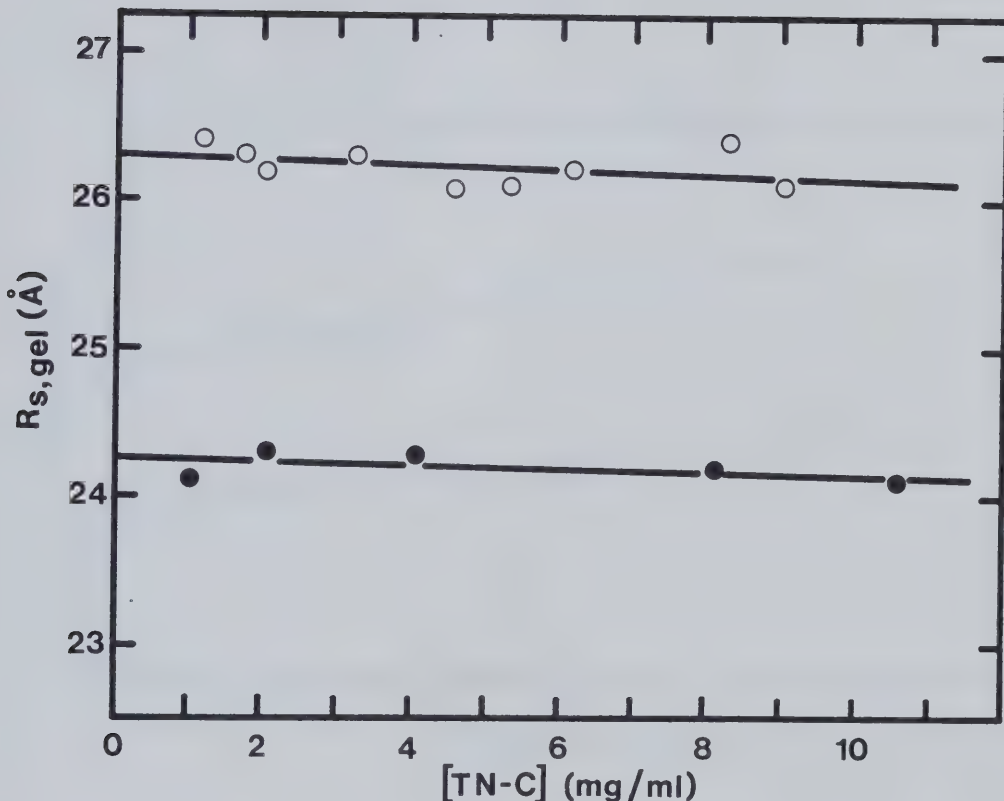


Figure 18. Stokes radius of TN-C as a function of protein concentration. Samples (300 μl) at the indicated concentrations were applied to a Sephadryl S-300 column (75 \times 1.1 cm) in 0.2 M KMED (pH 7.2). The flow rate was 15 ml/h and 0.4 ml fractions were collected. Ca^{2+} concentrations were: (○) no Ca^{2+} , (●) 2 mM Ca^{2+} .

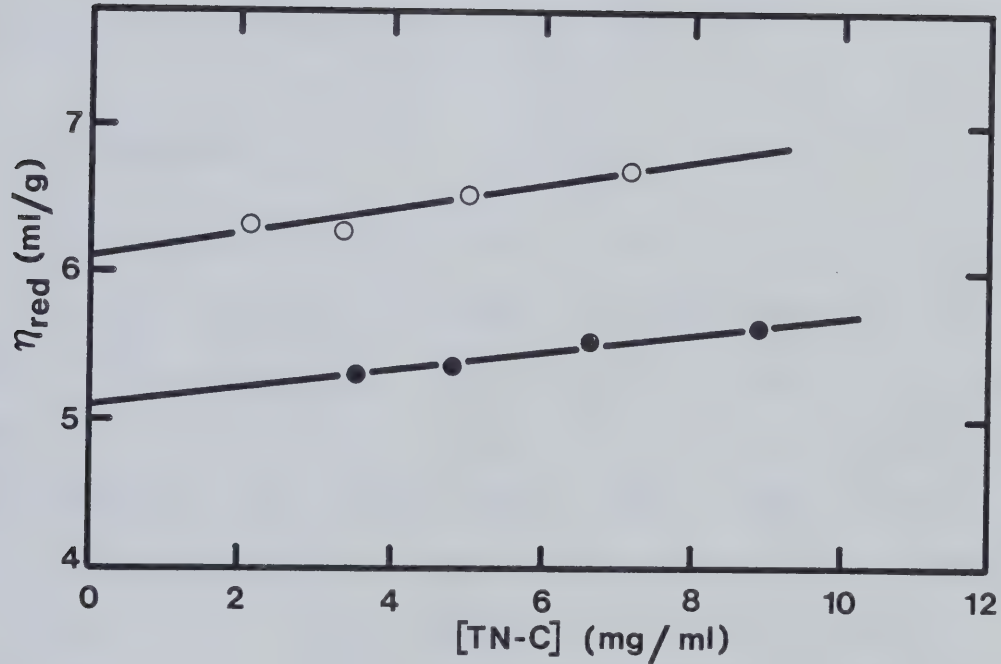


Figure 19. Viscosity of TN-C in 0.2 M KMED (pH 7.2). The uncorrected intrinsic viscosity values are 6.1 ml/g in the absence of Ca^{2+} (O) and 5.1 ml/g in the presence of 2 mM Ca^{2+} (●).

examined. Addition of 8 mM Mg²⁺ to TN-C (5 mg/ml) in 0.2 M KMED produced a decrease in η_{red} identical to that observed for Ca²⁺; subsequent addition of 2 mM Ca²⁺ resulted in no further change. The saturation of the high-affinity Ca²⁺/Mg²⁺-sites of TN-C ($K_a \sim 5 \times 10^3$) by Mg²⁺ was confirmed by circular dichroism (Burtnick, 1977).

B. DISCUSSION

The events which regulate striated muscle contraction on the thin filament originate with the binding of Ca²⁺ to TN-C. Thus, it is not surprising that so much effort has been devoted to the effects of Ca²⁺ on various properties of this subunit. For bovine cardiac TN-C, these effects include changes in the fluorescence of extrinsic probes (Johnson et al., 1980), increased α -helical content (Burtnick et al., 1975a), and perturbation of the aromatic amino acid environment as monitored by fluorescence (Leavis and Kraft, 1978), difference spectroscopy (Hincke et al., 1978), and NMR techniques (Hincke et al., 1981a,b). The thermal stabilization of cardiac TN-C by Ca²⁺ has also been investigated (Burtnick et al., 1975; McCubbin et al., 1980; Jacobson et al., 1981). The high solubility and stability of TN-C make it the easiest and most rewarding of the three subunits to study in solution.

The present results indicate that the binding of Ca²⁺

also affects the overall hydrodynamic shape of cardiac TN-C. The structural parameters ($\pm \text{Ca}^{2+}$) are summarized in Table III. The observed decrease in $R_{s,\text{gel}}$ and $[\eta]$, as well as the increase in $s_{20,w}^0$, suggests that TN-C in the absence of Ca^{2+} ($f/f_{\min} = 1.52$) undergoes a conformational change to a more globular shape ($f/f_{\min} = 1.40$) in the presence of Ca^{2+} . There is some evidence that a similar change occurs for rabbit skeletal TN-C on the basis of a Ca^{2+} -induced increase in $s_{20,w}^0$ (Mani et al., 1974) and intramolecular cross-linking (Gusev et al., 1980). This has been supported by a fluorescence study of this protein (van Eerd and Kawasaki, 1972). In contrast, Johnson et al. (1978b) could demonstrate no effect of Ca^{2+} on the size of skeletal TN-C measured by fluorescence depolarization. They found that dansyl-labelled TN-C rotates as a globular molecule (diameter $\sim 37 \text{ \AA}$) whether 0, 2, or 4 moles of Ca^{2+} are bound per mole of protein.

It has been fairly well established that the binding of Ca^{2+} to the single Ca^{2+} -specific site of TN-C constitutes the regulatory trigger in the cardiac myofibril (Johnson et al., 1978a, 1980). This occurs over a much more restricted range of Ca^{2+} concentration than that employed in the present study, in which added Ca^{2+} would be expected to fill both the Ca^{2+} -specific and $\text{Ca}^{2+}/\text{Mg}^{2+}$ sites. To establish whether the observed changes in the hydrodynamic properties

TABLE III: SUMMARY OF THE PHYSICAL PROPERTIES OF TN-C^a

| parameter | - Ca ²⁺ | + Ca ²⁺ (2 mM) |
|---|----------------------|---------------------------|
| E _{1%, 1 cm^b} 276 nm | 2.3 | -- |
| M _{w^c} | 17,500 | 18,000 |
| ̄v (ml/g) | 0.701 | 0.701 |
| R _{s,gel} (Å) | 26.3 | 24.3 |
| s _{20,w} (S) | 1.87 | 2.04 |
| R _{s,sed} (Å) | 26.2 | 24.0 |
| f/f _{min^d} | 1.52 | 1.40 |
| [η] (ml/g) ^e | 6.4 | 5.4 |
| β ^f | 2.14×10 ⁶ | 2.19×10 ⁶ |

^aAll experiments were performed in 0.2 M KMED (pH 7.2).

^bDetermined by the method of Babul and Stellwagen (1969), average of 13 samples (see also Hincke, 1981).

^cApparent weight-average molecular weight from Figure 16, where c is initial loading concentration.

^dFrom Equation 2, using the average of R_{s,gel} and R_{s,sed}. The value of R_o is 17.25 Å, calculated from the sequence molecular weight (M_r = 18,459, van Eerd and Takahashi, 1975).

^eDetermined from uncorrected intrinsic viscosity values (Figure 19).

^fCalculated from Equation 6.

of TN-C are physiologically-relevant, the effect of Mg^{2+} on the viscosity of the protein was examined. The addition of Mg^{2+} , which binds only to the Ca^{2+}/Mg^{2+} sites of TN-C, resulted in the same decrease in η_{red} seen with Ca^{2+} . This observation is in accord with circular dichroism studies (Hincke et al., 1978), indicating that the major Ca^{2+} -induced structural change accompanies the occupation of the Ca^{2+}/Mg^{2+} sites. Zot and Potter (1982) have demonstrated that cation binding to these sites is necessary to prevent the dissociation of skeletal TN-C from the myofibril and have suggested that they are required for the structural integrity of the troponin complex. Conversely, the regulatory Ca^{2+} -switch of cardiac TN-C would appear to involve a more modest conformational change, perhaps with subtle alterations occurring at regions of the protein surface that interact with other subunits.

Before attempting to interpret the hydrodynamic data in more detail, it is wise to consider possible alternative explanations for the Ca^{2+} -induced behaviour of cardiac TN-C. For example, the observed increase in $s_{20,w}$ when Ca^{2+} is added could also be caused by protein association. Indeed, rabbit skeletal TN-C has been shown to undergo self-association to a dimer (Margossian and Stafford, 1982), with aggregation becoming more prominent at Ca^{2+} concentrations above $10^{-4} M$ (Murray and Kay, 1972). However, aggregation

of cardiac TN-C does not appear to be an important factor in this study because sedimentation equilibrium experiments showed little tendency toward higher molecular weight species in 2 mM Ca^{2+} (Figure 16). This is particularly true at the lower protein concentrations to which most physical parameters are extrapolated. Moreover, an increase in molecular weight is clearly incompatible with the observed Ca^{2+} -induced decrease in the Stokes radius determined by gel filtration. It is also apparent from Figures 17 and 19 that the sedimentation and viscosity concentration profiles in Ca^{2+} are consistent with a monomeric protein. Aggregation of skeletal TN-C is probably enhanced when very low affinity ($K_a \sim 10^3 \text{ M}^{-1}$) Ca^{2+} -binding sites are occupied at millimolar Ca^{2+} levels, resulting in a less negatively charged molecule. Although such non-specific Ca^{2+} -binding sites have also been found on cardiac TN-C (Holroyde et al., 1980), they must play a reduced role in the intermolecular association until higher Ca^{2+} concentrations are reached.

The large net negative charge on TN-C at pH 7 might be expected to influence other properties of the protein in solution. In particular, the possibility of artifacts in gel filtration experiments should be considered. Although electrostatic interactions between proteins and the gel matrix are not usually observed at ionic strength above 0.2 M (Martenson, 1978), this problem does appear to affect

the characterization of calmodulin by gel filtration (Klee et al., 1980). However, the excellent agreement between R_s values obtained by gel filtration and sedimentation velocity (Table III) suggests that any gel-protein interactions are negligible under the conditions used. Of course, it is always possible that artifacts in both techniques could lead to the observed consistency, but this is highly unlikely.

It is clear that the anionic nature of TN-C also influences its partial specific volume. Electrostriction effects appear to be particularly prominent since the observed value of \bar{v} (0.701 ml/g) is substantially lower than that calculated from the amino acid composition (0.727 ml/g). This discrepancy ($\Delta\bar{v} = 0.026$ ml/g) is even larger than the corresponding difference in native troponin ($\Delta\bar{v} = 0.017$ ml/g), indicating that the TN-C subunit is mainly responsible for the electrostrictive effect in the whole protein. The importance of accurately knowing the partial specific volume can be illustrated for TN-C (- Ca²⁺) by contrasting the value of $R_{s, \text{sed}}$ (26.2 Å) determined using $\bar{v} = 0.701$ ml/g to the value (23.8 Å) calculated with $\bar{v} = 0.727$ ml/g, where $s_{20,w}^0 = 1.87$ (Table III). This represents a decrease in f/f_{\min} from 1.52 to 1.36. When Ca²⁺ was added to TN-C, \bar{v} remained constant, suggesting that if any further change in electrostriction occurs, it must be balanced by other factors such as excluded volume effects. Crouch and

Klee (1980) have reported that bovine brain calmodulin also exhibits a lower than average \bar{v} that is relatively insensitive to Ca^{2+} .

In order to describe cardiac TN-C in terms of an ellipsoid of revolution, both the Stokes radius and viscosity data should be consistent with the chosen model. Table IV lists various combinations of hydration and axial asymmetry derived from the experimental values of R_s and $[\eta]$. Although the maximum possible asymmetry of the TN-C molecule can be obtained by setting the degree of hydration (w) to zero, a more reasonable estimate of w is the value of 0.48 g/g protein calculated from the amino acid composition. With this estimate of hydration, an axial ratio of 5-6 would be expected for TN-C in the absence of Ca^{2+} (Table IV). In this case, the agreement between the two experimental approaches is better for the oblate model, having a width of about 60 Å. For TN-C in 2 mM Ca^{2+} , which may represent the more relevant state of the molecule in vivo, the data tend to favor a prolate ellipsoid (axial ratio ~ 4) with a length of 80-90 Å.

An alternate representation of these data can be made by using the hydrodynamic treatment of Scheraga and Mandelkern (1953). The value of β , which depends only on the axial ratio of the ellipsoid of revolution, is 2.14×10^6 for TN-C (- Ca^{2+}). This value is compatible with an

TABLE IV: STRUCTURAL PARAMETERS OF EQUIVALENT ELLIPSOIDS OF REVOLUTION BASED ON THE HYDRODYNAMIC PROPERTIES OF TN-C

| hydration w (g/g) | prolate axial ratio ^a calculated from | | oblate axial ratio calculated from | |
|----------------------|---|----------|---------------------------------------|----------|
| | R _S | [η] | R _S | [η] |
| - Ca ²⁺ | 9.6(156) ^b | 7.4(131) | 11.6(78) | 11.6(78) |
| | 7.0(126) | 5.7(110) | 8.0(69) | 8.1(69) |
| | 5.2(103) | 4.6(95) | 5.9(62) | 6.0(63) |
| | 4.1(88) | 3.8(84) | 4.4(56) | 4.6(57) |
| + Ca ²⁺ | 7.4(131) | 6.4(119) | 8.6(71) | 9.5(73) |
| | 5.2(104) | 4.9(100) | 5.8(62) | 6.5(64) |
| | 3.8(84) | 3.9(85) | 4.1(55) | 4.7(58) |
| | 2.8(68) | 3.1(73) | 2.9(49) | 3.5(52) |

^aAxial ratio values were estimated (see Table I) from the average Stokes radius (R_S) by using Equations 2 and 3 or from the intrinsic viscosity ([η]) using Equation 5.

^bThe longest unhydrated axis in Å, calculated from Equation 21, is shown in parentheses for each axial ratio value.

oblate model but not with a prolate model of axial ratio greater than about 3 (see Table I). On the other hand, the estimate of β for TN-C in 2 mM Ca^{2+} (2.19×10^6) is slightly higher than that expected for an oblate ellipsoid but is consistent with a prolate ellipsoid with an axial ratio of about 4. Caution is necessary in making these comparisons because the effect of experimental error on the calculation of β is rather large. However, this is a theoretically-sound treatment in which the hydrodynamic properties of TN-C are related to an equivalent ellipsoid of revolution without making any assumptions regarding protein hydration.

The interpretation of hydrodynamic data in terms of ellipsoidal models should not be taken too literally. Although the physical properties of TN-C (+ Ca^{2+}) are most consistent with a prolate ellipsoid of axial ratio 4 within the chosen framework of analysis, the data do not necessarily imply that the protein looks like this in solution. Moreover, it may be dangerous to extrapolate the hydrodynamic behaviour of TN-C in solution to its structure on the thin filament, where its interaction with other proteins could result in considerable deformation. Nevertheless, these results do indicate that cardiac TN-C is a mildly asymmetric protein, perhaps suggesting that the Ca^{2+} -binding domains are not folded in a compact arrangement. It is not yet known whether this conclusion

can be extended to the corresponding subunit from skeletal muscle, which has always been thought to be a strictly globular protein (Johnson et al., 1978b; Kretsinger and Barry, 1975). The concept of TN-C as a flattened or elongated protein with a maximum dimension of 60-80 Å is not inconsistent with electron microscopic evidence (Flicker et al., 1982) or with localization studies on the thin filament.

CHAPTER V

HYDRODYNAMIC PROPERTIES OF TROPONIN-T

A. RESULTS

1. Preparation of TN-T

An alternate method of purifying cardiac TN-T was developed, employing hydroxylapatite chromatography in 6 M urea at pH 7 (Figure 20). TN-T was applied to a Biogel HTP column and eluted with a linear Na-phosphate gradient (1-200 mM) at room temperature as described in Experimental Procedures. The material eluting at approximately 120 mM Na-phosphate consisted of a single component as monitored by SDS polyacrylamide gel electrophoresis (Figure 20, inset). Upon lyophilization, this purified TN-T was shown to be identical to that prepared by CM-Sephadex chromatography (Burtnick et al., 1976) by the criteria of amino acid composition and circular dichroism. Similar results were observed whether the hydroxylapatite chromatography step was performed on CM-Sephadex-treated TN-T (as in Figure 20) or on the crude TN-T fraction obtained from the initial separation of troponin subunits on DEAE-Sephadex (Burtnick et al., 1976).

The value of $E_{276 \text{ nm}}^{1\%, 1 \text{ cm}}$ for TN-T in 0.5 M NMED was

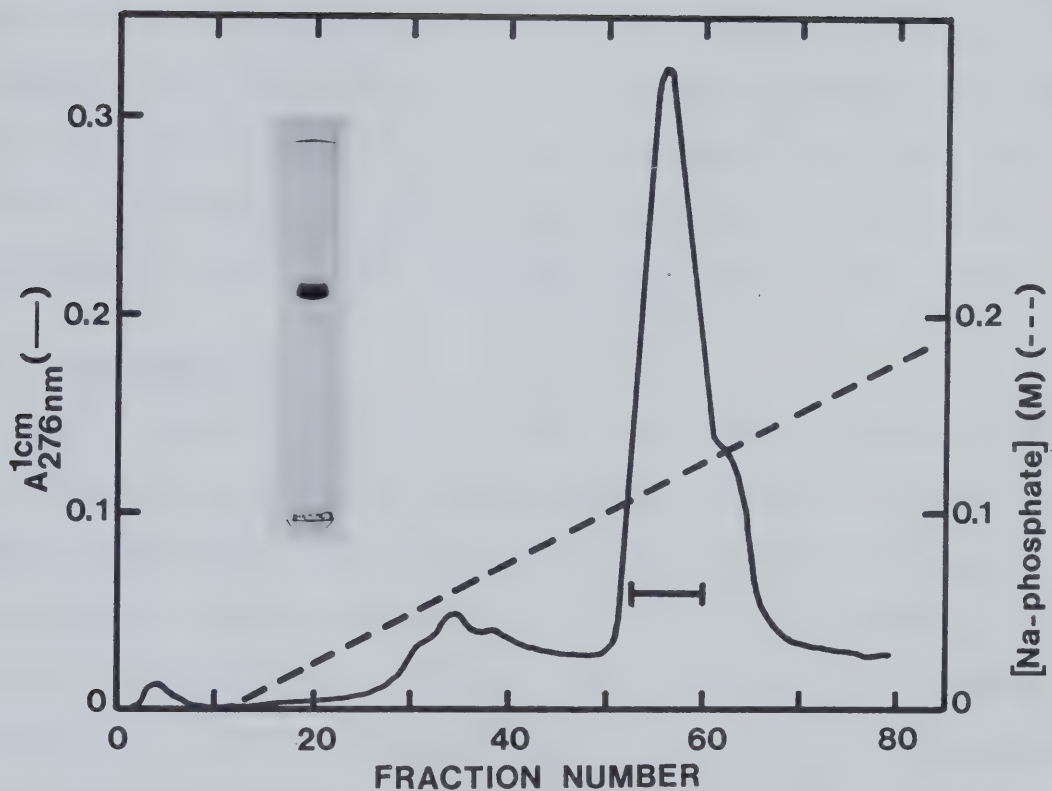


Figure 20. Purification of TN-T by hydroxylapatite chromatography. TN-T (50 mg) in 6 M urea, 1 mM Na-phosphate, 0.1 M NaCl, 0.5 mM DTT at pH 7 was applied to a Biogel HTP column (15 × 2.2 cm) and eluted with a linear 1-200 mM Na-phosphate gradient (500 ml total). The flow rate was 22 ml/h and 8 ml fractions were collected. The yield of lyophilized TN-T was 30 mg. Inset: SDS polyacrylamide gel of the major fraction.

4.4 ± 0.2 , established from refractometric measurements on 10 samples. This value is about 10% higher than the extinction coefficient previously determined for this subunit (Burtnick et al., 1976), but is consistent with the theoretical range of 4.4 to 5.0, calculated for TN-T in water and ethanol, respectively, assuming 4 tyrosine and 2 tryptophan residues per molecule (Burtnick et al., 1976).

2. Molecular Weight

The molecular weight of TN-T was measured by meniscus depletion sedimentation equilibrium. Conventional low-speed equilibrium experiments were not used due to the longer equilibrium times required and the resulting possibility of protein degradation. Moreover, any precipitation of this marginally-soluble subunit during the course of a low-speed run would be expected to violate the conservation of mass principle upon which this method is based.

The apparent molecular weight of TN-T in 0.5 M NMED (pH 7.2) increased as a function of protein concentration and was substantially higher than the monomeric value of 36,000 observed in 6 M urea (Figure 21). This aggregation of TN-T was not significantly influenced by various manipulations of the solvent conditions, such as increasing the NaCl concentration to 1 M, omitting DTT, or reducing the temperature to 5°C. Addition of 5 mM Mg²⁺, which causes a small decrease (of unknown significance) in the ellipticity

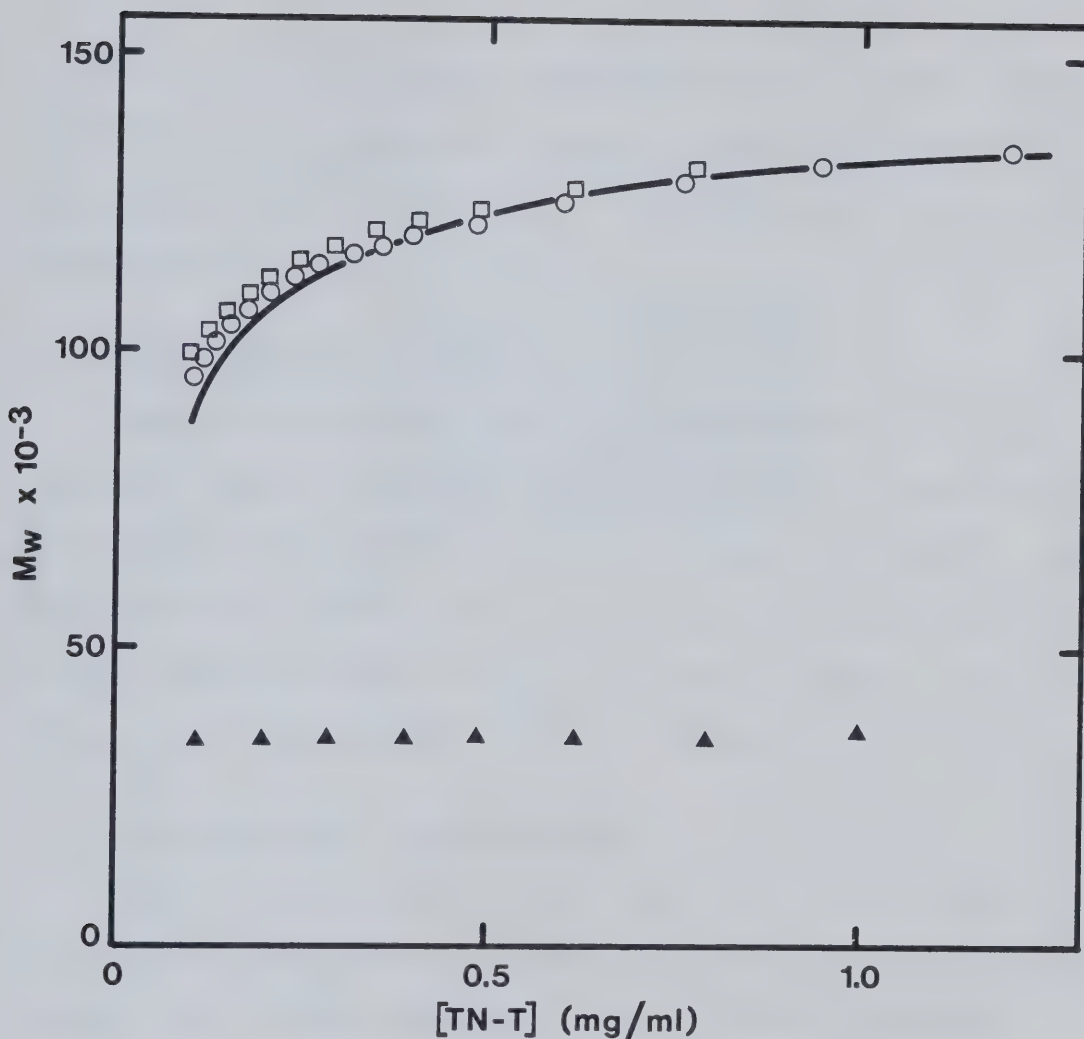


Figure 21. Molecular weight of TN-T as a function of protein concentration. Meniscus depletion sedimentation equilibrium experiments were performed on TN-T samples in 0.5 M NMED (○, □) or in 6 M urea, 0.2 M NMED (▲) at pH 7.2. Initial protein concentrations and equilibrium rotor speeds were: (○) 0.93 mg/ml, 17,000 rpm; (□) 0.31 mg/ml, 17,000 rpm; (▲) 0.57 mg/ml, 32,000 rpm. The theoretical molecular weight for TN-T undergoing an ideal monomer-tetramer equilibrium is also included (—), calculated from Equation 13 where $M_1 = 36,000$ and $K_a = 6 \times 10^3 \text{ ml}^3/\text{mg}^3$.

at 222 nm of this subunit (Burtnick et al., 1976), also had no effect on the molecular weight. Even the presence of 1 M guanidine hydrochloride or 2 M urea resulted in only partial dissociation.

3. Sedimentation Velocity

TN-T in 0.5 M NMED (pH 7.2) sedimented as a single schlieren peak, although a small shoulder was observed along the trailing edge of the boundary (Figure 22, inset). The sedimentation coefficient was relatively independent of protein concentration between 0.5 and 2.5 mg/ml. The value of $s_{20,w}$ in this region was 4.3 S (Figure 22).

4. Analytical Gel Chromatography

Figure 23 illustrates the Sephadryl S-300 elution behaviour of TN-T in 0.5 M NMED (pH 7.2). TN-T eluted in a single peak and the apparent Stokes radius increased dramatically with initial protein concentration. The values of $R_{s,gel}$ were unusually high (65-80 Å) by comparison to the largest protein standard, β -galactosidase ($R_s = 69 \text{ \AA}$, $M_r \sim 460,000$). This phenomenon was originally reported by Hincke et al. (1979).

5. Viscosity

The reduced viscosity of TN-T in 0.5 M NMED varied from 20 ml/g to over 25 ml/g in the concentration range examined (Figure 24). No attempt was made to estimate the intrinsic

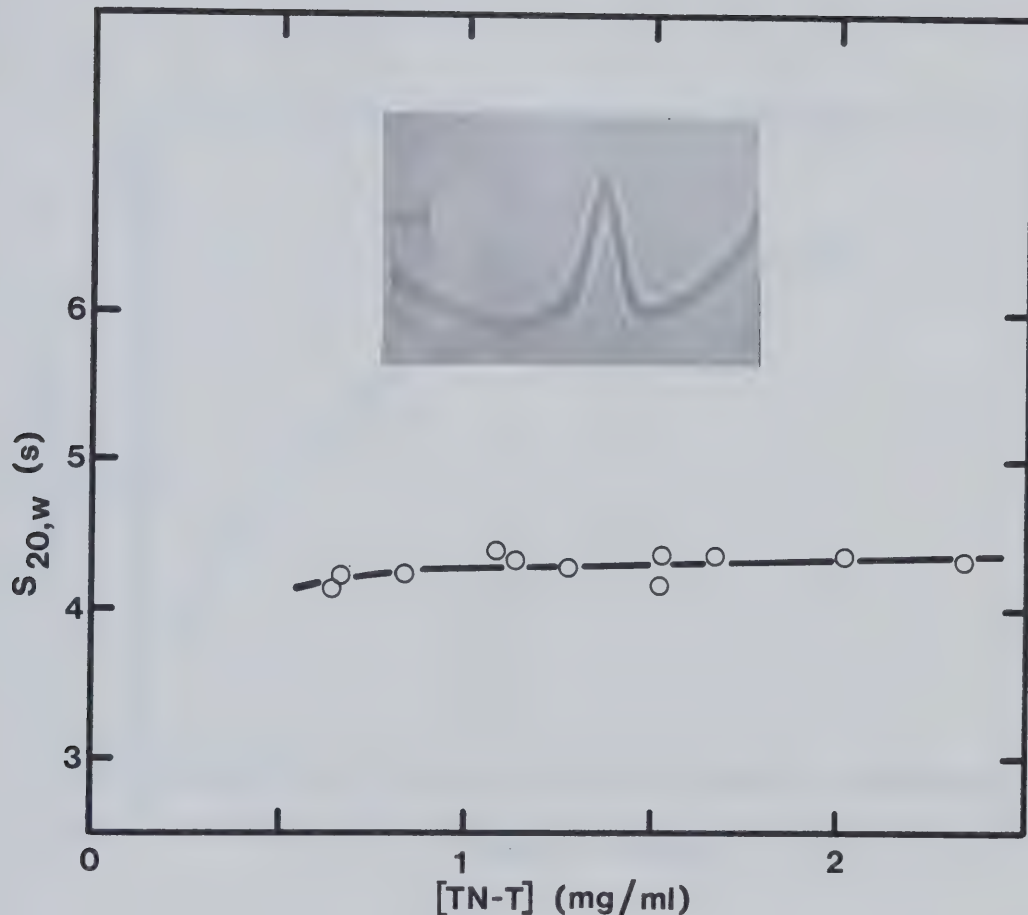


Figure 22. Effect of protein concentration on the sedimentation coefficient of TN-T. TN-T samples (0.4 ml) in 0.5 M NMED (pH 7.2) were sedimented at 60,000 rpm in aluminum synthetic boundary cells (12 mm). Schlieren photos were recorded at 16 min intervals. Inset: schlieren photo of TN-T (2.3 mg/ml), taken at 35 min.

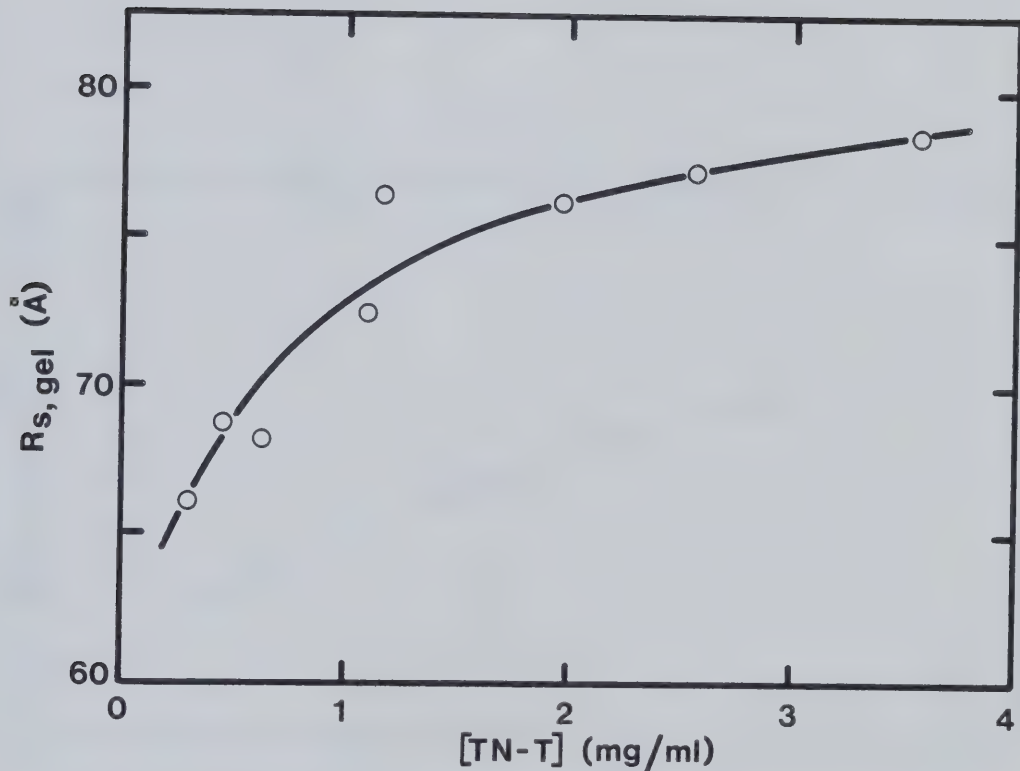


Figure 23. Effect of protein concentration on the apparent Stokes radius of TN-T. Samples (300 μ l) at the indicated concentrations were applied to a Sephadryl S-300 column (70 \times 1.1 cm) in 0.5 M NMED (pH 7.2). The flow rate was 14 ml/h and 0.4 ml fractions were collected.

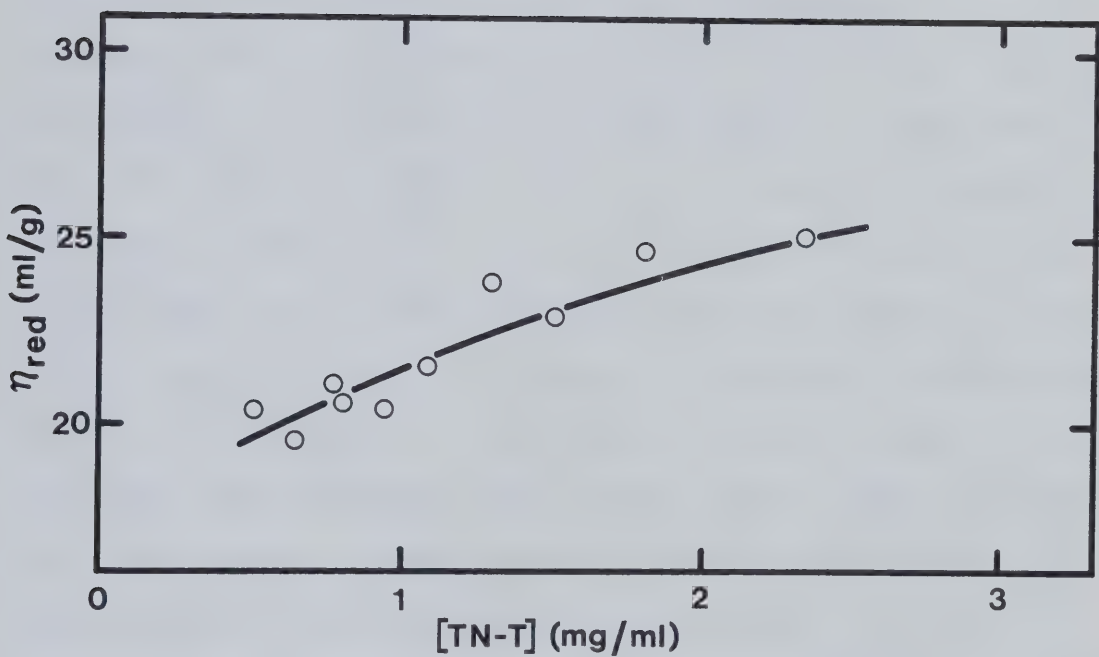


Figure 24. Viscosity of TN-T in 0.5 M NMED (pH 7.2).

viscosity of TN-T due to the extensive dissociation which occurs below 0.5 mg/ml.

B. DISCUSSION

A number of similar purification schemes for cardiac TN-T have been reported, employing ion-exchange chromatography on SP-Sephadex (Brekke and Greaser, 1976), CM-Sephadex (Burtnick et al., 1976; Potter, 1982) and CM-agarose (Stull and Buss, 1977) in 6 M urea. The method routinely used in our laboratory (Burtnick et al., 1976) gives good quality TN-T, although the purification is not always reproducible and a second CM-Sephadex chromatography step is often required. During the earlier stages of this project, good yields of pure subunit were seldom obtained for this reason. This situation has been improved considerably with the present introduction of a new purification procedure for TN-T: hydroxylapatite chromatography in 6 M urea (Figure 20). This method can be successfully used instead of, or in conjunction with, the traditional ion-exchange chromatography step. Some of the advantages offered by hydroxylapatite chromatography include the increased resolution of the TN-T peak and the relative ease of column regeneration in situ. Cardiac TN-T was obtained in reasonable yield (~60%) by this method and was comparable to our best previous preparations by several

criteria. Hydroxylapatite chromatography is commonly used as a final step in the purification of proteins and has been reviewed by Bernardi (1971,1973).

Once purified, TN-T is an unusually difficult protein to handle in solution, at least by comparison to normal globular proteins. Regardless of the source (skeletal or cardiac), this subunit is notoriously susceptible to proteolytic degradation (Drabikowski et al., 1971; Dabrowska et al., 1973). The virtual neglect of the physical properties of TN-T in solution can also be attributed to its poor solubility: the protein is soluble only at an unphysiologically high ionic strength (> 0.5 M) and concentrations of only a few milligrams per ml can be achieved. Furthermore, cardiac TN-T must be initially solubilized in a denaturing solvent, such as urea, before dialyzing against the analytical buffer (Burtnick et al., 1976). For these reasons, density measurements were not performed on either TN-T or TN-I. The value of \bar{v} used for TN-T (0.72 ml/g) was calculated from the amino acid composition (Burtnick et al., 1976). The errors involved in this assumption should not be as large as those encountered with TN-C. Since \bar{v} of TN-C (0.70 ml/g) is less than that of whole troponin (0.71 ml/g), the true partial specific volumes of the remaining subunits (TN-T and TN-I) are probably more in line with their calculated values.

Like native troponin, cardiac TN-T appears to be highly aggregated in non-denaturing buffers, in agreement with earlier studies (Burtnick et al., 1976). Moreover, as with the native molecule, the present results favor a reversible protein association reaction rather than the presence of multiple non-interacting species in solution. Figure 21 shows that the apparent molecular weight of TN-T is independent of initial loading concentration, which differs by a factor of three in the two experiments illustrated. This overlap would not be expected in a non-associating system. Moreover, only single peaks were observed in sedimentation velocity and gel filtration experiments, with $R_{s, \text{gel}}$ exhibiting a large dependence on sample concentration (Figure 23). The insensitivity of $s_{20,w}$ to protein concentration probably reflects the fact that the association reaction is essentially complete at concentrations above 1 mg/ml.

Analysis of the sedimentation equilibrium data according to monomer-polymer and isodesmic indefinite modes of association is illustrated in Figure 25. This treatment suggests that TN-T associates to a tetramer ($M_r = 144,000$) with an association constant (K_a) of $6 \times 10^3 \text{ ml}^3/\text{mg}^3$. This value of K_a has been used to generate a theoretical M_w vs concentration curve, which is included in Figure 21, for comparison to the experimental data. As mentioned

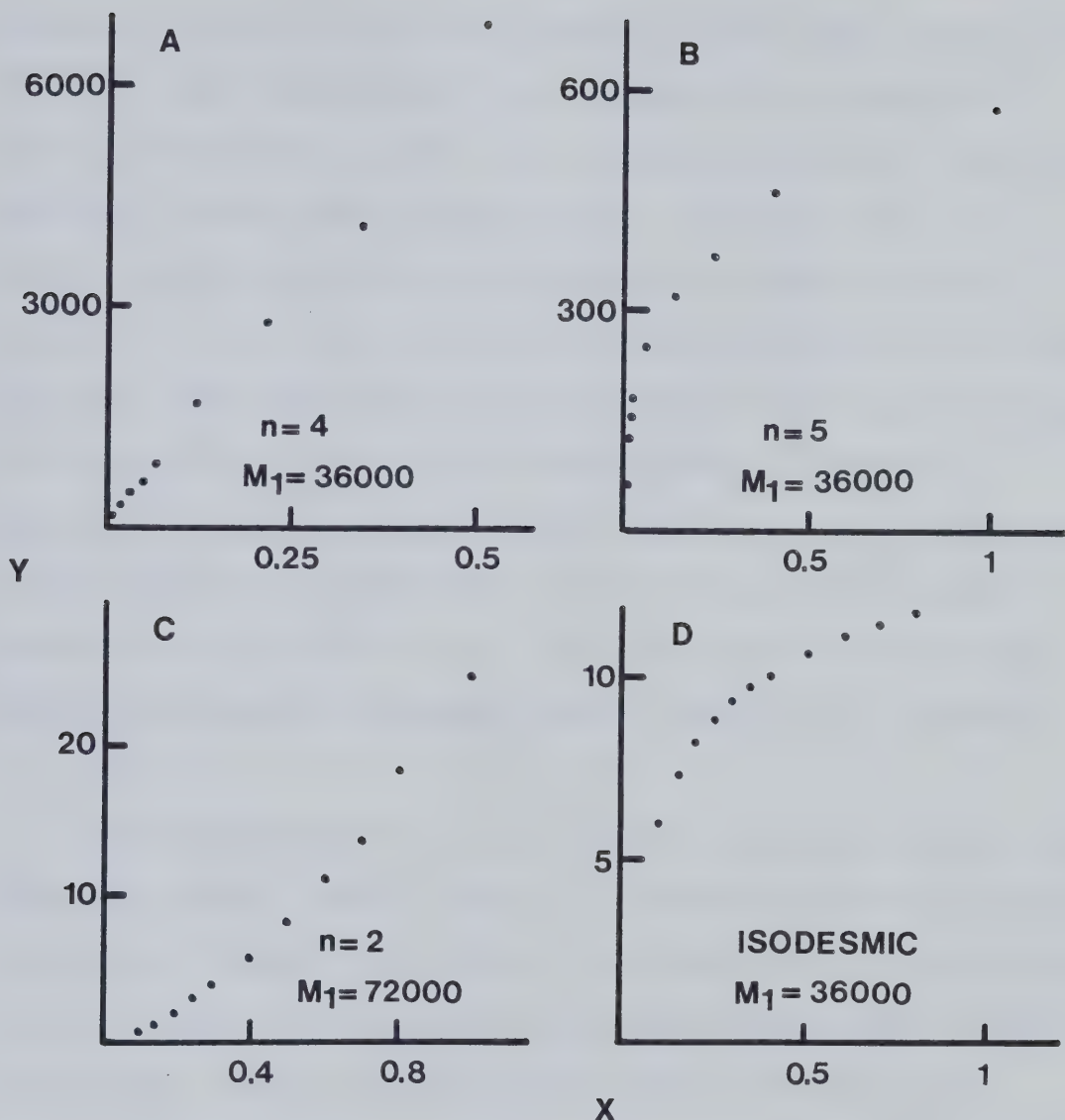


Figure 25. Protein association models for TN-T in 0.5 M NMED (pH 7.2). M_w vs concentration data from Figure 21 (experimental points) were treated according to Equations 13 and 15, where the coordinates X and Y are defined. Panels A-C: Monomer-n-mer association (Equation 12). Panel D: isodesmic indefinite association (Equation 14).

previously regarding native troponin, this simple method of analysis does not consider the effects of non-ideality which, if a factor, would tend to decrease M_w and thus the estimated degree of polymerization. However, the polymerization of TN-T to a tetramer is supported by a comparison of the sedimentation velocity and gel filtration results. The value of $R_{s, \text{sed}}$ calculated from Equation 9 is 83 Å, assuming $s_{20,w}$ (4.3 S) corresponds to the TN-T tetramer. This is similar to the values of $R_{s, \text{gel}}$ observed in gel filtration experiments when concentrated protein samples were applied (Figure 23). Analogous calculations based on pentamer or hexamer models give $R_{s, \text{sed}}$ values of over 100 Å.

The aggregation of native troponin probably occurs via the TN-T subunit, even though the sedimentation equilibrium data do not necessarily suggest the same mode of association in both cases. This lack of agreement could simply be due to the much larger concentration range included in the analysis for troponin. Nevertheless, it is interesting to compare the slopes of corresponding plots in Figure 15 (troponin) and Figure 25 (TN-T). It is clear that the association of TN-T is much stronger than that of whole troponin in 0.5 M NMED. Perhaps some of the sites responsible for aggregation in TN-T are involved in the binding of the other subunits in native troponin. Based on

its amino acid composition and behaviour on ion-exchange columns, TN-T has only a small net negative charge at pH 7.2. Certainly the observed molecular weight of this subunit is much less sensitive than native troponin to changes in the ionic strength of the solvent.

The strong tendency of TN-T to self-associate makes it virtually impossible to use conventional hydrodynamic techniques to study the monomeric form of the molecule. This is unfortunate since it is the TN-T monomer which presumably exists in vivo. In contrast to native troponin, there is no indication that even the lowest $R_s,_{gel}$ values measured correspond to the completely dissociated subunit. An attempt was made to discover solvent conditions that would reverse the self-association of TN-T without disrupting the secondary and tertiary structure of the molecule. However, aggregation persists even at moderate concentrations of denaturants such as guanidine hydrochloride and urea. The results obtained from this investigation do indicate that cardiac TN-T forms asymmetric aggregates in solution. Assuming TN-T is a tetramer with a Stokes radius of 83 Å, the frictional ratio would be 2.4, even larger than the value for troponin ($f/f_{min} = 1.85$). The reduced viscosity of TN-T (Figure 24) is also significantly larger than that of the native protein (Figure 13) at the same protein concentrations.

The physical properties of native troponin in solution are most likely dominated by the asymmetry of the TN-T subunit. As noted in Chapter III, skeletal TN-T has been localized over an extended region of tropomyosin on the thin filament. Immunoelectron microscopy (Ohtsuki, 1979), affinity chromatography (Pearlstone and Smillie, 1981) and cross-linking studies (Chong and Hodges, 1982a) have all demonstrated that the C-terminal half of TN-T can interact with tropomyosin. This section of TN-T is probably situated in the same general vicinity as TN-C and TN-I, about 130 Å from the tropomyosin overlap region (Figure 2). However, TN-T binding also occurs at the extreme C-terminus of tropomyosin (Ohtsuki, 1979; Mak and Smillie, 1981; Pato et al., 1981). A highly-helical region in the N-terminal half of TN-T, encompassed by a cyanogen bromide fragment (CB2, residues 71-151) has been implicated in this interaction (Jackson et al., 1975; Pearlstone and Smillie, 1977). The extended nature of TN-T suggested by these studies has recently been supported by an electron microscopic investigation of the skeletal protein (Flicker et al., 1982). These workers observed that TN-T corresponds to the tail section of rotary-shadowed troponin, a long rod-like molecule with a length of 165 ± 20 Å.

Thus, the current picture of skeletal TN-T is that of an elongated molecule consisting of several distinct domains

which are involved in interactions with other thin filament components. Analysis of the TN-T sequence reveals an almost complete absence of clusters of nonpolar residues in the polypeptide chain, suggesting that this subunit might lack the hydrophobic core necessary for extensive chain folding (Pearlstone et al., 1976). This is also consistent with the increased susceptibility of TN-T to proteolytic degradation. Most of the ordered secondary structure in skeletal TN-T is located in the cyanogen bromide fragment CB2, which also binds to tropomyosin (Pearlstone and Smillie, 1977). It is conceivable that this fragment, containing about 80% α -helix, could interact with the tropomyosin coiled-coil near the overlap region. A study is currently underway in our laboratory to isolate and characterize cyanogen bromide fragments from cardiac TN-T; it will be interesting to see if a helical region corresponding to CB2 exists in this protein.

CHAPTER VI

HYDRODYNAMIC PROPERTIES OF TROPONIN-I

A. RESULTS

1. Preparation of TN-I

In view of the success achieved in the purification of TN-T by hydroxylapatite chromatography in 6 M urea, this method was also applied to the TN-I subunit of bovine cardiac muscle. The procedure used was basically the same as for TN-T, although a shallower Na-phosphate gradient (1-120 mM) was employed. The results from different preparations were somewhat variable; a typical experiment is illustrated in Figure 26. The starting material for this purification was crude TN-I which had been subjected to a single CM-Sephadex chromatography step (Burtnick et al., 1975b), yet still contained a significant number of low molecular weight impurities. TN-I eluted from the Biogel HTP column in two partially-separated peaks (fractions A and B, Figure 26). Both peaks consisted mainly of TN-I (Figure 26, inset), although the later peak (B) was also contaminated with other components. The yield of lyophilized protein from fractions A and B was 25% and 32%, respectively, relative to the amount of TN-I applied to the

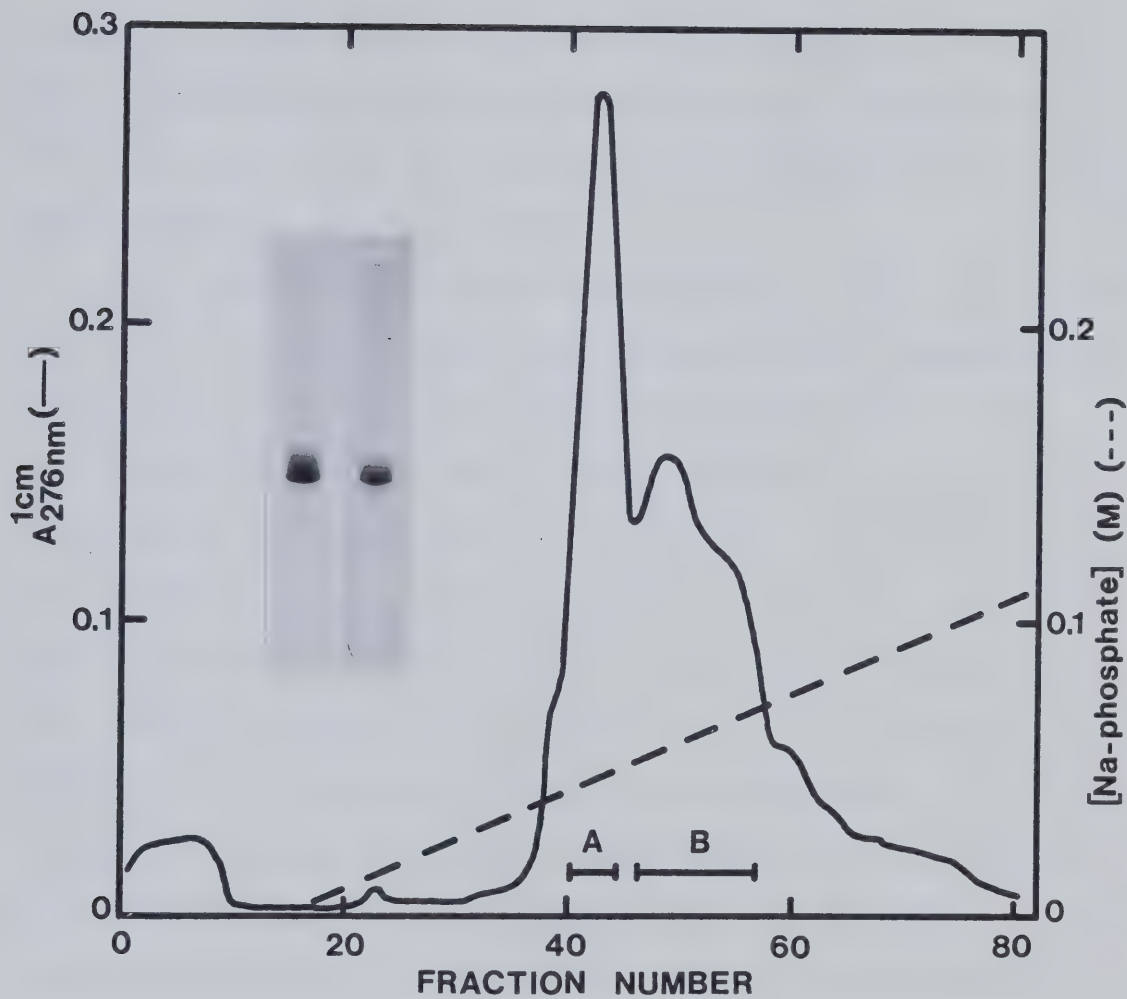


Figure 26. Purification of TN-I by hydroxylapatite chromatography. TN-I (75 mg) in 6 M urea, 0.1 M NaCl, 1 mM Na-phosphate, 0.5 mM DTT at pH 7 was applied to a Biogel HTP column (21 × 2.2 cm) and eluted with a linear 1-120 mM Na-phosphate gradient (500 ml total). The flow rate was 23 ml/h and 8 ml fractions were collected. The yield of lyophilized material was: A (19 mg), B (24 mg). Inset: SDS polyacrylamide gels of pooled fractions A (left) and B.

column. No significant difference was found in the amino acid compositions of the two fractions; the compositions of both were identical to that previously reported for cardiac TN-I (Burtnick et al., 1975b).

The observed extinction coefficient ($E_{276 \text{ nm}}^{1\%, 1 \text{ cm}}$) of TN-I was 5.2 ± 0.2 , determined from refractometric measurements on a total of 10 samples from 3 different preparations. This value is significantly higher than that originally established for this subunit ($E_{278 \text{ nm}}^{1\%, 1 \text{ cm}} = 3.7$; Burtnick et al., 1975b). It is also outside the range calculated from the tyrosine (3) and tryptophan (1) content (Burtnick et al., 1975b): from 4.0 (in water) to 4.6 (in ethanol). However, for a detailed comparison of extinction coefficients, the calculated value should be increased by 10-15% to account for the contribution due to light scattering of TN-I. Indeed, this subunit exhibited considerably more scattering at wavelengths above 310 nm than either TN-C or TN-T.

2. Molecular Weight

Meniscus depletion sedimentation equilibrium was used to measure the molecular weight of TN-I; conventional equilibrium experiments were not employed for reasons already outlined with regard to TN-T. Initial molecular weight studies performed in the absence of reducing agent (Figure 27) or in 0.5 M NMED (pH 7.2) buffer containing 0.5

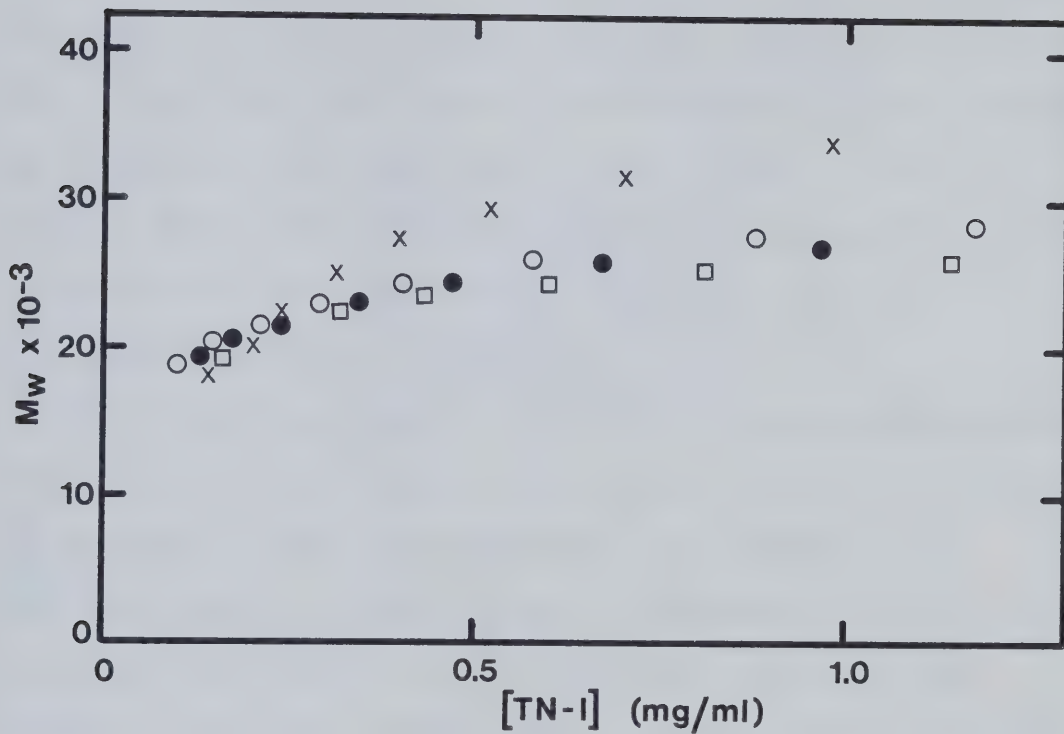


Figure 27. Effect of protein concentration on the molecular weight of TN-I and CMC-TN-I. Meniscus depletion sedimentation equilibrium experiments were performed on samples of TN-I in 0.5 M NMED (2 mM DTT) (\circ , \square), TN-I in 0.5 M NME (no DTT) (x), and CMC-TN-I in 0.5 M NME (no DTT) (\bullet), all at pH 7.2. Initial protein concentrations and equilibrium rotor speeds were: (\circ) 0.60 mg/ml, 36,000 rpm; (\square) 0.85 mg/ml, 34,000 rpm; (x) 0.84 mg/ml, 36,000 rpm; (\bullet) 0.82 mg/ml; 36,000 rpm.

or 1 mM DTT, gave variable results which indicated substantial aggregation of this subunit. This effect was diminished in the presence of 2 mM DTT and M_w throughout most of the cell was closer to the value of 23,000 expected for monomeric TN-I (Burtnick et al., 1975b). Even at elevated DTT concentrations, however, some higher molecular weight material was observed at the bottom of the ultracentrifuge cell (Figure 27).

The molecular weight behaviour of carboxamidomethylated (CMC) TN-I, in which both cysteine residues of the subunit are protected, was also measured. As expected, the molecular weight of CMC-TN-I was independent of DTT concentration, and M_w for the modified subunit in the absence of DTT (0.5 M NME, Figure 27) was similar to that observed for TN-I in the presence of reducing agent.

The value of \bar{v} used for TN-I and CMC-TN-I (0.73 ml/g) was calculated from the amino acid composition.

3. Sedimentation Velocity

Only a single schlieren peak was observed in sedimentation experiments with TN-I in 0.5 M NMED (pH 7.2) (Figure 28, inset). The sedimentation coefficient increased slightly as a function of protein concentration over the limited solubility range of the subunit and the value of $s_{20,w}$ at the lowest concentrations was about 1.9-2.0 S (Figure 28).

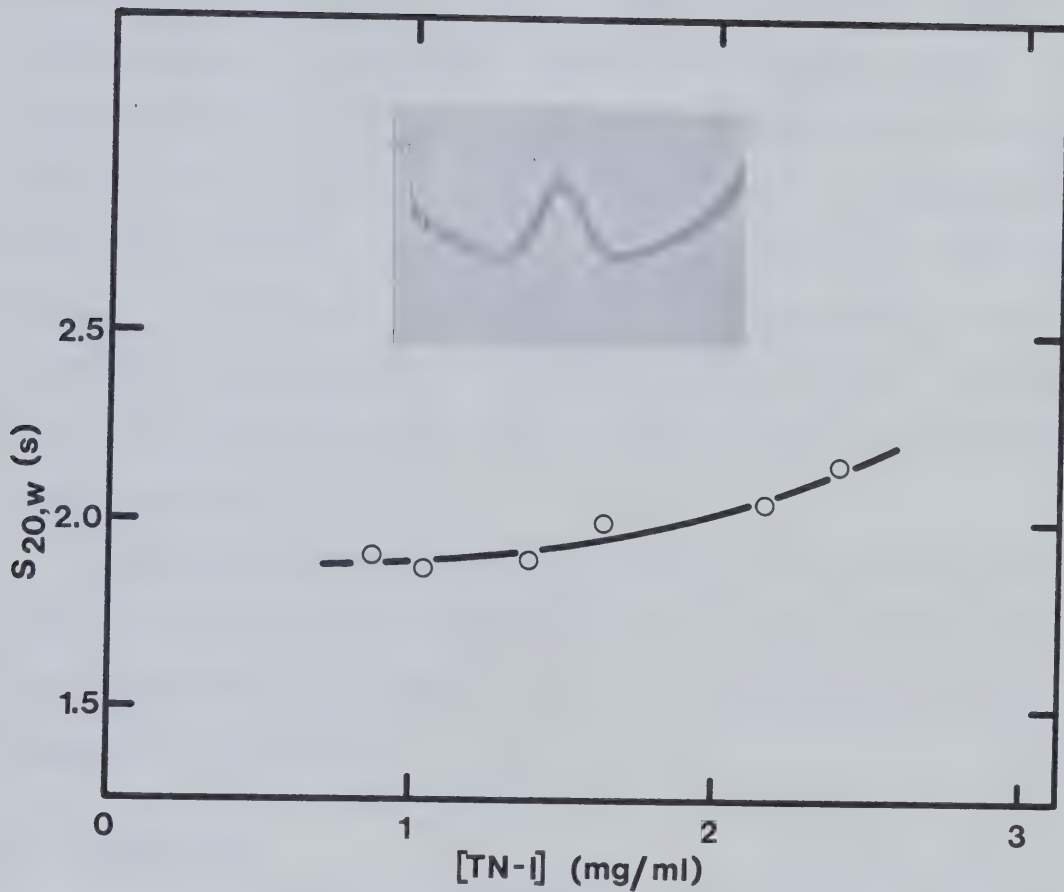


Figure 28. Sedimentation coefficient of TN-I as a function of protein concentration. TN-I samples (0.4 ml) in 0.5 M NMED (pH 7.2) were sedimented at 60,000 rpm in aluminum synthetic boundary cells (12 mm). Schlieren photos were recorded at 16 min intervals. Inset: schlieren photo of TN-I (2.4 mg/ml) taken at 50 min.

4. Analytical Gel Chromatography

TN-I eluted in a single peak from Sephadryl S-300 columns equilibrated with 0.5 M NMED (2 mM DTT). Only a small increase in apparent Stokes radius with sample concentration was observed and the limiting value of $R_{s,gel}$ at low concentration was 29 Å (Figure 29). In experiments performed without DTT in the solvent, a separate faster peak ($R_{s,gel} \sim 38$ Å) was also present. This material, which comprised about 25% of the total protein eluted, was shown to be intermolecularly disulfide-linked TN-I using SDS gel electrophoresis (\pm DTT).

Carboxamidomethylated TN-I eluted in a single peak regardless of the DTT concentration in the solvent; no difference in $R_{s,gel}$ from that of the unmodified subunit was observed (Figure 29).

5. Viscosity

The reduced viscosity of TN-I in 0.5 M NMED (pH 7.2) varied from 6 to 10 ml/g in the protein concentration range examined (Figure 30). Attempts to measure η_{red} at lower concentrations were unsuccessful due to the small difference in flow time between the solvent and protein solution. Viscosity measurements performed with CMC-TN-I in the same solvent indicated no change in this parameter (Figure 30).

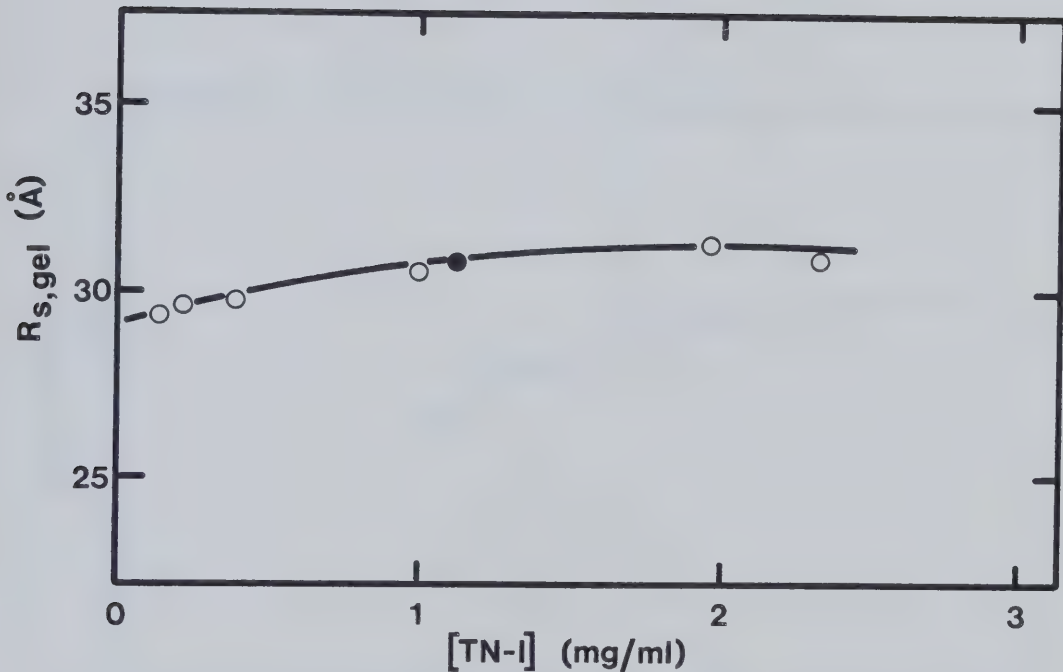


Figure 29. Effect of protein concentration on the apparent Stokes radius of TN-I (O) and CMC-TN-I (●). Samples (500 μl) at the indicated concentrations were applied to a Sephadryl S-300 column (90 \times 1.3 cm) in 0.5 M NMED (pH 7.2). The flow rate was 20 ml/h and 0.6 ml fractions were collected.

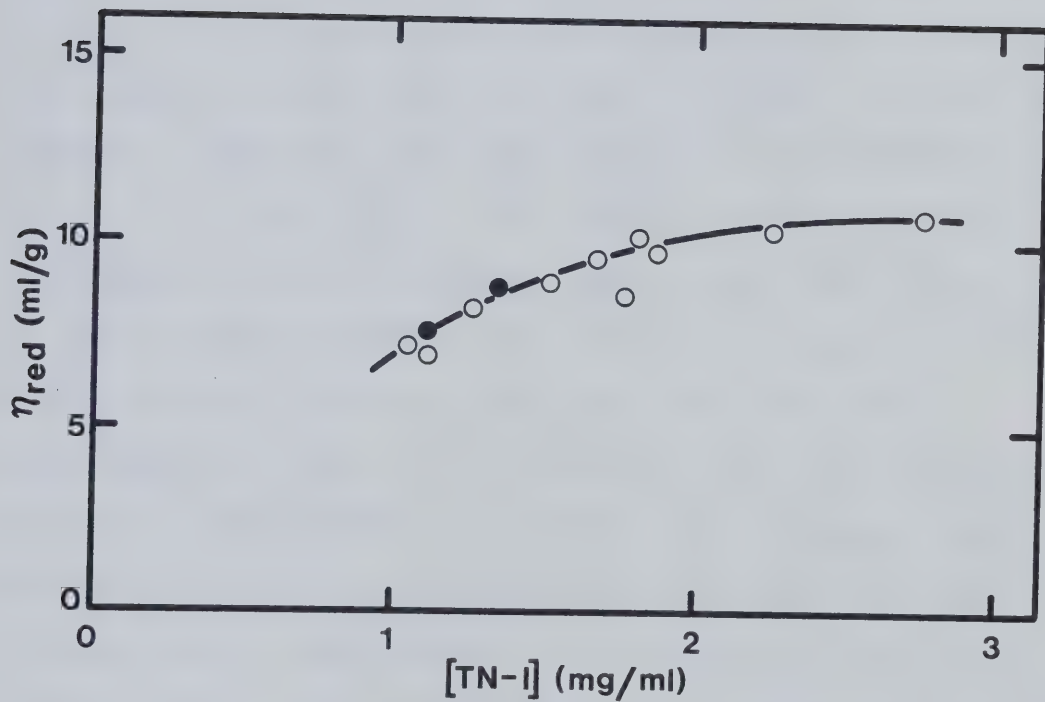


Figure 30. Viscosity of TN-I (○) and CMC-TN-I (●) in 0.5 M NMED (pH 7.2).

B. DISCUSSION

In contrast to TN-T, hydroxylapatite chromatography of cardiac TN-I does not appear to offer many advantages in purity or yield over existing methods (Brekke and Greaser, 1976; Burtnick et al., 1975b; Potter, 1982). However, the unusual elution profile illustrated in Figure 26, in which TN-I appears in at least two separate peaks, deserves some comment. Bernardi (1973) has noted that phosphoproteins have a very high affinity for hydroxylapatite, since phosphate groups will readily compete for the calcium sites in the calcium phosphate gel. Thus, it is possible that these different elution peaks represent different phosphorylated forms of the subunit, although this was not confirmed experimentally. Cardiac TN-I contains three specific phosphorylation sites, at least one of which (serine 20) is considered to be biologically important (Perry, 1979). If hydroxylapatite chromatography does, in fact, fractionate TN-I on this basis, the method should perhaps be further developed to aid in the study of protein phosphorylation.

TN-I shares with TN-T a number of unpleasant handling characteristics in solution, including its poor solubility and sensitivity to proteolysis (Drabikowski et al., 1971; Martin, 1981). The increased tendency of the TN-I cysteine residues to undergo oxidation poses additional problems in

working with this subunit. Disulfide oxidation in skeletal (Horwitz et al., 1979) and cardiac (Hincke et al., 1979) TN-I has been shown to adversely affect the interaction with other troponin subunits. The present results indicate that this loss of TN-I function is at least partially due to intermolecular disulfide-bond formation. Both sedimentation equilibrium and gel filtration experiments revealed the increased presence of TN-I aggregates in the absence of reducing agent (DTT). Although cardiac TN-C and TN-T also contain cysteine residues, no similar dependence of the molecular weight on DTT concentration was ever observed with these proteins.

The problem of cysteine oxidation has led some investigators to take special precautions in the preparation of TN-I solutions (Hincke et al., 1979; Horwitz et al., 1979). In particular, these workers have reported that continuous bubbling of nitrogen through the solvent during sample dialysis is necessary to completely maintain the sulfhydryl groups in the reduced state. This protocol was not followed in the present study, since the use of freshly-made DTT solutions (2 mM) was found to be sufficient to overcome the problem of TN-I oxidation. The physical properties of TN-I were not noticeably altered when DTT concentrations higher than 2 mM were used, or when nitrogen flushing was carried out during sample preparation. Horwitz

et al. (1979) have pointed out that DTT oxidation is very rapid in air-exposed solutions at elevated pH values; at pH 8.5, for example, 2 mM DTT has a half-life of about 1 h. However, the half-life of 2 mM DTT in 0.5 M NMED (pH 7.2) was over 80 h when no special precautions were adopted, as monitored by both the loss of free sulfhydryl groups (Ellman, 1959) and by the increase in absorbance at 283 nm (Cleland, 1964). In addition, the free sulfhydryl concentration was periodically checked following sedimentation equilibrium runs with TN-I. Although increased oxidation in the sample relative to the solvent was usually observed, the effective DTT concentration was never less than 70% of the initial value.

Due to the important status of sulfhydryl groups in cardiac TN-I, Hincke et al. (1979) have examined the structural and functional consequences of modifying both cysteine residues of this protein by carboxamido-methylation. Although they observed that this modification does not adversely affect the inhibitory activity of TN-I, or its complex formation with TN-C, they discovered that the ability of the subunit to interact with TN-T is lost. Furthermore, a significant increase (~15%) in the amount of secondary structure of TN-I was observed, a result which they attributed to an enhanced α -helix-forming potential of the modified amino acid. The present hydrodynamic evidence

indicates, however, that carboxamidomethylation does not result in a gross conformational change, since the gel filtration (Figure 29) and viscosity (Figure 30) behaviour could detect no difference between TN-I and CMC-TN-I. It is more likely that the structural change (i.e. α -helix formation) induced by this modification is a local event, perhaps occurring at the TN-T interaction site on the surface of the TN-I molecule (Hincke et al., 1979). In bovine cardiac TN-I, this site probably corresponds to the region surrounding cysteines 75 and/or 92 in the homologous rabbit cardiac subunit (see Figure 6).

Cardiac TN-I undergoes much less self-association than the TN-T subunit. In the presence of sufficient reducing agent, TN-I appears to be essentially monomeric at protein concentrations below 0.5-1 mg/ml, as monitored by sedimentation equilibrium (Figure 27). This is supported by the relatively mild variation in R_s ,gel with protein concentration (Figure 29). Nevertheless, the concentration dependence of all the parameters measured suggests that some association does occur over the limited solubility range of TN-I, even in the absence of intermolecular disulfide cross-linking. Aggregation has previously been reported for both skeletal (Greaser and Gergely, 1973; Mani et al., 1973) and cardiac (Burtnick et al., 1975b) TN-I.

Of the physical parameters examined in this study, only gel filtration is capable of measurement at protein concentrations sufficiently low to ensure complete dissociation. Using the value of $R_{s,\text{gel}}$ extrapolated to zero concentration (29 Å), and assuming the subunit to be completely monomeric ($M_r = 23,000$) under these conditions the calculated frictional ratio for TN-I is 1.53. This value is similar to that determined for TN-C (- Ca²⁺) and suggests that TN-I is also a moderately asymmetric protein in solution. Although less reliable due to the aggregation of TN-I, the sedimentation velocity and viscosity data are in accord with the results from gel chromatography on Sephadryl S-300. For example, the estimated sedimentation coefficient for a protein of $M_r = 23,000$ and $f/f_{\min} = 1.53$ (Equation 9) is 1.9 S, very close to the values of $s_{20,w}$ observed at the lowest concentration examined (Figure 28). However, using a value of f/f_{\min} more typical of globular proteins (1.3), the calculated value of $s_{20,w}$ is significantly higher (2.3 S). Nevertheless, the lack of reliable hydrodynamic data obtained for TN-I precludes a more detailed structural analysis, of the type performed for TN-C (Chapter IV).

Very little is known about the three-dimensional structure of TN-I. Although antibodies to skeletal TN-I stain thin filaments over a fairly narrow region (Ohtsuki,

1975), there is some circumstantial evidence indicating that this subunit may not be a compact, symmetrical molecule. To begin with, TN-I is capable of interacting with every other thin filament protein; in the case of TN-C and TN-T, more than one region of contact may even be involved (see Chapter VII). It is difficult to rationalize these multiple interaction sites with a completely globular structure for TN-I. In addition, both skeletal (McCubbin and Kay, 1982) and cardiac (Burtnick, 1977) TN-I possess the least amounts of ordered secondary structure in their respective troponin systems. This fact, along with the high sensitivity to proteolysis exhibited by TN-I, suggests that the polypeptide chain may exist in a relatively open, expanded conformation. However, more chemical and physical studies are required, both in solution and on the thin filament, to determine whether TN-I is indeed an asymmetric protein, as indicated by its hydrodynamic properties.

CHAPTER VII

TROPONIN SUBUNITS: BINARY COMPLEXES AND RECONSTITUTION OF WHOLE TROPONIN

A. RESULTS

Interactions between cardiac troponin subunits were studied in both 0.2 M and 0.5 M NMED buffer systems. Since all three subunits are individually soluble in 0.5 M NMED, while only TN-C is soluble in 0.2 M NMED, troponin complexes were prepared by two different methods. Complexes in 0.5 M NMED were formed by dissolving the subunits in urea and separately dialyzing them vs the analytical buffer. The subunits were then mixed in the appropriate molar ratio. Complexes in 0.2 M NMED were prepared by mixing the subunits prior to the removal of urea by dialysis. Molar protein concentrations were determined using the following parameters: TN-C ($E_{276 \text{ nm}}^{1\%, 1 \text{ cm}} = 2.3$, $M_r = 18,500$), TN-I ($E_{276 \text{ nm}}^{1\%, 1 \text{ cm}} = 5.2$, $M_r = 23,000$) and TN-T ($E_{276 \text{ nm}}^{1\%, 1 \text{ cm}} = 4.4$, $M_r = 36,000$).

1. TN-IC

Binary complex formation between troponin subunits was monitored by gel filtration as well as by velocity and equilibrium ultracentrifugation. TN-I and TN-C mixed in a

1:1 mole ratio in 0.5 M NMED (pH 7.2) eluted from Sephadryl S-300 in a single, symmetrical peak with an apparent Stokes radius of 36 Å (Figure 31). This value is larger than that expected for either TN-I (30 Å) or TN-C (24 Å) alone, indicating that these proteins form a stable bimolecular complex (TN-IC). Similar results were observed for TN-IC in 0.2 M NMED, where TN-I was induced into solution by its interaction with TN-C. Addition of 2 mM Ca^{2+} to TN-IC in either solvent system produced no significant change in R_s, gel .

The molecular weight behaviour of TN-IC in 0.5 M NMED (pH 7.2), examined by meniscus depletion sedimentation equilibrium, is shown in Figure 32. In the absence of Ca^{2+} , the molecular weight of TN-IC was close to the value expected for the complex ($M_r = 41,500$), except at the meniscus. The reduced M_w observed in this region of the cell could be due either to partial dissociation of the complex at low protein concentration or to a slight excess of one subunit over the other. The molecular weight of TN-IC was increased in 2 mM Ca^{2+} , suggesting further aggregation of the complex (Figure 32). Similar results were observed in 0.2 M NMED.

TN-IC in 0.2 M NMED (pH 7.2) exhibited a single schlieren boundary in sedimentation velocity experiments

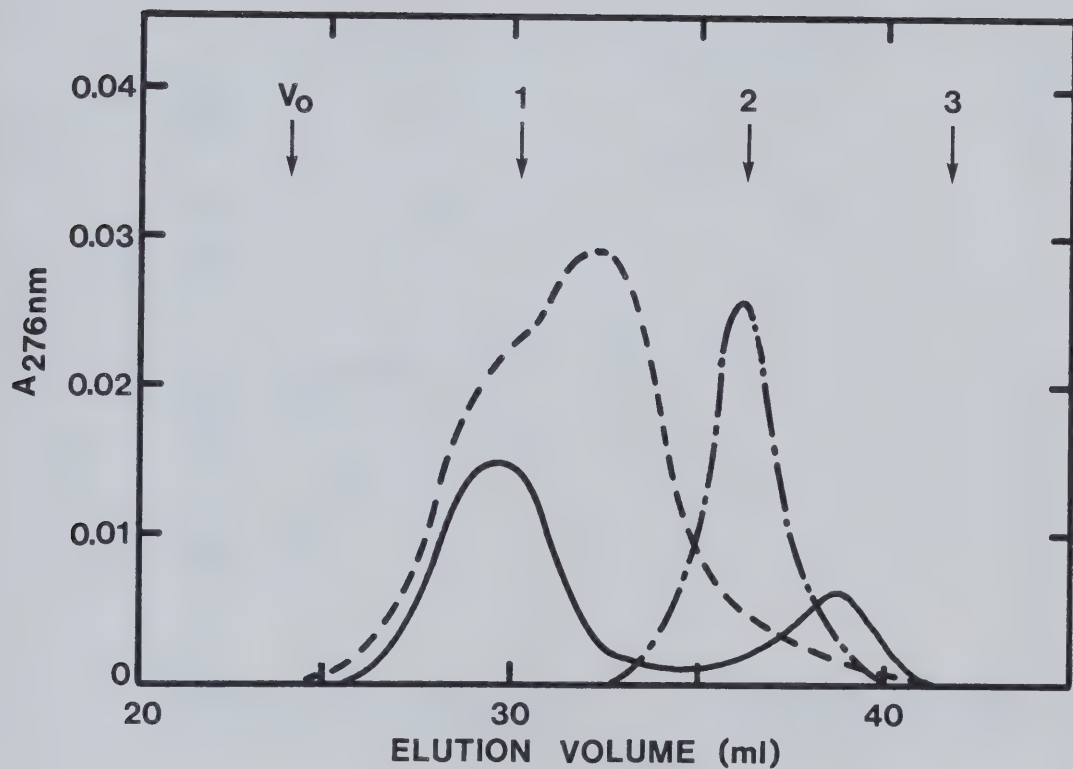


Figure 31. Analytical gel filtration of binary troponin complexes on Sephadryl S-300. Samples (0.4-0.8 mgs in 300 μ l) of TN-IC (---), TN-CT (—) and TN-IT (- - -) were applied to the column (58 \times 1.1 cm) in 0.5 M NMED (pH 7.2). The flow rate was 13 ml/h and 0.4 ml fractions were collected. The void volume (V_o) was measured with Blue dextran. Protein standards and Stokes radii were: 1 β -galactosidase (69 Å); 2 BSA (35 Å); 3 myoglobin (19.8 Å).

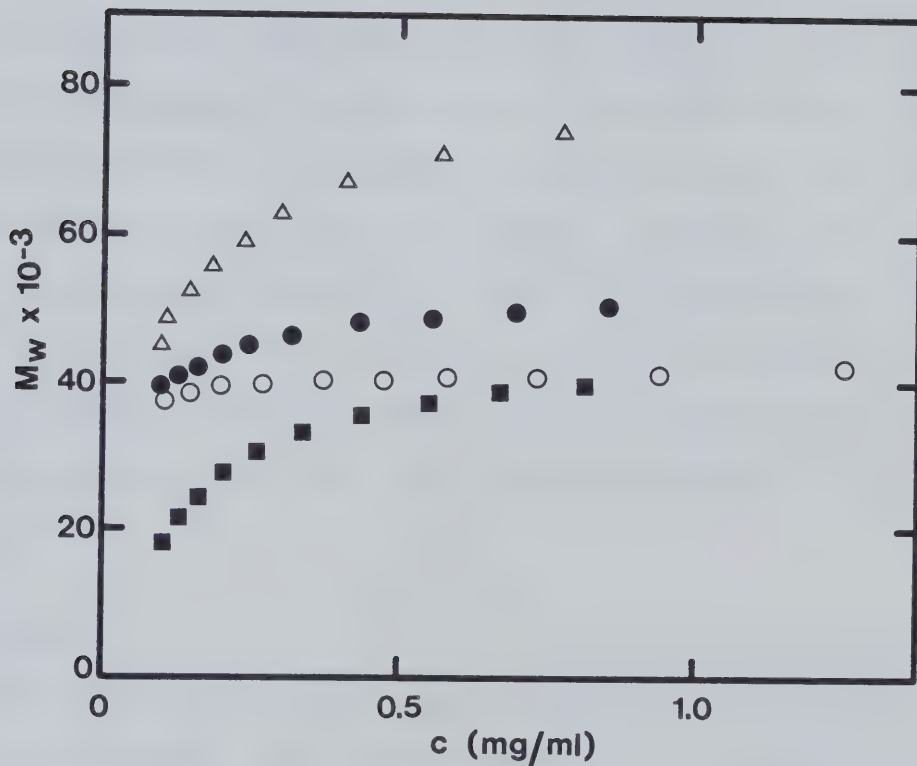


Figure 32. Effect of protein concentration on the molecular weight of binary troponin complexes. Meniscus depletion sedimentation equilibrium experiments were performed on samples of TN-IC (\circ , \bullet), TN-CT (\blacksquare) and TN-IT (\triangle) in 0.5 M NMED (pH 7.2). Initial protein concentrations and equilibrium rotor speeds were: (\circ) 0.85 mg/ml, 28,000 rpm; (\bullet , \blacksquare) 0.68 mg/ml, 28,000 rpm; (\triangle) 0.60 mg/ml, 24,000 rpm. Ca^{2+} concentrations were: (\circ , \triangle) no Ca^{2+} ; (\bullet , \blacksquare) 2 mM Ca^{2+} .

(Figure 33). The sedimentation coefficient was relatively independent of protein concentration and $s_{20,w}$ was 2.9 S (Figure 34A). Since this value is substantially higher than expected for the individual subunits ($s_{20,w} \sim 2$ S), this technique supports the existence of a stable TN-IC complex. The sedimentation coefficient of TN-IC was not significantly affected by the addition of 2 mM Ca^{2+} (Figure 34A).

The reduced viscosity of TN-IC in 0.2 M NMED ($\pm \text{Ca}^{2+}$) was also measured as a function of protein concentration (Figure 34B). The corrected intrinsic viscosity of TN-IC in the absence of Ca^{2+} (8.7 ml/g) was reduced to 6.9 ml/g in 2 mM Ca^{2+} .

2. TN-CT

In contrast to TN-IC, no interaction between TN-C and TN-T was observed when these subunits were mixed in a 1:1 mole ratio. Both gel filtration (Figure 31) and sedimentation velocity (Figure 33) experiments in 0.5 M NMED (pH 7.2) exhibited bimodal profiles with elution and schlieren peaks corresponding to the individual subunits. Moreover, dialysis of TN-C and TN-T, mixed in urea, against 0.2 M NMED resulted in the precipitation of most of the TN-T. This subunit, unlike TN-I, is not solubilized by TN-C at the lower ionic strength. Identical results were obtained in the presence of 2 mM Ca^{2+} or when the complex (in urea) was dialyzed vs buffer containing 1 M NaCl prior to

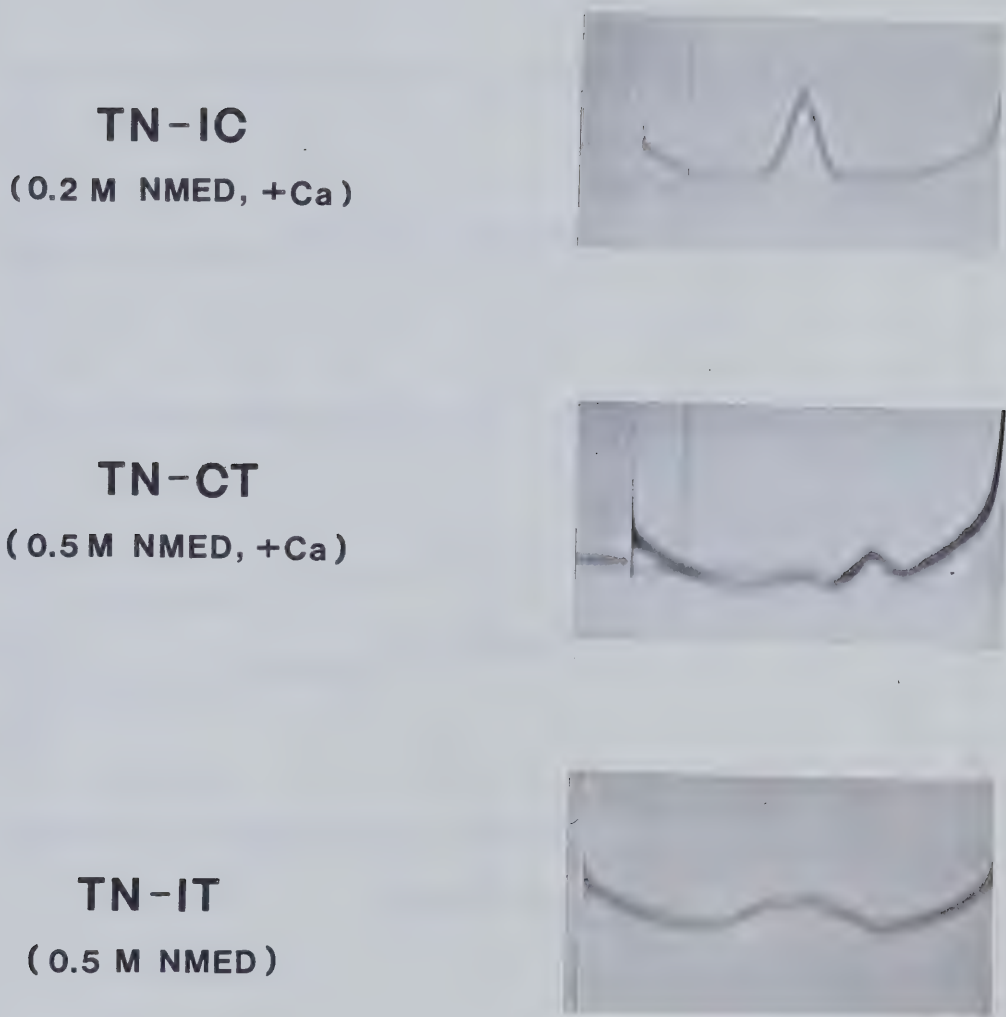


Figure 33. Schlieren photographs of binary troponin complexes (pH 7.2). Sedimentation velocity runs were performed at 60,000 rpm (20°C) using aluminum synthetic boundary cells. Sample concentrations and photo times were: TN-IC (2.0 mg/ml, 20 min); TN-CT (1.7 mg/ml, 50 min); TN-IT (2.0 mg/ml, 40 min).

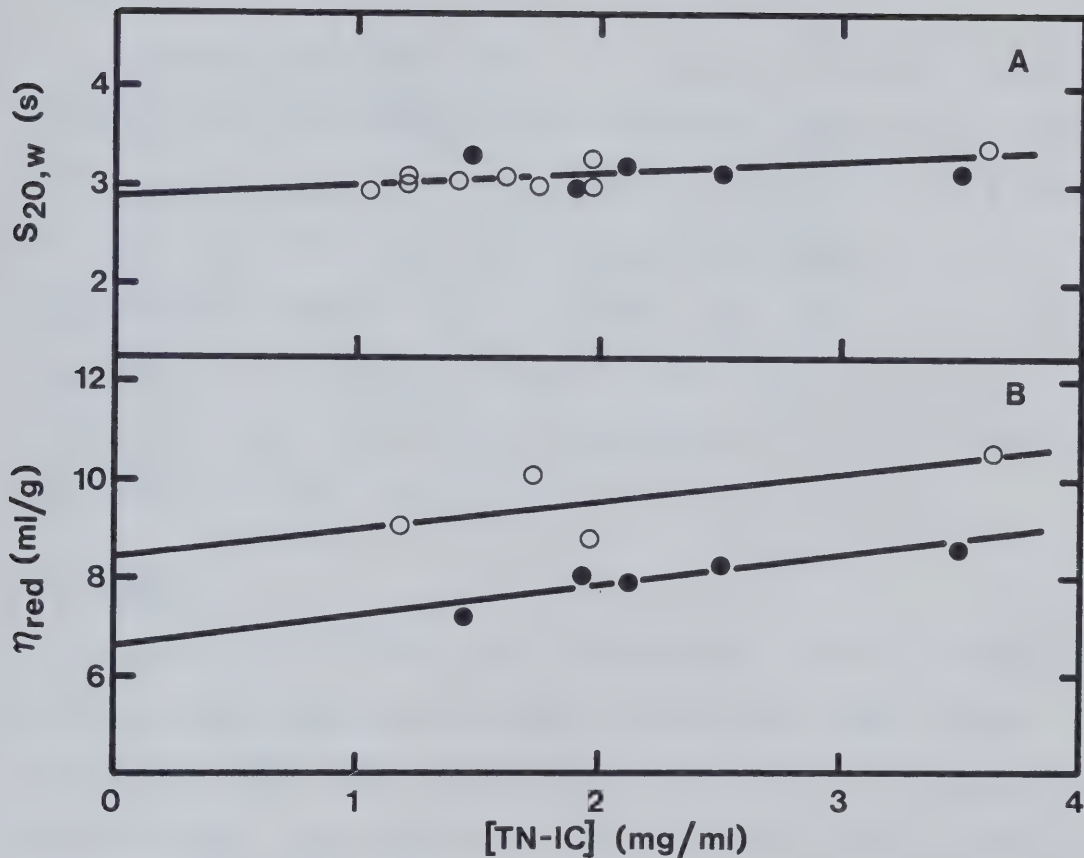


Figure 34. Physical properties of TN-IC. (A) Concentration dependence of the sedimentation coefficient of TN-IC in 0.2 M NMED (pH 7.2). Samples (0.4 ml) were sedimented at 60,000 rpm in aluminum synthetic boundary cells (12 mm). The value of $s_{20,w}^0$ (2.90 S) was calculated using the $- \text{Ca}^{2+}$ data only. (B) Viscosity of TN-IC in 0.2 M NMED (pH 7.2). The uncorrected intrinsic viscosity values are 8.4 ml/g ($- \text{Ca}^{2+}$) and 6.6 ml/g ($+ \text{Ca}^{2+}$). Calcium concentrations were: (○) no Ca^{2+} ; (●) 2 mM Ca^{2+} .

equilibration with the analytical solvent (Holroyde et al., 1980).

Further evidence that TN-C and TN-T do not interact strongly was provided by sedimentation equilibrium (Figure 32). The observed molecular weight of TN-CT in 0.5 M NMED (+ Ca²⁺) was well below the value expected for the bimolecular complex ($M_r = 54,500$). In fact, M_w near the meniscus was similar to that of TN-C ($M_r = 18,500$), indicating that most of the aggregated TN-T is sedimented to the bottom of the cell in this type of experiment.

3. TN-IT

Evidence for TN-I-TN-T interaction in 0.5 M NMED (pH 7.2) was obtained by all three techniques used. The Sephadryl S-300 elution profile (Figure 31) revealed a new protein peak, eluting at a position between the individual subunits. SDS polyacrylamide gels of fractions in this region indicated the presence of both TN-I and TN-T. However, the shape of the elution profile shown in Figure 31 suggests that TN-IT complex formation is incomplete. This conclusion is supported by sedimentation velocity experiments (Figure 33), in which a number of poorly-resolved schlieren peaks were observed. Moreover, the apparent molecular weight of the TN-IT mixture was quite variable over the cell (Figure 32). The lack of material with M_w corresponding to TN-I ($M_r = 23,000$) indicates that

TN-T interacts more strongly with this subunit than with TN-C.

4. Reconstituted Troponin

The stability of the ternary TN-ICT complex, reconstituted from the subunits in an equimolar ratio, was investigated in 0.5 M NMED (pH 7.2) by gel chromatography and sedimentation equilibrium. The Sephadryl S-300 elution behaviour of TN-ICT and native undissociated troponin were indistinguishable: both proteins eluted in a single sharp peak which contained all three subunits as determined by SDS polyacrylamide gel electrophoresis (Figure 35A). No effect of Ca^{2+} was observed. Gel filtration was also used to examine the effect of varying the subunit ratio on the reconstitution of troponin (Figure 35B). When troponin was prepared with an extra mole of TN-I ($\text{TN-I}_2\text{CT}$) or TN-C ($\text{TN-IC}_2\text{T}$), this excess subunit did not appear to associate with the troponin complex on Sephadryl S-300. Rather, the additional TN-I and TN-C eluted in separate peaks, exhibiting R_s ,gel values expected for the individual subunits in each case.

Meniscus depletion and conventional sedimentation equilibrium experiments also provided evidence for the stability of the TN-ICT complex (Figure 36). The apparent molecular weight of TN-ICT was similar to that of native troponin over the entire protein concentration range

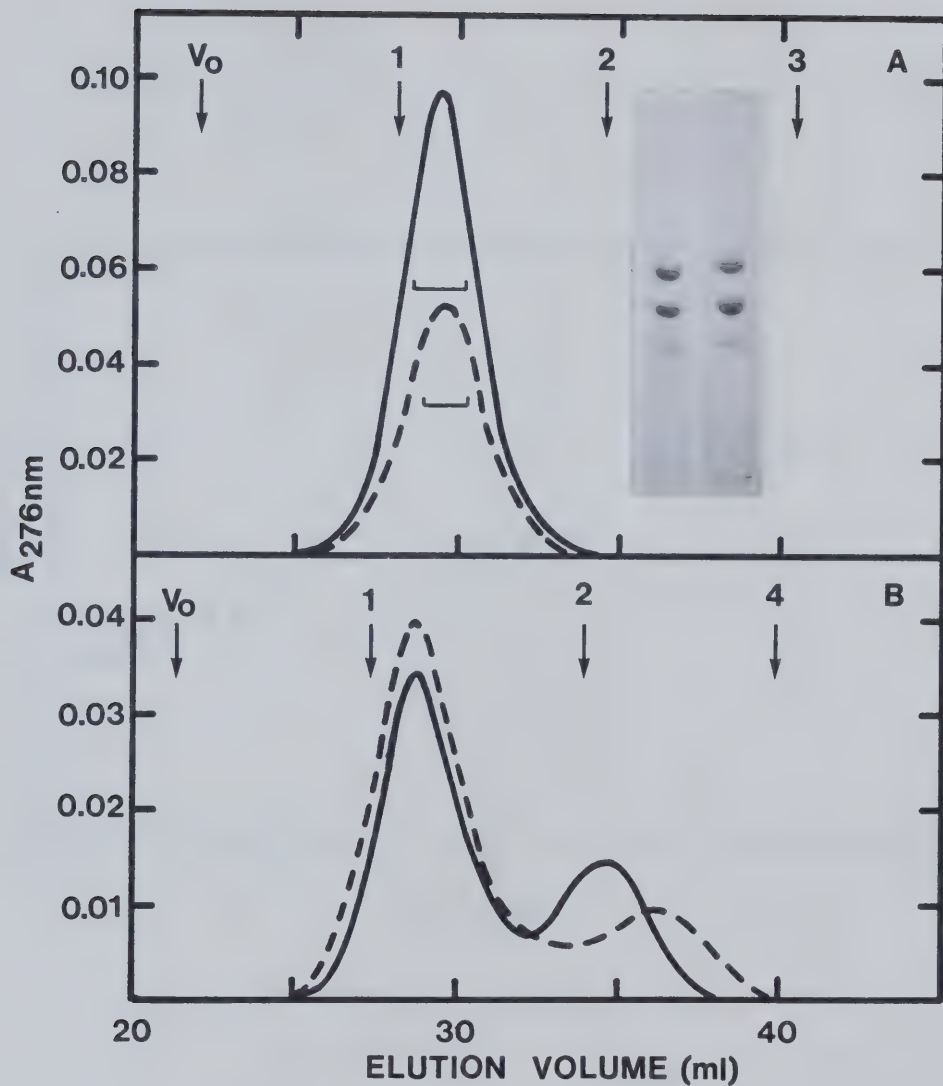


Figure 35. Analytical gel filtration of native and reconstituted troponin on Sephadex S-300. (A) Native troponin (—) and TN-ICT (---). Inset: SDS polyacrylamide gels of the indicated native (left) and reconstituted troponin fractions. (B) TN-I₂CT (—) and TN-IC₂T (---). Samples (0.4-0.8 mgs in 300 μ l) were applied to the column (58×1.1 cm) in 0.5 M NMED (pH 7.2). The flow rate was 13 ml/h and 0.4 ml fractions were collected. The void volume (V_0) was measured with Blue dextran. Protein standards and Stokes radii were: 1 β -galactosidase (69 Å); 2 BSA (35 Å); 3 myoglobin (19.8 Å); 4 cytochrome c (17.2 Å).

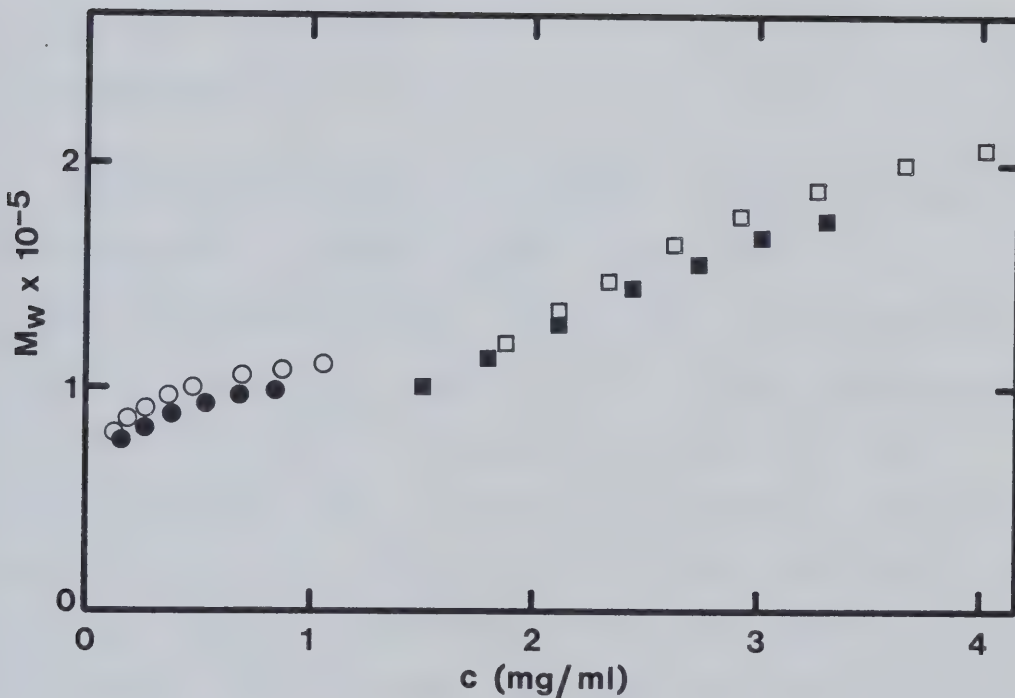


Figure 36. Effect of protein concentration on the molecular weight of native troponin (\circ, \square) and reconstituted TN-ICT (\bullet, \blacksquare). Meniscus depletion (circles) and conventional (squares) sedimentation equilibrium experiments were performed on samples in 0.5 M NMED (- Ca²⁺) at pH 7.2. Initial protein concentrations and equilibrium rotor speeds were: (\circ, \bullet) 1.0 mg/ml, 17,000 rpm; (\square) 2.8 mg/ml, 4,800 rpm; (\blacksquare) 2.0 mg/ml, 5,200 rpm.

examined, although M_w for the complex was slightly lower.

As with TN-IC, this decreased M_w could be due to either some dissociation or subunit excess in the mixture.

B. DISCUSSION

Interactions within the troponin complex are central to the mechanism of striated muscle regulation. Most thin filament regulatory models, such as the steric blocking hypothesis (Figure 3), invoke a Ca^{2+} -induced conformational change in TN-C which is propagated through the other troponin subunits and tropomyosin, ultimately relaying control to the force-generating actomyosin machinery. Much effort has thus been devoted to characterizing the nature of these subunit interactions, including the specific primary structure regions involved for each protein. The most valuable information has been obtained by chemical methods, such as cross-linking or side chain reactivity experiments, or by studying the interactions between chemically or proteolytically defined fragments of the troponin subunits. For rabbit skeletal troponin subunits, these mutual contact sites are now understood in a fair amount of detail (reviewed by Perry, 1979; McCubbin and Kay, 1980).

The ability of cardiac troponin subunits to interact with each other is evident in the preparation and handling

of these proteins. The subunits firmly adhere together during several stages in the purification of native troponin and are only separated in the presence of strong denaturants, such as 6 M urea. The enhanced solubility of Tn-I and TN-T in the whole troponin complex is further proof that interaction alters the properties of the individual subunits. Due to the importance of intersubunit interactions in troponin, there has been some interest in comparing the skeletal and cardiac proteins in this regard. Much of this work has originated from our own laboratory (Burtnick, 1977; Hincke, 1981). The experiments described in this chapter were intended not simply to provide additional evidence for interaction, but also to examine the structural properties of any stable complexes formed.

Of the possible binary subunit combinations, only TN-I and TN-C are capable of forming a stable equimolar complex which is suitable for hydrodynamic characterization. Cardiac TN-I-TN-C interaction has previously been demonstrated by circular dichroism (Burtnick and Kay, 1976), affinity chromatography (Syska et al., 1974), gel electrophoresis (Burtnick et al., 1975b) and differential scanning calorimetry (Jacobson et al., 1981). This interaction is also manifested in the functions of these proteins, since the Ca^{2+} -binding properties of TN-C

(Holroyde et al., 1980) and the inhibitory properties of TN-I (Burtnick et al., 1975b) are each substantially altered in the presence of the other subunit. Both cardiac (Burtnick et al., 1975b) and skeletal (Head and Perry, 1974) TN-IC complexes are stable even in 6 M urea, although the skeletal proteins require Ca^{2+} for this interaction.

The regions of primary structure involved in interaction have been thoroughly investigated for skeletal TN-C and TN-I. TN-C interaction sites are located on two positively-charged fragments of the skeletal TN-I molecule, involving residues 1-47 and 96-117 (Syska et al., 1976). This latter fragment is particularly interesting since it also contains the inhibitory activity of TN-I. Indeed, a cyanogen bromide fragment of TN-C (residues 83-134), which encompasses Ca^{2+} -binding site III, is able to form Ca^{2+} -dependent complex with TN-I, thus neutralizing the inhibition by this subunit (Weeks and Perry, 1978). This work has been supported by cross-linking (Chong and Hodges, 1981) and sulfhydryl reactivity studies (Chong and Hodges, 1982b), which have demonstrated the proximity of TN-C cysteine 98 to TN-I in the complex. Using a variety of TN-C fragments, Grabarek et al. (1981) have shown that no less than three regions of TN-C are involved in complex formation with TN-I. These regions are the three flanking helices on the N-terminal side of Ca^{2+} -binding sites II, III and IV.

Interactions involving the first two sites appear to require Ca^{2+} .

In order to use the present hydrodynamic data to structurally characterize the cardiac TN-IC complex, it is necessary to assume that the measured physical parameters correspond to the bimolecular unit of $M_r = 41,500$. This is an oversimplification since there is evidence for both dissociation of the complex at low protein concentration and possible aggregation at higher concentrations, especially in the presence of Ca^{2+} . Nevertheless, this assumption appears reasonable because of the excellent agreement in the Stokes radius values determined by gel filtration and sedimentation velocity, two techniques which are sensitive to protein size and shape in different fashions. The value of $R_{s,\text{sed}}$ for TN-IC ($- \text{Ca}^{2+}$) is 36 Å, calculated from Equation 9 where $s_{20,w}^0 = 2.9$ S (Figure 34A). This value is indistinguishable from $R_{s,\text{gel}}$ obtained by Sephadryl S-300 chromatography (Figure 31). Thus, the translational frictional ratio (f/f_{\min}) of TN-IC is 1.58, using Equation 2 where $R_o = 22.7$ Å. Since this value of f/f_{\min} is similar to that for both TN-I and TN-C alone ($f/f_{\min} \sim 1.5$), these subunits would appear to combine in a manner that does not substantially alter the hydrodynamic properties relative to the individual molecules. Asymmetry of the TN-IC complex is also indicated by the relatively large intrinsic viscosity of the protein

(8.7 ml/g, Figure 34B). Preliminary electron microscopy studies suggest that the "head region" of skeletal troponin, which consists mainly of TN-I and TN-C, may be somewhat flattened with a width of 100 Å (Flicker et al., 1982). However, the frictional ratio of TN-IC is still somewhat less than that of native troponin ($f/f_{min} = 1.85$), so the hydrodynamic properties are not inconsistent with the more restricted disposition of these subunits schematically represented in Figure 2.

The effect of Ca^{2+} on the hydrodynamic properties of TN-IC is complicated by its influence on the degree of protein association. While addition of Ca^{2+} increased the apparent molecular weight of the complex, only minor changes in $s_{20,w}$ and $R_{s,gel}$ were observed. On the basis of a Ca^{2+} -induced decrease in viscosity, it is tempting to speculate that TN-IC, like TN-C alone, undergoes a conformational change to a more compact shape. However, it is difficult to assess the relative contributions of tertiary and quaternary structure changes to the viscosity behaviour.

The inability of hydrodynamic techniques to detect complex formation between cardiac TN-C and TN-T would seem to be in conflict with various reports demonstrating such an interaction. These have provided evidence based on circular dichroism (Burtnick and Kay, 1976), electron microscopy (Yamaguchi and Greaser, 1979), gel electrophoresis (Burtnick

et al., 1976) and calorimetry (Jacobson et al., 1981). However, the transport methods used in this investigation are only sensitive to the overall physical properties of the proteins involved and might not be expected to detect weak subunit interactions. Indeed, gel electrophoresis studies have indicated that only a small fraction of the total TN-C and TN-T mixed is involved in complex formation (Burtnick et al., 1976). Experiments with the corresponding subunits from skeletal muscle have also suggested that this interaction is decidedly weaker than that between TN-C and TN-I (van Eerd and Kawasaki, 1973; Mani et al., 1974). These studies showed that the strength of skeletal TN-C-TN-T interaction is increased in the presence of Ca^{2+} ; no such effect was observed here with the cardiac proteins.

From the sequence of skeletal TN-T, Pearlstone et al. (1976) suggested that the highly basic C-terminal portion of the molecule might be involved in binding the acidic TN-C subunit. This proposal has since been supported experimentally by studying the binding of TN-T fragments to a TN-C-Sepharose affinity column (Pearlstone and Smillie, 1978) and by measuring the relative reactivity of TN-T lysine residues in the complex (Hitchcock et al., 1981). Immunoelectron microscopy has also indicated that the C-terminal region of TN-T is near both TN-C and TN-I on the thin filament (Ohtsuki, 1979).

Interaction between skeletal TN-I and TN-T was originally suggested on the basis of electron microscopic evidence (Margossian and Cohen, 1973) as well as the tendency of these proteins to copurify (Hartshorne and Mueller, 1969). However, early studies with the purified subunits could find no explicit evidence for such an interaction (van Eerd and Kawasaki, 1973). Hitchcock (1975) eventually demonstrated that TN-I and TN-T could be cross-linked in troponin and suggested that they must be located within 6 Å of each other. TN-IT complex formation in skeletal (Horwitz et al., 1979) and cardiac (Hincke et al., 1979) troponin have more recently been confirmed by a number of spectroscopic and physical methods. These studies have shown that this interaction is very sensitive to the oxidation state of the cysteine residues in TN-I, which may explain the failure of earlier investigators to detect the TN-IT complex. It is now believed that TN-I interacts mainly with the C-terminal half of the TN-T molecule, based on fragment interaction (Katayama, 1979; Pearlstone and Smillie, 1980) and lysine reactivity (Hitchcock et al., 1981) studies. It is possible that this interaction is even affected by Ca^{2+} in the presence of TN-C (Hitchcock-DeGregori, 1982). A very recent cross-linking investigation suggests that the region of skeletal TN-I around cysteines 48 and 64 may be involved in the binding of TN-T (Chong and

Hodges, 1982c). These residues probably correspond to cysteines 75 and 92 in (rabbit) cardiac TN-I, which are thought to be important in the interaction with TN-T (Hincke et al., 1979).

In agreement with the earlier results from our laboratory (Hincke et al., 1979), partial formation of a cardiac TN-IT complex in 0.5 M NMED is indicated by gel filtration and sedimentation velocity. While the complicated boundaries observed by these techniques do not permit an accurate hydrodynamic analysis, a few points are worthy of mention. If the new protein peak seen by gel filtration (Figure 31) indeed represents the TN-IT complex, the fact that it elutes between the individual subunits suggests that TN-T is dissociated from its normal aggregated state by the TN-I subunit. Although partially obscured in an elution profile that is probably the sum of at least three separate components, this proposed TN-IT complex appears to have a Stokes radius in the range of 50-60 Å. It is interesting that this value is similar to the limiting $R_s,_{gel}$ of native troponin (52 Å), perhaps indicating that the removal of TN-C does not grossly alter the hydrodynamic properties of the whole complex.

Whereas bimolecular interactions between the cardiac troponin subunits exhibit a wide range of stability, the combination of all three subunits results in a tightly-

associated complex, similar in its physical properties to native troponin. This stabilization of troponin, by mutual subunit interactions, was also observed in a thermodynamic study on the cardiac system (Jacobson et al., 1981). By measuring thermal denaturation using differential scanning calorimetry, these workers concluded that there is a considerably higher degree of order in the ternary complex than in the bimolecular units. Moreover, Burtnick and Kay (1976) noted that reconstituted troponin contains a larger amount of ordered secondary structure than expected by simply adding the circular dichroism contributions of the individual subunits. TN-I would appear to have a special significance in the reconstitution of troponin since it is the only subunit that interacts strongly with each of the other two subunits in a binary fashion.

Potter and his coworkers (Johnson et al., 1980) have also reported the reconstitution of cardiac troponin, from subunits mixed in urea. The present study indicates that reassembly of the complex does not require the presence of urea, but rather can proceed with previously-refolded subunits in a non-denaturing solvent (0.5 M NMED). Similarly, skeletal troponin can be reconstituted from subunits in a native-like conformation (Eisenberg and Kielley, 1974; Mani et al., 1974), despite earlier claims to the contrary (Greaser and Gergely, 1971). It should not be

forgotten that, in addition to the structural stability demonstrated here, reconstituted cardiac troponin is also biologically-active (Burtnick et al., 1976).

It is almost universally accepted that skeletal troponin, on the thin filament, consists of one molecule each of TN-C, TN-I and TN-T. Early electron microscopic evidence indicated that troponin, tropomyosin and actin are present in a molar ratio of 1:1:7 (Ebashi et al., 1969). This finding was supported by Potter (1974), who separated all the myofibrillar proteins by SDS polyacrylamide gel electrophoresis and further demonstrated that the TN-C:TN-I:TN-T molar ratio is 1:1:1. However, this rather fundamental tenet has recently been challenged by Sperling et al. (1979), who have reported that skeletal troponin actually contains two TN-I subunits per molecule. They have claimed that the observed variability of subunit composition is due to proteolytic degradation during troponin purification and have introduced a casein-Sepharose chromatography step to remove these endogenous proteases. Although no similar conflict has developed regarding cardiac troponin, the importance of determining the subunit stoichiometry of this protein is obvious by analogy.

The available evidence suggests that native cardiac troponin prepared by our methodology is 1:1:1 with respect to its constituents. Native troponin was compared to

reconstituted TN-ICT using densitometric scans of SDS polyacrylamide gels, such as those shown in Figure 35. Although the staining intensity of TN-C was rather weak and somewhat variable, the TN-T:TN-I staining ratios were identical (about 1.2:1) in both the native and reconstituted proteins. The amino acid composition of native troponin was also compared to that expected for TN-ICT and TN-I₂CT. Table V indicates that the amino acid composition is not a very sensitive function of the assumed subunit stoichiometry, probably because of the overall similarity among the subunits. Nevertheless, where there are significant expected differences between TN-ICT and TN-I₂CT, the composition of our native troponin more closely resembles that of the equimolar complex for most amino acids.

These considerations still do not address the question raised by Sperling et al. (1979), i.e. whether troponin isolated from muscle corresponds to the protein on the thin filament. However, the gel filtration results (Figure 35) do indicate that, unlike TN-ICT, complexes reconstituted with an extra mole of TN-I (or TN-C) are unstable. It could still be argued that the purification of troponin somehow destroys the binding site of a second TN-I subunit, or that this extra subunit is very weakly associated with the complex in vivo. However, the simplest interpretation of

TABLE V: COMPARISON OF THE AMINO ACID COMPOSITION OF NATIVE BOVINE CARDIAC TROPONIN TO THAT EXPECTED FOR TN-ICT AND TN-I₂CT

| Amino Acid | Number of Residues ^a | | | |
|------------|---------------------------------|----------------------|------------------------------|------------------------------|
| | TN-ICT ^b | TN-I ₂ CT | Native Troponin ^c | Native Troponin ^d |
| Asx | 72 | 67 | 73.7 | 69.8 |
| Thr | 25 | 25 | 23.2 | 27.1 |
| Ser | 22 | 23 | 20.4 | 27.7 |
| Glx | 148 | 126 | 136.9 | 140.6 |
| Pro | 20 | 21 | 21.0 | 17.4 |
| Gly | 38 | 36 | 39.8 | 41.7 |
| Ala | 56 | 56 | 56 | 56 |
| Val | 29 | 27 | 31.9 | 33.8 |
| Met | 20 | 17 | 19.0 | 18.6 |
| Ile | 28 | 25 | 27.5 | 28.0 |
| Leu | 53 | 52 | 54.2 | 51.9 |
| Tyr | 10 | 9 | 11.3 | 13.4 |
| Phe | 20 | 17 | 23.5 | 22.8 |
| His | 7 | 7 | 10.2 | 11.5 |
| Lys | 70 | 66 | 71.6 | 65.8 |
| Arg | 60 | 58 | 64.8 | 58.1 |

^a All data were normalized to a standard alanine content of 56 residues per molecule, based on a molecular weight for TN-ICT of 78,000.

^b The data for TN-ICT and TN-I₂CT were calculated from the sequence of bovine cardiac TN-C (van Eerd and Takahashi, 1975) as well as the amino acid compositions of cardiac TN-I (Burtnick et al., 1975b) and TN-T (Burtnick et al., 1976).

^c Our DEAE-Sephadex-purified cardiac troponin (60 h hydrolyzate).

^d Cardiac troponin preparation reported by Lin and Cassim (1978).

these results is that cardiac troponin, in its natural state, consists of the three subunits in an equimolar ratio. There is evidence for a precursor pool of unassembled TN-I in rat cardiac myofibrils (Martin, 1981), but there is presently no reason to believe that this surplus protein has an active role in the function of troponin.

CHAPTER VIII

GENERAL DISCUSSION

The earliest pictoral representation of troponin was that of a globular protein situated at periodic intervals along the thin filament (Ebashi et al., 1969). In recent years, however, several lines of evidence have indicated that troponin is more elongated, perhaps spanning as much as one-third of the tropomyosin period length, or about 130 Å. This new knowledge has been derived mainly from the localization of skeletal TN-T fragments on tropomyosin; this approach has demonstrated that TN-T is an extended molecule with at least two well-separated tropomyosin-binding domains. On the other hand, little is known about the possible shapes of TN-C and TN-I in the troponin complex.

For the most part, the results of the present project on bovine cardiac troponin support this more modern view. While these proteins are certainly not asymmetric in comparison to other muscle components such as myosin and tropomyosin, hydrodynamic experiments have indicated that neither troponin nor its subunits should be thought of as typical globular proteins. At physiological concentrations of Mg^{2+} and Ca^{2+} , TN-C would appear to be the most compact subunit, with a frictional ratio of about 1.4. TN-I would

be slightly more asymmetric ($f/f_{\min} = 1.53$). The 1:1 mole complex of these two subunits (TN-IC) also seems to be moderately asymmetric ($f/f_{\min} = 1.58$). Native troponin ($f/f_{\min} = 1.85$) and TN-T are probably even more elongated, at least based on their properties in solution. Of course, these generalizations can be made only under the assumption that all other contributing factors, such as hydration, are equal among the proteins. Although no comparable hydrodynamic study has yet been reported for skeletal troponin, the results obtained with the cardiac proteins are not inconsistent with the structural information that is available for this more popular muscle system.

The general limitations of hydrodynamic analysis have already been outlined in the Introduction to this thesis. However, it is necessary at this time to reiterate some of the special problems involved in working with cardiac troponin and its subunits. To begin with, this is not a "clean" system. TN-T and TN-I, in particular, are very insoluble proteins and unnatural solvent conditions are required to achieve what little solubility is possible. Secondly, many of these proteins, such as native troponin, TN-T, and to a lesser extent TN-I and TN-IC, tend to self-associate in non-denaturing solvents. As a result, many physical parameters must be estimated by extrapolation through a concentration range in which this equilibrium is

occurring. These parameters will be weight averages at those concentrations. Thirdly, the use of ellipsoidal models (or any other "smooth" model) is clearly invalid for proteins, like native troponin and the TN-IC complex, which are composed of non-identical subunits. This may not be a serious limitation in view of the relatively low amount of detail afforded by hydrodynamic techniques, but it should be kept in mind. Finally, troponin and its subunits are not designed to function free in solution. The constraints of interaction with each other and with other proteins on the thin filament could result in quite different structures for these proteins in situ.

It is this latter consideration that has led some investigators to question the usefulness of experiments involving the isolated troponin subunits. Lin and Cassim (1978) have claimed that the harsh conditions required to dissociate troponin into subunits result in significant and irreversible conformational perturbation of these proteins. They have suggested that such studies may therefore not be biologically-relevant. We cannot agree with this view. The present investigation, as well as many others, have indicated that troponin is a reasonably hardy oligomeric protein, capable of being dissociated and reconstituted with few ill effects. Furthermore, the individual subunits exhibit characteristics related to their

specific functions in vivo: TN-C alone binds Ca^{2+} ; TN-T alone binds tropomyosin; TN-I alone inhibits the actomyosin ATPase. When these subunits are recombined a stable complex is formed, similar in its physical and biological properties to native troponin. As will be discussed in the following paragraphs, problems in the interpretation of results do arise when troponin is considered in isolation from other thin filament components. Nevertheless, the study of troponin and its constituents in solution is, without question, invaluable to a complete understanding of striated muscle regulation.

It is difficult to imagine a thin filament regulatory mechanism that does not involve some form of Ca^{2+} -induced conformational change originating at the troponin complex. However, no definitive evidence for such a change was obtained by the hydrodynamic methods used in this investigation. Even with TN-C, most of the observed structural effects probably arise from cation binding to the non-regulatory $\text{Ca}^{2+}/\text{Mg}^{2+}$ sites, since Mg^{2+} can fully replace Ca^{2+} in decreasing the intrinsic viscosity of this subunit. These results would tend to suggest that the Ca^{2+} -trigger on the thin filament involves a relatively minor conformational alteration. Cross-linking experiments have also indicated that the topology of skeletal troponin in solution is not substantially influenced by Ca^{2+} (Sutoh,

1980).

How can the observed structural insensitivity of these proteins to Ca^{2+} be reconciled with a control mechanism, such as the steric blocking hypothesis, in which fairly large protein motions are presumed to occur? In fact, there may be no discrepancy at all. It is important to remember that only part of the thin filament regulatory unit has been examined in the present study. Since troponin contains sites which interact with both tropomyosin and actin, it is conceivable that a rather small Ca^{2+} -induced conformational change within the troponin complex would be amplified when relayed to these other proteins. For example, a slight rotation of one troponin subunit relative to the others might escape detection by hydrodynamic techniques while still causing a substantial change in the orientation of these interaction sites. Alternatively, one or more interaction sites (i.e. between TN-I and actin) could be strengthened or weakened in a Ca^{2+} -dependent manner, thus allowing troponin to move relative to tropomyosin and/or actin. Indeed, changes of this nature have been observed by fluorescence in reconstituted thin filaments (Miki, 1979) and by cross-linking experiments between troponin and tropomyosin (Chong and Hodges, 1982a). Of course, all possible mechanistic models will have to be analyzed within a framework of chemical equilibrium and cooperativity along

the thin filament. This cooperativity between adjacent troponin-tropomyosin units has become very interesting in light of the present knowledge that TN-T extends to the tropomyosin overlap region.

BIBLIOGRAPHY

Adelstein, R.S., and Eisenberg, E. (1980) Annu. Rev. Biochem. 49, 921-956.

Andrews, P. (1965) Biochem. J. 96, 595-606.

Babul, J., and Stellwagen, E. (1969) Anal. Biochem. 28, 216-221.

Barskaya, N.V., and Gusev, N.B. (1981) Biochem. Int. 2, 43-49.

Bernardi, G. (1971) Methods Enzymol. 22, 325-339.

Bernardi, G. (1973) Methods Enzymol. 27, 471-479.

Bloomfield, V., Dalton, W.O., and Van Holde, K.E. (1967) Biopolymers 5, 135-148.

Bradbury, J.H. (1970) in Physical Principles and Techniques of Protein Chemistry (Leach, S.J., Ed.) Part B, pp 99-145, Academic Press, New York.

Bradford, M.M. (1976) Anal. Biochem. 72, 248-254.

Brekke, C.J., and Greaser, M.L. (1976) J. Biol. Chem. 251, 866-871.

Bremel, R.D., Murray, J.M. and Weber, A. (1972) Cold Spring Harb. Symp. Quant. Biol. 37, 267-275.

Burtnick, L.D. (1977) Ph.D. Thesis, University of Alberta.

Burtnick, L.D., and Kay, C.M. (1976) FEBS Lett. 65, 234-237.

Burtnick, L.D., and Kay, C.M. (1977) FEBS Lett. 75, 105-110.

Burtnick, L.D., McCubbin, W.D., and Kay, C.M. (1975a) Can. J. Biochem. 53, 15-20.

Burtnick, L.D., McCubbin, W.D., and Kay, C.M. (1975b) Can. J. Biochem. 53, 1207-1213.

Burtnick, L.D., McCubbin, W.D., and Kay, C.M. (1976) Can. J. Biochem. 54, 546-552.

Byers, D.M., and Kay, C.M. (1982a) Biochemistry 21, 229-233.

Byers, D.M., and Kay, C.M. (1982b) J. Biol. Chem., in press.

Byers, D.M., and Kay, C.M. (1982c) FEBS Lett., in press.

Byers, D.M. McCubbin, W.D., and Kay, C.M. (1979) FEBS Lett. 104, 106-110.

Cann, J.R. (1970) Interacting Macromolecules, pp 102-133, Academic Press, New York.

Cantor, C.R., and Schimmel, P.R. (1980) Biophysical Chemistry, Part II, pp 539-590, W.H. Freeman and Co., San Francisco.

Carlson, F.D. and Wilkie, D.R. (1974) Muscle Physiology, Prentice-Hall, New Jersey.

Casassa, E.F., and Eisenberg, H. (1964) Adv. Protein Chem. 19, 287-395.

Chalovich, J.M., Chock, P.B., and Eisenberg, E. (1981) J. Biol. Chem. 256, 575-578.

Chalovich, J.M., and Eisenberg, E. (1982) J. Biol. Chem. 257, 2432-2437.

Chervenka, C.H. (1969) A Manual of Methods for the Analytical Ultracentrifuge, p 45, Spinco Division of Beckman Instruments, Inc., Palo Alto, California.

Chong, P.C.S., and Hodges, R.S. (1981) J. Biol. Chem. 256, 5071-5076.

Chong, P.C.S., and Hodges, R.S. (1982a) J. Biol. Chem. 257, 9152-9160.

Chong, P.C.S., and Hodges, R.S. (1982b) J. Biol. Chem. 257, 2549-2555.

Chong, P.C.S., and Hodges, R.S. (1982c) J. Biol. Chem. 257, 11667-11672.

Chothia, C. (1975) Nature 254, 304-308.

Cleland, W.W. (1964) Biochemistry 3, 480-482.

Cohn, E.J., and Edsall, J.T. (1943) Proteins, Amino Acids and Peptides, pp 370-381, Reinhold, New York.

Collins, J.H. (1974) Biochem. Biophys. Res. Commun. 58, 301-308.

Collins, J.H., Potter, J.D., Horn, M.J., Wilshire, G., and Jackson, N. (1973) FEBS Lett. 36, 268-272.

Crouch, T.H., and Klee, C.B. (1980) Biochemistry 19, 3692-3698.

Cummins, P., and Perry, S.V. (1978) Biochem. J. 171, 251-259.

Dabrowska, R., Barylko, B., Nowak, E., and Drabikowski, W. (1973) FEBS Lett. 29, 239-242.

Dedman, J.R., Potter, J.D., Jackson, R.L., Johnson, J.D., and Means, A.R. (1977) J. Biol. Chem. 252, 8415-8422.

de Riel, J.K., and Paulus, H. (1978) Biochemistry 17, 5141-5146.

Drabikowski, W., Rafalowska, U., Dabrowska, R., Szpacenko, A., and Barylko, B. (1971) FEBS Lett. 19, 259-263.

Eaton, B.L. (1976) Science 192, 1337-1339.

Ebashi, S. (1963) Nature 200, 1010.

Ebashi, S., Ebashi, F., and Kodama, A. (1967) J. Biochem. (Tokyo) 62, 137-138.

Ebashi, S., Endo, M., and Ohtsuki, I. (1969) Quart. Rev. Biophys. 2, 351-384.

Ebashi, S., and Kodama, A. (1965) J. Biochem. (Tokyo) 58, 107-108.

Ebashi, S., Masaki, T., and Tsukui, R. (1974a) Adv. Cardiol. 12, 59-69.

Ebashi, S., Mikawa, T., Hirata, M., and Nonomura, Y. (1978) Ann. N.Y. Acad. Sci. 307, 451-461.

Ebashi, S., Ohnishi, S., Abe, S., and Maruyama, K. (1974b) in Calcium Binding Proteins (Drabikowski, W., Strzelecka-Golaszewska, H., and Carafoli, E., Eds.), pp 179-195, Elsevier, Amsterdam.

Eisenberg, E., and Kielley, W.W. (1974) J. Biol. Chem. 249, 4742-4748.

Ellman, G.L. (1959) Arch. Biochem. Biophys. 82, 70-77.

England, P.J. (1975) FEBS Lett. 50, 57-60.

Erickson, H.P. (1982) Biophys. J. 37, 96a.

Fiske, C.H., and SubbaRow, Y. (1925) J. Biol. Chem. 66, 375-400.

Flicker, P.F., Phillips, G.N., and Cohen, C. (1982) Biophys. J. 37, 266a.

Gilbert, G.A. (1955) Disc. Faraday Soc. 20, 68-71.

Grabarek, Z., Drabikowski, W., Leavis, P.C., Rosenfeld, S.S., and Gergely, J. (1981) J. Biol. Chem. 256, 13121-13127.

Grand, R.J.A., Wilkinson, J.M., and Mole, L.E. (1976) Biochem. J. 159, 633-641.

Greaser, M.L., and Gergely, J. (1971) J. Biol. Chem. 246, 4226-4233.

Greaser, M.L. and Gergely, J. (1973) J. Biol. Chem. 248, 2125-2133.

Greene, L.E., and Eisenberg, E. (1980) Proc. Natl. Acad. Sci. USA 77, 2616-2620.

Gusev, N.B., Sajgo, M., and Friedrich, P. (1980) Biochim. Biophys. Acta 625, 304-309.

Harrington, W.F. (1979) in The Proteins (Neurath, H., and Hill, R.L., Eds.), Vol. 4, pp 245-409, Academic Press, New York.

Hartshorne, D.J., and Mueller, H. (1969) Biochim. Biophys. Acta 175, 301-319.

Head, J.F., and Perry, S.V. (1974) Biochem. J. 137, 145-154.

Henn, S.W., and Ackers, G.K. (1969) J. Biol. Chem. 244, 465-470.

Higashi, S., and Ooi, T. (1968) J. Mol. Biol. 34, 699-701.

Hincke, M.T. (1981) Ph.D. Thesis, University of Alberta.

Hincke, M.T., McCubbin, W.D., and Kay, C.M. (1977) FEBS Lett. 83, 131-136.

Hincke, M.T., McCubbin, W.D., and Kay, C.M. (1978) Can. J. Biochem. 56, 384-395.

Hincke, M.T., McCubbin, W.D., and Kay, C.M. (1979) Can. J. Biochem. 57, 768-775.

Hincke, M.T., Sykes, B.D., and Kay, C.M. (1981a) Biochemistry 20, 3286-3294.

Hincke, M.T., Sykes, B.D., and Kay, C.M. (1981b) Biochemistry 20, 4185-4193.

Hirabayashi, T., and Perry, S.V. (1974) Biochim. Biophys. Acta 351, 273-289.

Hitchcock, S.E. (1975) Biochemistry 14, 5162-5167.

Hitchcock-DeGregori, S.E. (1982) J. Biol. Chem. 257, 7372-7380.

Hitchcock, S.E., Huxley, H.E., and Szent-Györgyi, A.G. (1973) J. Mol. Biol. 80, 825-836.

Hitchcock, S.E., Zimmerman, C.J., and Smalley, C. (1981) J. Mol. Biol. 147, 125-151.

Holroyde, M.J., Robertson, S.P., Johnson, J.D., Solaro, R.J., and Potter, J.D. (1980) J. Biol. Chem. 255, 11688-11693.

Horwitz, J., Bullard, B., and Mercola, D. (1979) J. Biol. Chem. 254, 350-355.

Huxley, H.E. (1972) Cold Spring Harb. Symp. Quant. Biol. 37, 361-376.

Jackson, P., Amphlett, G.W., and Perry, S.V. (1975) Biochem. J. 151, 85-97.

Jacobson, A.L., Devin, G., and Braun, H. (1981) Biochemistry 20, 1694-1701.

Johnson, J.D., Charlton, S.C., and Potter, J.D. (1979) J. Biol. Chem. 254, 3497-3502.

Johnson, J.D., Collins, J.H., Robertson, S.P., and Potter, J.D. (1978a) Circulation 58, II-71.

Johnson, J.D., Collins, J.H., and Potter, J.D. (1978b) *J. Biol. Chem.* 253, 6451-6458.

Johnson, J.D., Collins, J.H., Robertson, S.P., and Potter, J.D. (1980) *J. Biol. Chem.* 255, 9635-9640.

Johnson, J.D., and Potter, J.D. (1978) *J. Biol. Chem.* 253, 3775-3777.

Johnson, P., Stockmal, V.B., and Braselton, S.E.H. (1981) *Int. J. Biol. Macromol.* 3, 267-268.

Katayama, E. (1979) *J. Biochem. (Tokyo)* 85, 1379-1381.

Katz, A.M. (1970) *Physiol. Rev.* 50, 63-158.

Kay, C.M. (1960) *Biochim. Biophys. Acta* 38, 420-427.

Klee, C.B., Crouch, T.H., and Richman, P.G. (1980) *Annu. Rev. Biochem.* 49, 489-515.

Kratky, O., Leopold, H., and Stabinger, H. (1973) *Methods Enzymol.* 27, 98-110.

Kretsinger, R.H., and Barry, C.D. (1975) *Biochim. Biophys. Acta* 405, 40-52.

Kretsinger, R.H., and Nockolds, C.E. (1973) *J. Biol. Chem.* 248, 3313-3326.

Kuntz, I.D., and Kauzmann, W. (1974) *Adv. Protein Chem.* 28, 239-345.

Leavis, P.C., and Kraft, E.L. (1978) *Arch. Biochem. Biophys.* 186, 411-415.

Leavis, P.C., Rosenfeld, S.S., Gergely, J., Grabarek, Z., and Drabikowski, W. (1978) *J. Biol. Chem.* 253, 5452-5459.

Lehman, W. (1978) *Nature* 274, 80-81.

Lehninger, A.L. (1970) *Biochemistry*, p 585, Worth Publishers, Inc., New York.

Lin, T., and Cassim, J.Y. (1978) *Biochem. J.* 175, 137-147.

Linderstrøm-Lang, K. (1950) *Cold Spring Harb. Symp. Quant. Biol.* 14, 117-126.

Lovell, S.J., and Winzor, D.J. (1977) Biochem. J. 167, 131-136.

Lynn, R.W., and Taylor, E.W. (1970) Biochemistry 10, 4617-4624.

Mak, A.S., and Smillie, L.B. (1980) Fed. Proc. 39, 1622.

Mak, A.S., and Smillie, L.B. (1981) J. Mol. Biol. 149, 541-550.

Mani, R.S., McCubbin, W.D., and Kay, C.M. (1973) FEBS Lett. 29, 243-247.

Mani, R.S., McCubbin, W.D., and Kay, C.M. (1974) Biochemistry 13, 5003-5007.

Mannherz, H.G. and Goody, R.S. (1976) Annu. Rev. Biochem. 45, 427-465.

Margossian, S.S., and Cohen, C. (1973) J. Mol. Biol. 81, 409-413.

Margossian, S.S., and Stafford, W.F. (1982) J. Biol. Chem. 257, 1160-1165.

Martson, S.B., Trevett, R.M., and Walters, M. (1980) Biochem. J. 185, 355-365.

Martenson, R.E. (1978) J. Biol. Chem. 253, 8887-8893.

Martin, A.F. (1981) J. Biol. Chem. 256, 964-968.

McCubbin, W.D., Hincke, M.T., and Kay, C.M. (1980) Can. J. Biochem. 58, 683-691.

McCubbin, W.D., and Kay, C.M. (1980) Acc. Chem. Res. 13, 185-192.

McCubbin, W.D., and Kay, C.M. (1982) Methods Enzymol. 85, 677-698.

McLachlan, A.D., and Stewart, M. (1976) J. Mol. Biol. 106, 1017-1022.

Miki, M. (1979) Biochim. Biophys. Acta 578, 96-106.

Moir, A.J.G., Solaro, R.J., and Perry, S.V. (1980) Biochem. J. 185, 505-513.

Moore, S., and Stein, W.H. (1963) Methods Enzymol. 6, 819-831.

Moore, P.B., Huxley, H.E., and DeRosier, D.J. (1970) J. Mol. Biol. 50, 279-295.

Murray, A.C., and Kay, C.M. (1971) Biochem. Biophys. Res. Commun. 44, 237-244.

Murray, A.C., and Kay, C.M. (1972) Biochemistry 11, 2622-2627.

Nonomura, Y., Drabikowski, W., and Ebashi, S. (1968) J. Biochem. (Tokyo) 64, 419-422.

Ohtsuki, I. (1975) J. Biochem. (Tokyo) 77, 633-639.

Ohtsuki, I. (1979) J. Biochem. (Tokyo) 86, 491-497.

Oikawa, K., Kay, C.M., and McCubbin, W.D. (1968) Biochim. Biophys. Acta 168, 164-167.

Oncley, J.L. (1941) Ann. N.Y. Acad. Sci. 41, 121-150.

Parry, D.A.D., and Squire, J.M. (1973) J. Mol. Biol. 75, 33-55.

Pato, M.D., Mak, A.S., and Smillie, L.B. (1981) J. Biol. Chem. 256, 602-607.

Pearlstone, J.R., Carpenter, M.R., Johnson, P., and Smillie, L.B. (1976) Proc. Natl. Acad. Sci. USA 73, 1902-1906.

Pearlstone, J.R., and Smillie, L.B. (1977) Can. J. Biochem. 55, 1032-1038.

Pearlstone, J.R., and Smillie, L.B. (1978) Can. J. Biochem. 56, 521-527.

Pearlstone, J.R., and Smillie, L.B. (1980) Can. J. Biochem. 58, 649-654.

Pearlstone, J.R., and Smillie, L.B. (1981) FEBS Lett. 128, 119-122.

Perrin, F. (1936) J. Phys. Radium 7, 1-11.

Perry, S.V. (1979) Biochem. Soc. Trans. 7, 593-617.

Potter, J.D. (1974) Arch. Biochem. Biophys. 162, 436-441.

Potter, J.D. (1982) Methods Enzymol. 85, 241-263.

Potter, J.D., and Gergely, J. (1974) Biochemistry 13, 2697-2703.

Potter, J.D., and Gergely, J. (1975) J. Biol. Chem. 250, 4628-4633.

Potter, J.D., Robertson, S.P., and Johnson, J.D. (1981) Fed. Proc. 40, 2653-2656.

Potter, J.D., and Zot, H.G. (1982) Biophys. J. 37, 43a.

Reid, R.E., and Hodges, R.S. (1980) J. Theor. Biol. 84, 401-444.

Richards, E.G., Teller, D.C., and Schachman, H.K. (1968) Biochemistry 7, 1054-1076.

Robertson, S.P., Johnson, J.D., Holroyde, M.J., Kranias, E.G., Potter, J.D., and Solaro, R.J. (1982) J. Biol. Chem. 257, 260-263.

Schachman, H.K. (1959) Ultracentrifugation in Biochemistry, pp 236-247, Academic Press, New York.

Schaub, M.C., Perry, S.V., and Häcker, W. (1972) Biochem. J. 126, 237-249.

Scheraga, H.A., and Mandelkern, L. (1953) J. Am. Chem. Soc. 75, 179-184.

Siegel, L.M., and Monty, K.J. (1966) Biochim. Biophys. Acta 112, 346-362.

Simha, R. (1940) J. Phys. Chem. 44, 25-34.

Sin, I.L., Fernandes, R., and Mercola, D. (1978) Biochem. Biophys. Res. Commun. 82, 1132-1139.

Seymour, J., and O'Brien, E.J. (1980) Nature 283, 680-682.

Shapiro, A.L., Vinuela, E., and Maizel, J.V. (1967) Biochem. Biophys. Res. Commun. 28, 815-820.

Smillie, L.B. (1976) PAABS Revista 5, 183-190.

Sobieszek, A. (1982) J. Mol. Biol. 157, 275-286.

Solaro, R.J., Moir, A.J.G., and Perry, S.V. (1976) Nature 262, 615-617.

Sperling, J.E., Feldmann, K., Meyer, H., Jahnke, U., and Heilmeyer, L.M.G. (1979) *Eur. J. Biochem.* 101, 581-592.

Squire, P.G., and Himmel, M.E. (1979) *Arch. Biochem. Biophys.* 196, 165-177.

Squire, J. (1981) *Nature* 291, 614-615.

Stewart, M., and McLachlan, A.D. (1976) *J. Mol. Biol.* 103, 251-269.

Strasburg, G.M., Greaser, M.L., and Sundaralingam, M. (1980) *J. Biol. Chem.* 255, 3806-3808.

Stull, J.T., and Buss, J.E. (1977) *J. Biol. Chem.* 252, 851-857.

Sutoh, K. (1980) *Biochemistry* 19, 1977-1983.

Svedberg, T., and Pedersen, K.O. (1940) *The Ultracentrifuge*, p 273, Oxford University Press, London.

Syska, H., Perry, S.V., and Trayer, I.P. (1974) *FEBS Lett.* 40, 253-257.

Syska, H., Wilkinson, J.M., Grand, R.J.A., and Perry, S.V. (1976) *Biochem. J.* 153, 375-387.

Talbot, J.A., and Hodges, R.S. (1981a) *J. Biol. Chem.* 256, 2798-2802.

Talbot, J.A., and Hodges, R.S. (1981b) *J. Biol. Chem.* 256, 12374-12378.

Tanford, C. (1955) *J. Phys. Chem.* 59, 798-799.

Tanford, C. (1961) *Physical Chemistry of Macromolecules*, pp 317-456, John Wiley and Sons, New York.

Taylor, K.A., and Amos, L.A. (1981) *J. Mol. Biol.* 147, 297-324.

Teller, D.C. (1973) *Methods Enzymol.* 27, 346-441.

Teller, D.C., Swanson, E., and deHaen, C. (1979) *Methods Enzymol.* 61, 103-124.

Tsukui, R., and Ebashi, S. (1973) *J. Biochem. (Tokyo)* 73, 1119-1121.

van Eerd, J.-P., and Kawasaki, Y. (1972) *Biochem. Biophys. Res. Commun.* 47, 859-865.

van Eerd, J.-P., and Kawasaki, Y. (1973) Biochemistry 12, 4972-4980.

van Eerd, J.-P., and Takahashi, K. (1975) Biochem. Biophys. Res. Commun. 64, 122-127.

Van Holde, K.E. (1975) in The Proteins (Neurath, H., and Hill, R.L., Eds.), Vol. 1, pp 225-291, Academic Press, New York.

Wagner, P.D., and Giniger, E. (1981) J. Biol. Chem. 256, 12647-12650.

Wakabayashi, T., and Ebashi, S. (1968) J. Biochem. (Tokyo) 64, 731-732.

Wakabayashi, T., Huxley, H.E., Amos, L.A., and Klug, A. (1975) J. Mol. Biol. 93, 477-497.

Weber, K., and Osborn, M. (1969) J. Biol. Chem. 244, 4406-4412.

Weeks, R.A., and Perry, S.V. (1978) Biochem. J. 173, 449-457.

Wilkinson, J.M., and Grand, R.J.A. (1978) Nature 271, 31-35.

Wilkinson, J.M., Perry, S.V., Cole, H.A., and Trayer, I.P. (1972) Biochem. J. 127, 215-228.

Wolodko, W.T. (1974) Ph.D. Thesis, University of Alberta.

Wuthrich, K., Wider, G., Wagner, G., and Braun, W. (1982) J. Mol. Biol. 155, 311-319.

Yamaguchi, M., and Greaser, M.L. (1979) J. Mol. Biol. 131, 663-667.

Yamaguchi, M., Greaser, M.L., and Cassens, R.G. (1974) J. Ultrastruct. Res. 48, 33-58.

Yanagida, T., Taniguchi, M., and Oosawa, F. (1974) J. Mol. Biol. 90, 509-522.

Yang, J.T. (1961) Adv. Protein Chem. 16, 323-400.

Yphantis, D.A. (1964) Biochemistry 3, 297-317.

Zot, H.G., and Potter, J.D. (1982) J. Biol. Chem. 257, 7678-7683.

B30370